TARGETING CYCLIN DEPENDENT KINASES 4/6 ACTIVITY IN PANCREATIC DUCTAL ADENOCARCINOMA

APPROVED BY SUPERVISORY COMMITTEE

_____
Erik S. Knudsen, Ph.D.

_____
Rolf Brekken, Ph.D.

_____
Sandeep Burma, Ph.D.

_____
Gray Pearson, Ph.D.

DEDICATION

This dissertation is dedicated to Jorge Sr. & Maria Franco, and Marisa Leal for their love and sacrifice.

'

Acknowledgements

This dissertation was carried out in the laboratory of Erik Knudsen Ph.D. at UT Southwestern Medical Center. I would like to thank my mentor Erik for the given opportunity to participate in this research projects.

TARGETING CYCLIN DEPENDENT KINASES 4/6 ACTIVITY IN PANCREATIC DUCTAL ADENOCARCINOMA

By

Jorge Franco, Ph.D.

DISSERTATION

Presented to the Faculty of the Graduate School of Biomedical Sciences

The University of Texas Southwestern Medical Center at Dallas

In Partial Fulfillment of the Requirements

For the Degree of

DOCTOR OF PHILOSOPHY

The University of Texas Southwestern Medical Center at Dallas

Dallas, Texas

August, 2016

TARGETING CYCLIN DEPENDENT KINASES 4/6 ACTIVITY IN PANCREATIC DUCTAL ADENOCARCINOMA

Jorge Franco

The University of Texas Southwestern Medical Center at Dallas, 2016

Erik Knudsen Ph.D.

Pancreatic ductal Adenocarcinoma (PDA) is an aggressive and lethal disease that lacks an adequate treatment. Given that patients with PDA only marginally benefit from the current therapies, there is an urgent need to develop more effective approaches that specifically target PDA. Because a significant portion of PDA tumors lose p16 expression and often over-express Cyclin D1, we hypothesized that CDK4/6 activity is deregulated leading to uncontrolled proliferation. Thus, PDA would represent a good candidate for treatment with recently developed CDK4/6 inhibitors.

Our study first investigated the sensitivity of PDA cells to CDK4/6 inhibition and found that PDA cells exhibit variable responses to CDK4/6 inhibition, incling models that display significant resistance. Interestingly, these models showed a novel mechanism of resistance to CDK4/6 inhibition. Prior to this study, RB loss was the only mechanism known to circumvent CDK4/6 inhibition. However, herein, we uncovered that CDK4/6 inhibition can lead to aberrant Cyclin E expression, which can compensate for CDK4/6 activity loss and maintain RB in a hyper-phosphorylated state. Subsequent findings demonstrated that this resistance could be blocked by combination therapy with MTOR inhibitors, which prevented aberrant Cyclin E expression and reinforced RB activation.

Our second study found that prolonged CDK4/6 inhibition led to an altered metabolic state with an increased in oxidative respiration and glycolysis accompanied by mitochondria accumulation and increase cellular complexity. This heightened metabolic state was mediated by MTOR signaling, which activity was stimulated by amino acid accumulation and an increase in lysosome production in CDK4/6 treated PDA cells. Lastly, we unveiled new combination therapies that targeted the altered metabolism state of CDK4/6 inhibitor treated cells by impinging on antioxidants such as Hemoxygenase 1 (HO-1) and catalase (CAT), whose expression was enhanced post treatment, or by targeting BCL-2/BCL-XL using ABT-737.

Taken together our data demonstrate that targeting PDA with CDK4/6 inhibitors can represent an efficacious route for treatment. Activation of MTOR and perhaps other signaling pathways likely contribute to intrinsic and acquired resistance to CDK4/6. These combined data would support the combined use of CDK4/6 with MTOR inhibitors and other agents for the treatment of pancreatic cancer.

TABLE OF CONTEXT

PUBLICATIONS

1. Franco, J., Balaji, U., Freinkman, E., Witkiewicz, A. K. & Knudsen, E. S. (2016) Metabolic Reprogramming of Pancreatic Cancer Mediated by CDK4/6 Inhibition Elicits Unique Vulnerabilities, *Cell reports*. **14**, 979-90.

2. Ortega, S. B., Kashi, V. P., Cunnusamy, K., Franco, J. & Karandikar, N. J. (2015) Autoregulatory CD8 T cells depend on cognate antigen recognition and CD4/CD8 myelin determinants, *Neurology(R) neuroimmunology & neuroinflammation*. **2**, e170.

3. Witkiewicz, A. K., Borja, N. A., Franco, J., Brody, J. R., Yeo, C. J., Mansour, J., Choti, M. A., McCue, P. & Knudsen, E. S. (2015) Selective impact of CDK4/6 suppression on patient-derived models of pancreatic cancer, *Oncotarget*. **6**, 15788-801.

4. Knudsen, E. S., McClendon, A. K., Franco, J., Ertel, A., Fortina, P. & Witkiewicz, A. K. (2015) RB loss contributes to aggressive tumor phenotypes in MYC-driven triple negative breast cancer, *Cell Cycle*. **14**, 109-22.

5. Franco, J., Witkiewicz, A. K. & Knudsen, E. S. (2014) CDK4/6 inhibitors have potent activity in combination with pathway selective therapeutic agents in mdels of pancreatic cancer, *Oncotarget*. **5**, 6512-25.

6. Cunnusamy, K., Baughman, E. J., Franco, J., Ortega, S. B., Sinha, S., Chaudhary, P., Greenberg, B. M., Frohman, E. M. & Karandikar, N. J. (2014) Disease exacerbation of multiple sclerosis is characterized by loss of terminally differentiated autoregulatory CD8+ T cells, *Clin Immunol*. **152**, 115-26.

LIST OF FIGURES

LIST ABBREVIATIONS

5-FU	Fluorouracil
ATP	Adenosine Triphosphate
ATP	Adenosine triphosphate
BCL2	B-cell lymphoma 2
BRAF	v-raf murine sarcoma viral oncogene homolog B1
BrdU	Bromodeoxyuridine
BSO	L-buthionine-S,R-sulfoximine
CAFs	Cancer-Associated Fibroblasts
CAT	Catalase
CCND1	Cyclin D1
CCNE1	Cyclin E1
CDK	Cyclin-dependent kinases
CDK2	Cyclin-dependent kinase 2
CDK4/6	Cyclin Dependent Kinases 4 and 6
CDKN2A	Cyclin-Dependent Kinase Inhibitor 2A
DCK	deoxycytidine kinase
DHFR	Dihydrofolate reductase
DNA	deoxyribonucleic acid
dNTP	Deoxynucleotide
ECR	extracellular acidification rate
FDA	Food and Drug Administration
FDG-PET	fluorodeoxyglucose- positron emission tomography
FLT-PET	fluorothymidine-positron emission tomography
FOXM1	Forkhead box protein M1
GAP	GTPase activating proteins
GDP	Guanosine diphosphate
GEF	nucleotide exchange factors
GTP	Guanosine triphosphate
HK	Hexokinase
HMOX1	Heme Oxygenase 1
HO-1	Hemeoxygenase
KRAS	Kirsten rat sarcoma
LDHA	Lactate Dehydrogenase A
MCL1	Myeloid Cell Leukemia 1
MCM7	Minichromosome Maintenance Complex Component 7
MCT4	Monocarboxylate transporter 4
MEK	Mitogen-activated protein kinase kinase
MTOR	mammalian target of rapamycin
NADPH	Nicotinamide adenine dinucleotide phosphate
NQO1	NAD(P)H Dehydrogenase, Quinone 1

OCR	oxygen consumption rate
PanIN	Pancreatic Intraepithelial Neoplasia
PCNA	Proliferating cell nuclear antigen
PDA	Pancreatic ductal adenocarcinoma
PDX	patient-derived xenograft
PDX	Pancreatic and duodenal homeobox 1
PFS	progression-free survival
PI3K	Phosphatidylinositol 3-kinase
PI3K	Phosphoinositide 3-kinase
PLK1	Polo-Like Kinase 1
Ptf1a	pancreas transcription factor 1 complex
RB	Retinoblastoma 1
ROS	Reactive oxygen species
ROS	Reactive oxygen species
RPPA	Reverse phase protein array
RT	Room temperature
S6	Ribosomal protein S6
SA-b-Gal)	beta-galactosidase
TCA	Tricarboxylic acid cycle
TORC1	mammalian target of rapamycin complex 1
TS	thymidylate synthase

CHAPTER I: General Introduction

1.1: Pancreas' Anatomy and Function:

The pancreas is located behind the lower portion of the stomach. It is surrounded by the spleen, small intestine, gallbladder and duodenum. It is composed of three main sections: the head, body, and tail. This organ has two distinct functions: an endocrine and exocrine function. The endocrine component of the pancreas is made up of islet cells, which are ubiquitously located in the pancreatic parenchyma. They are responsible for the production and secretion of important hormones such as insulin and glucagon. These molecules maintain adequate blood glucose levels, which are essential for proper organ homeostasis. The pancreas also contains exocrine glands that secrete zymogens, pro-enzymes, and bile into the intestine, which facilitate carbohydrate, fat, and protein digestion. These molecules are shuttled via a network of ducts that are branched throughout the pancreatic parenchyma and drained into the duodenum. It is here in these ducts that 95% of all pancreatic tumors develop. These tumors are referred to as Pancreatic Ductal Adenocarcinomas (PDA)[1].

1.2: Pancreatic Ductal Adenocarcinoma's Epidemiology and Etiology:

PDA has a dire prognosis with a 5-year survival rate of less than 5%. It is recognized as the 4th leading cause of cancer deaths in the United States (US), but it has also been projected that in the next decade PDA will become the 2nd leading cause of cancer deaths[2]. This ascent is the result of an increasing survival trend seen in patients with breast and prostate cancers due to more effective screening and/or more efficacious therapies, which currently lead PDA in cancer deaths, while no significant progress is

predicted in PDA. There are about 50,000 new cases of PDA diagnosed every year in the US with a median age of diagnosis at around 71 years old [3]. The etiology of PDA is still unclear, but various risks factors have been identified including smoking, long-term diabetes, and chronic pancreatitis[4-7]. However, how these factors influence PDA development remains discovered. In addition to the risk factors mentioned, a genetic component has also been identified and is thought to account for about 10% of PDA cases. Inherited germline mutations to multiple genes (CDKN2A, BRCA1, BRCA2, ATM, etc.) have been found to be associated with a predisposition to PDA[8]. Not surprisingly, combinations of genetic and environmental factors have been shown to hold the greatest risk in the development of PDA[9].

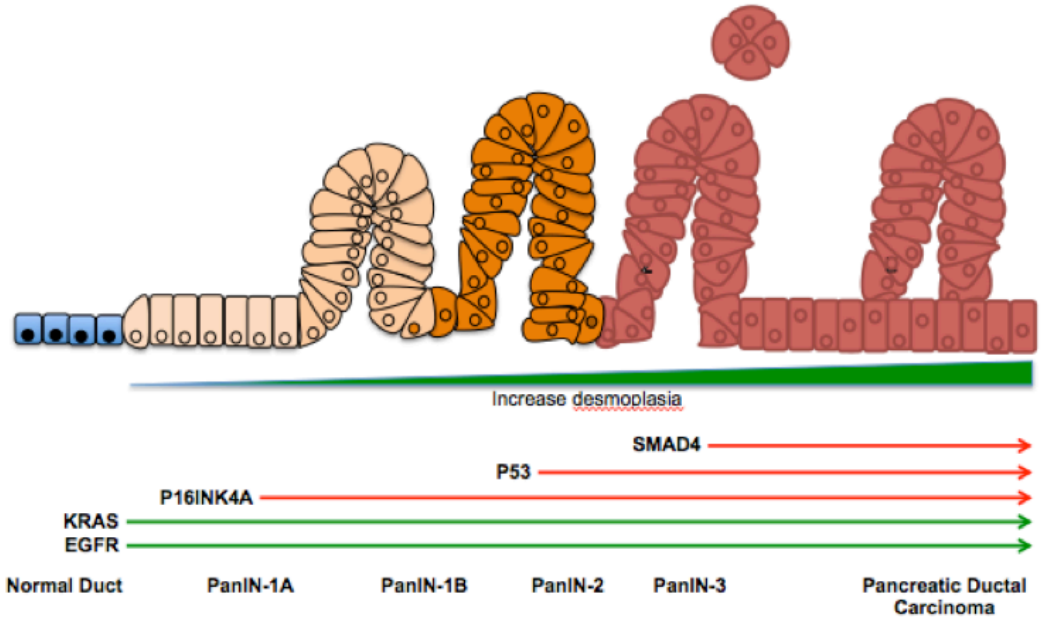

1.3: PDA Progression:

Figure 1.1. **The genetic progression of PDA.** The model shows the morphological and architectural changes experienced by normal duct epithelium until the development of PDA, which occurs through a series of histological defined stages called Pancreatic intraepathlium neoplasia (PanIN). The earliest genetic alterations occur in KRAS, which are then followed by P16INK4A and later by P53 and SMAD4[10].

PDA develops through a multistep process, whereby normal healthy ductal cells accumulate genetic changes that subsequently lead to its malignant transformation. The process of PDA cancer initiation and progression can be summarized in four distinct stages, as illustrated in Figure 1.1. The first stage is called pancreatic intraepithelial neoplasia-1(PanIN-1). Here, normally ductal cells usually lose their regular morphology, changing from non-mucinous cuboidal to mucinous tall columnar epithelium. As the cells

accumulate more genetic aberrations, the ductal lining becomes increasingly more disorganized, entering the second stage called PanNI-2. In the third stage, PanIN-3 lesions cells are often seen detaching into the PanIN lumen. Lastly, in fourth stage, PanIN-3 cells develop to adenocarcinoma, where cells undergo an epithelial to mesenchymal transition to become migratory. These migratory cells often metastasize to tissues including local and distant lymph nodes as well as the liver, brain and lungs [11].

1.4: Current Pancreatic Cancer Therapeutics

Even though there has been an increase in knowledge regarding the progression of PDA, there ultimately has been very little progress in the development of effective therapies to target PDA. For the last 30 years, Gemcitabine, a nucleoside analog, has been used as the major medical treatment for PDA even though the benefit has only led to an increase in overall survival in advance disease by about a month[12]. Recently, two new standard therapies have been employed: Folfirinox or Nab-paclitaxel with Gemcitabine. Folfirinox is a multiple chemotherapy combination containing fluorouracil [5-FU], leucovorin, irinotecan and oxaliplatin; while, Nab-paclitaxel is an albumin nanoparticle that allows better delivery of paclitaxel due to its greater solubility in water. Similar to Gemcitabine these drug combinations work by non-selectively targeting all proliferating cells. Presently, these combinations have only shown a modest benefit in the overall survival of patients possibly due to PDA's recalcitrant nature[13, 14]. Several studies have attempted to use more targeted approaches to PDA but results have been less then modest. For instance, Epidermal growth factor receptor (EGFR) was considered an attractive target due to the fact that its high expression is correlated with more advanced disease and poor survival[15]. This led to the evaluation of EGFR antagonists erlotinib

with Gemcitabine in the clinic, but unexpectedly this combination only increased overall survival by about two weeks[16-18]. Other similar studies testing other potential candidates such farnesyl transferase, thought to play an essential in KRAS attachment to cell membrane, however results showed no significant benefit [19]. Together, this suggests that new candidates need to be identified and targeted that could potentially be more efficacious.

1.5: Overview of Cell Cycle:

PDA growth is thought to result from a disruption in the cell cycle control. Normally, the mammalian cell cycle is divided into four discrete phases, G_1, S, G_2 and M. The cell cycle begins at G_1, where the cell prepares for genomic replication by inducing early cell cycle genes. The G_1 phase is followed by genome replication during the S phase. When genomic replication is completed the cells will enter G_2. Here, the cell continues to grow and produce proteins that are important for proper genomic separation. Lastly, cells will go through an ordered series of stages during mitosis (prophase, prometaphase, metaphase, anaphase, telophase and cytokinesis) to generate two daughter cells, thus completing the cell cycle. Oscillating regulatory subunits called cyclins closely regulate these orchestrated processes. The fluctuating expression of cyclins is created by their rapid expression and quick degradation by the proteasome to coordinate the transition between the various cell cycle phases[20]. Each cyclin is specific for distinct phases of the cell cycle. The primary role of cyclins is to activate Cyclin-dependent kinases (CDKs), which are responsible for phosphorylating and activating cell cycle machinery components[21, 22]. Each of these phases is associated with a different cyclin/CDK complexes as illustrated in Figurec 1.3 [23]. This process is closely regulated

by surveillance mechanisms referred to as checkpoints, which are driven by major transcriptional regulators (RB, P53 etc.)[24-26]. These checkpoints exist to halt replication progression should a problem arise. Present at several points of the cell cycle (G_1 - S, G_2 - M and metaphase - anaphase transitions), these checkpoints can by readily activated following DNA damage or other cellular stresses[27]. In healthy cells, activation of these checkpoints will lead to cell cycle arrest until the problem is repaired. If the damage is irreversible cell death will be initiated via apoptosis. Interestingly, in cancer many of these regulatory processes are disrupted due to loss function of cell cycle regulators such as RB and/or P53 leading to uncontrollable cell cycle progression, which has been shown to be essential for cancer progression[28].

1.6: Deregulation of Tumor Suppressors

It is speculated that loss of tumor suppressors is an important step for PDA development[29]. This is supported by animal studies showing that when tumor suppressors are lost, PDA arises[30].Tumor suppressors such as P53 and SMAD4 have been investigated and shown to be actively involved in PDA suppression, but their loss is often found at later stages in PDA[1, 31]. Unlike P53 and SMAD4, CDKN2A loss is found in much earlier lesions and at higher rates, thus suggesting that loss of CDKN2A is the first hurtle PDA needs to overcome[32, 33]. This is in accordance with familial studies, where germline mutations to CDKN2A were significantly associated with PDA[34].

1.7: Loss CDKN2A a Common Occurrence in PDA:

One of the hallmark genetic events in PDA is the loss of the CDKN2A tumor suppressor locus[9]. This locus normally encodes for a pair of tumor suppressors: ARF and p16. ARF functions as a stabilizer of the tumor suppressor protein p53 by antagonizing E3 ubiquitin-protein ligase, MDM2; while p16 is an inhibitor of CDK4/6. The mechanism by which p16 exerts its inhibitory effect occurs via binding to CDK4/6 thus preventing their association with Cyclin D1, a complex responsible for the induction of cell cycle genes[35]. Interestingly, oncogenic KRAS induces a senescent-like growth arrest state in the presence of p16[36]. In accordance with this data, genetic engineered animal models have also demonstrated that constitutively active forms of KRAS are not sufficient for PDA development. It is only when tumor suppressors such as p16 are deleted in conjunction with KRAS oncogene induction that PDA develop. Together, this evidence suggests that there is a highly selective pressure for p16 loss, which precedes PDA development[37].

1.8: CDK/RB/E2F Axis:

CDK4/6, threonine/serine kinases, are key components of the cell cycle machinery. These low-weight molecular proteins are responsible for initiating transition from G_1 to S phase. In response to mitotic signals, CDK4/6 together with D-Type cyclins (D1, D2, and D3) initiate the hyper-phosphorylation of RB, which is a main gatekeeper of cell cycle. Subsequent to CDK4/6 phosphorylation other CDK/Cyclin complexes are responsible for maintaining RB in a hyper-phosphorylated state throughout the cell cycle[38]. For instance, Cyclin E1 /CDK2 complex plays a pivotal role in RB

phosphorylation following CDK4/6 mono-phosphorylation of RB[39]. Thus, it is speculated that a possible mechanism of resistance to CDK4/6 inhibition may occur as a consequence of deregulation of compensatory CDK/cyclin complexes such as Cyclin E/CDK2. RB is responsible for binding to E2F transcription factor and recruiting histone modifying complexes that prevent induction of cell cycle genes. However, when RB is hyper-phosphorylated in part by the CDK4/6/CylinD1 complex, RB becomes inactive and E2F transcriptional factors are released. Consequently, transcription of cell cycle genes is re-initiated and the progression of the cell cycle continues[40].

1.9: CDK4/6 Inhibitors:

Normal cell cycle progression is tightly controlled by multiple regulatory mechanisms. Disruption of these mechanisms can contribute to malignant transformation. In PDA, RB is often maintained in a hyper-phosphorylated state along with the up-regulation of Cyclin D1 expression, alluding to a possible deregulation of CDK4/6 activity, which may be responsible for the uncontrolled proliferation seen in PDA[41, 42]. Until recently, CDKs were considered untargetable due to lack of specificity; however, more recent developments have changed this perspective[43]. Currently, several CDK4/6 inhibitors have been developed (Palbociclib, Lee-001 and LY2832519), unlike their predecessors; these inhibitors exhibit greater specificity in the nanomolar range (Figure 1.2)[44]. They were developed from a group of pyridopyrimidines, which are selective ATP-competitive inhibitors. These inhibitors effectively dephosphorylate RB and inhibit cell cycle progression, halting cells at G_1 thus they are considered cytostatic drugs[45]. Recent clinical studies have shown that CDK4/6 inhibitors can exert a potent effect as a single agent in several cancer types, which are highly dependent on

CDK4/6 activity[46, 47]. Additionally, in breast cancer, CDK4/6 inhibitors were shown to be very efficacious in combination with anti-estragon therapy increasing Tumor Free Progression (TFP) by more than 10 months[48].

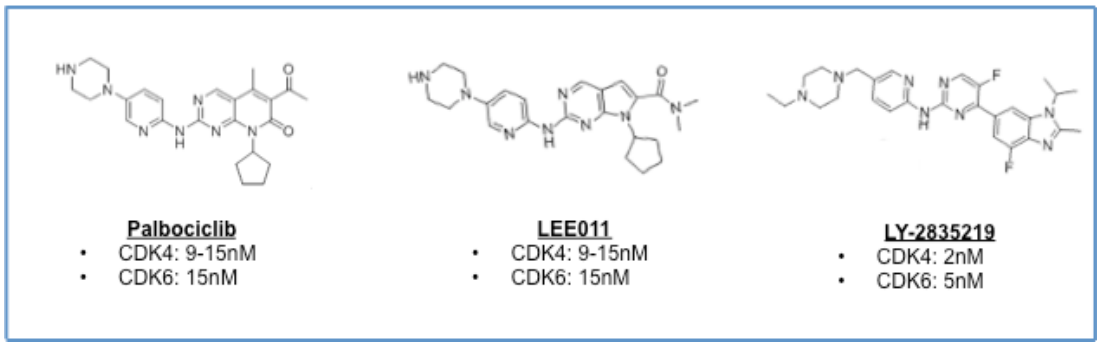

Figure 1.2 **CDK4/6 inhibitors specificity.** All CDK4/6 inhibitors target CDK4 and CDK6 at namomolar range.

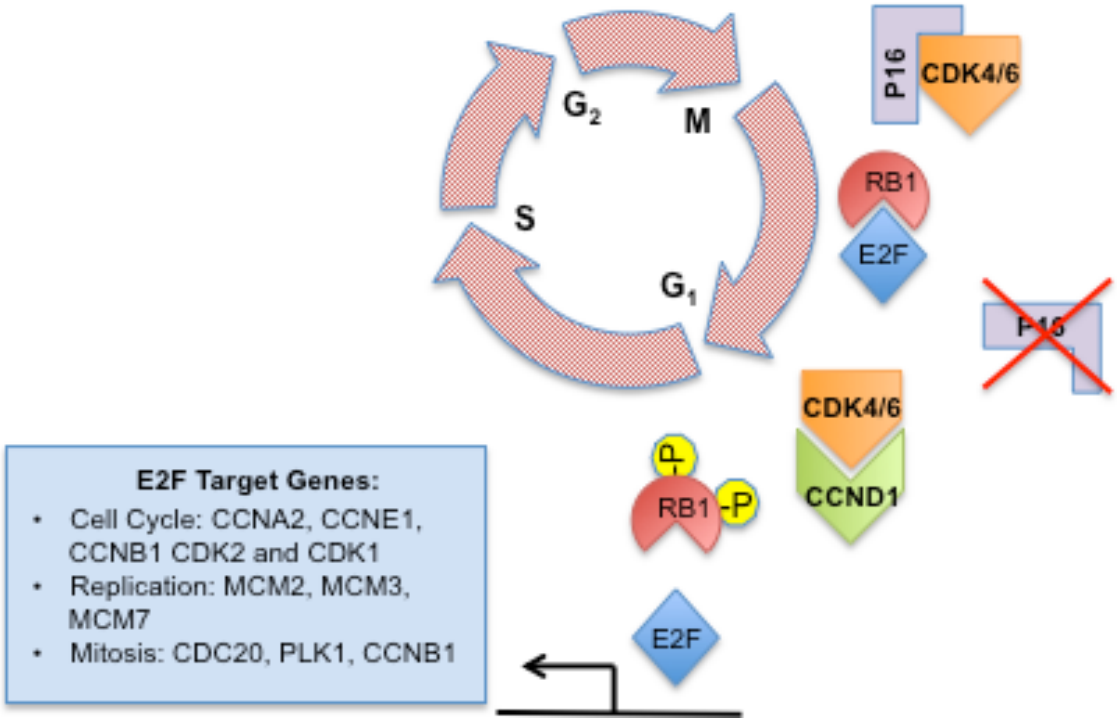

Figure 1.3 Cell Cycle Regulation at G_1 to S transition: P16 maintains RB in its active and hypo-phosphorylated by inhibiting CDK4/6 activity. When P16 is loss, RB is hyper-phosphorylated by CDK4/6 leading to release of E2F transcriptional actors and subsequent induction of cell cycle genes.

1.10: KRAS oncogene in PDA:

PDA is a disease that originates from the deregulation of cellular mechanisms important in maintaining normal cell growth leading to oncogenic transformation. The

progression from normal pancreas to PDA occurs via a series of well-established genetic alterations. The most common genetic alteration in PDA occurs in KRAS (name derived from Kirsten rat sarcoma)[49]. KRAS is member of a family of GTPases possessing intrinsic GTPase activity that plays an important role in transmitting mitogenic messages from the cell membrane. Normally, KRAS activity is regulated by nucleotide exchange factors (GEFs) and GTPase activating proteins (GAPs). When bound to GEFs, KRAS is activated by the substitution of GDP to GTP; conversely, when bound to GAPs, KRAS is inactivated by the hydrolysis of bound GTP to form GDP[50]. However, in PDA, these regulatory mechanisms become impaired. The most common mutations found in KRAS are G12, G13, or Q61, which disrupt KRAS GTP hydrolysis thus rendering KRAS in a constitutive active state[51, 52]. These activating mutations are found in >95% in PDA tumors and in 30% of PanIN lesions. Since activation of KRAS is both an early and predominant event in the formation of pancreatic cancer, it is considered to play a critical role in the formation of PDA tumors[53]. These findings are consistent with genetic engineered animal models (PDX-1-Cre, LSL-$Kras^{G12D}$ or Ptf1a-Cre, LSL-$Kras^{G12D}$) where KRAS is constitutively expressed in pancreatic tissue. These models have shown that introduction of KRAS in the pancreas, in conjunction with tumor suppressor (p53, pRB, CDKN2A, etc…) ablation, is sufficient to drive PDA in mice. [54, 55].

1.11: KRAS signaling in PDA:

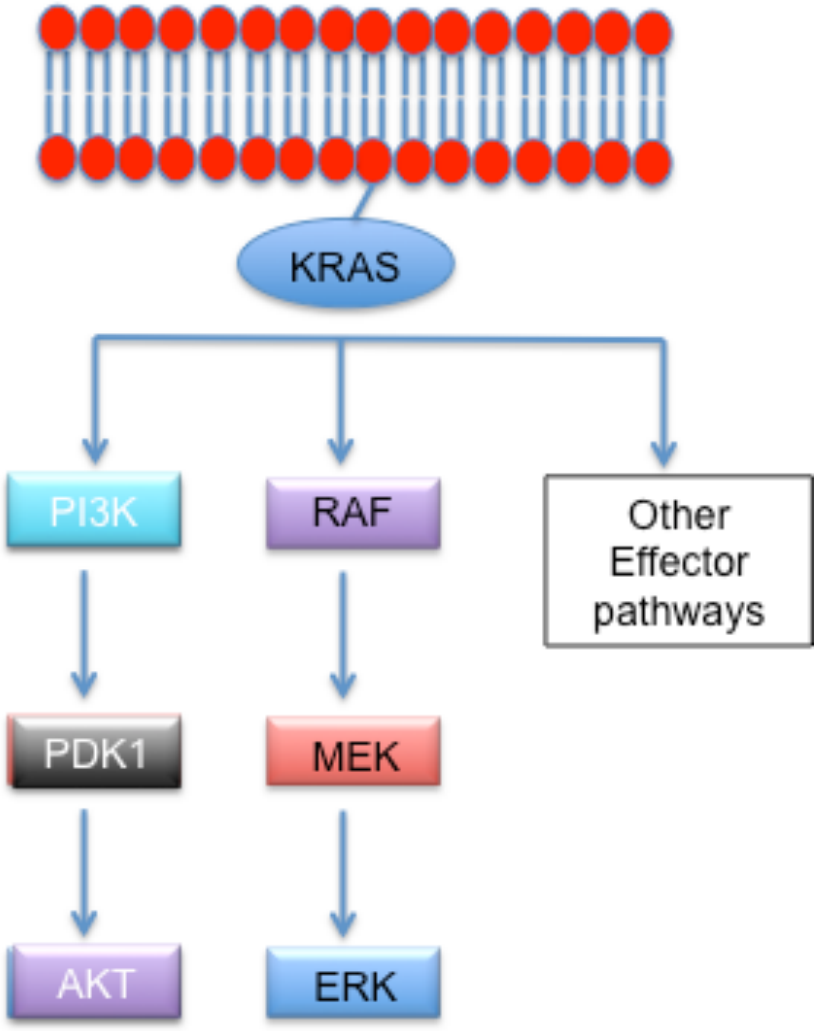

Figure 1.4. **Oncogenic KRAS *signaling.*** *Oncogenic* KRAS activates multiple signaling pathways. *Two* of the major pathways that are activated by KRAS are BRAF, mitogen-activated protein kinase, and PI3K.

KRAS signaling is relayed through various signaling cascades, as illustrated in Figure 1.4. There are several major signaling pathways that are engaged by KRAS signaling including PI3K and MEK signaling[53]. The importance of these pathways on PDA development has been investigated using genetic engineered mouse models, where constitutively active forms of PI3K (*PIK3CA)* or MEK (RAF) signaling are introduced into pancreatic ductal epithelium[56, 57]. Interestingly, these models were capable of phenocopying KRAS-driven pancreatic carcinoma, thus emphasizing the importance of these pathways in PDA development. Furthermore, studies have examined the effects of impinging on these signaling pathways on PDA growth using pharmacological agents. Results have found that disrupting a single KRAS driven pathways only exerts a modest effect, but when intruding on multiple singling pathways by using combination therapies, a more significant outcome can be achieved[58, 59]. How this relates to human disease however, is still unknown. Multiple clinical trials that are interested in investigating the dependency of PDA on these signaling pathways are underway.

1.12: KRAS and Metabolism:

KRAS signaling influences beyond proliferation in PDA. It plays a pivotal role in regulating metabolic processes, in the cytoplasm and mitochondria that are essential for fueling the rampant proliferation observed in PDA. KRAS drives major metabolic processes such as glycolysis and glutaminolysis, which dividing cells rely heavily on for energy and raw material[53, 60]. Glycolysis is essential for the production of ATP as well as primary intermediates that are important in the synthesis of nucleotides and nucleic acids required for DNA replication. Glutaminolysis supports lipid and nucleotide

biosynthesis as well as maintaining the redox balance by replenishing Nicotinamide adenine dinucleotide phosphate (NADPH). KRAS has been shown to steer cells toward glycolysis and glutaminolysis by inducing the expression of rate-limiting enzymes such as Hexokinase (HK1), Hexokinase 2 (Hk2), and Lactate Dehydrogenase A (LDHA), aspartate transaminase 1(GOT1)[60, 61]. In addition, several KRAS down-stream signaling pathways have been implicated in regulating metabolic processes including MEK and MTOR signaling[62]. For instance, our group has shown that MEK signaling regulates monocarboxylate transporter MCT4 expression, which mediates lactic acid efflux, presumably helping maintain proper intracellular pH and cellular homeostasis[63].

1.13: Metabolism and ROS Production in PDA

It is speculated that the heightened metabolic state exhibited by PDA cells could become a liability due to the production of by-products such as reactive oxygen species (ROS). Various metabolic processes occurring in the mitochondria and the cytoplasm produce ROS. In the mitochondria, generation of ROS is produced by the electron transport chain; while, in the cytoplasm, NADPH oxidase is the major contributor[64]. It has been shown that high levels of ROS can potentially lead to DNA damage, which is detrimental for cancer cells; however, paradoxically, ROS can also act as a second messenger responsible for prosurvival and anti-apoptotic signals in PDA[65]. A study showed that ROS produced by NADPH-activated JAK2 kinases mitigated apoptosis by inhibiting key protein tyrosine phosphatases (PTPs)[66]. However, ROS levels need to be closely regulated as they can still exert much damage. Interestingly, KRAS regulates ROS levels by multiple mechanisms including the induction of NRF2. NRF2 is key transcriptional factor that regulates the expression of antioxidants, such as NADPH

Dehydrogenase, Quinone 1 (NQO1) and Heme Oxygenase 1 (HMOX1), which play an important role in ROS quenching[67].

CHAPTER II: CDK4/6 inhibitors have potent activity in combination with pathway selective therapeutic agents in models of pancreatic cancer

2.1: Abstract

Pancreatic ductal adenocarcinoma (PDA) has a poor prognosis, in part, due to the therapy-recalcitrant nature of the disease. Loss of the CDK4/6 inhibitor CDKN2A is a signature genetic event in PDA. Therefore, PDA may be amenable to treatment with pharmaceutical CDK4/6 inhibitors. Surprisingly, response to CDK4/6 inhibition was highly variable in PDA models, and associated with differential suppression of gene expression. Mitotic genes were repressed and FOXM1 was uniformly attenuated; however, genes involved in DNA replication were uniquely suppressed in sensitive models. Aberrant induction of Cyclin E1 was associated with resistance, and knockdown demonstrated synergistic suppression of the cell cycle with CDK4/6 inhibition. Combination therapies are likely required for the effective treatment of disease, and drug screening demonstrated additive/antagonistic interactions with CDK4/6 inhibitors. Agents dependent on mitotic progression (taxanes/PLK1 inhibitors) were antagonized by CDK4/6 inhibition, while the response to 5-FU and gemcitabine exhibited drug specific interactions. PI3K/MTOR and MEK inhibitors potently cooperated with CDK4/6 inhibition. These agents were synergistic with CDK4/6 inhibition, blocked the aberrant upregulation of Cyclin E1, and yielded potent inhibition of tumor cell growth. Together, these data identify novel mechanisms of resistance to CDK4/6 inhibitions and provide a roadmap for combination therapies in the treatment of PDA.

2.2: Introduction:

Pancreatic ductal adenocarcinoma (PDA) has a terrible prognosis with a 5-year survival of approximately 6% [68-70]. The approved systemic therapies have a relatively modest impact on survival, and PDA is considered a therapy recalcitrant disease [68, 69, 71]. The treatment of PDA has remained largely dependent on the use of systemic chemotherapy regimens, and there are basically no targeted approaches to treatment that exploit the underlying genetic features of pancreatic cancer. PDA is largely driven by oncogenic events (e.g. KRAS), which historically are considered "non-actionable" from a therapeutic perspective. However, PDA exhibits a range of genetic alterations some of which could be amenable to targeted therapy. One of these alterations is the genetic loss or epigenetic silencing of the CDKN2A tumor suppressor [49, 72-74].

The CDKN2A gene encodes the p16INK4a protein that is a potent inhibitor of Cyclin Dependent Kinases 4 and 6 (CDK4/6). Physiologically, p16ink4a represents a key barrier to oncogenic transformation, as it is induced by oncogenic stress and leads to senescence in multiple disease relevant settings [75]. In the context of PDA, it has been hypothesized that p16ink4a loss is selected for to enable the progression of KRAS mutated cells [76-79]. Correspondingly, it has been shown that the over-expression of p16ink4a is dominant to the effects of KRAS in cell culture models and is capable of re-establishing a senescence-like arrest in established cancer models [80-83]. The only known functional target of p16ink4a are the kinases CDK4 and CDK6, and a plethora of data support this concept [75, 84-89]. For example, p16ink4a-mediated arrest is selectively bypassed by CDK4 mutations that disrupt the association with the inhibitor

[90, 91]. Similarly, loss of RB, which is the down stream target for CDK4/6 bypasses the growth inhibitory activity of p16ink4a [75, 92]. Furthermore, analysis of mutual-exclusivity in cancer demonstrates that there is a pronounced reciprocal relationship between the loss of p16ink4a, deregulation of CDK4/6, and loss of RB [91, 93, 94]. Thus these events describe a single pathway, wherein the predominant event occurring in PDA is loss of p16ink4a, and suggest that restoring its biological function could represent a key means to limit the growth of KRAS driven cancers.

While multiple CDK-inhibitory agents have been evaluated in clinical trials, only recently have highly specific CDK4/6 inhibitory drugs been developed [45, 95]. Consistent with the function of p16ink4a, they induce a highly potent G1-arrest that is dependent on the suppression of CDK4/6 and the presence of RB tumor suppressor (RB) [96-98]. RB is a critical downstream effector of CDK4/6 and regulates the expression of a host of target genes through interactions with E2F and other transcription factor complexes [99]. These targets include CDK/Cyclin subunits (e.g. Cyclin E and Cyclin A), DNA replication factors (e.g. MCM7 and PCNA), genes involved in dNTP metabolism (e.g. thymidylate synthase and ribonucleotide reductase), and mitotic progression (e.g. PLK1 and CDC20). In preclinical models, activation of RB via CDK4/6 inhibition can induce senescent-like arrest [45, 95, 100-104]. An important parallel effector of CDK4/6 is FOXM1, which is stabilized by direct CDK4/6 mediated phosphorylation and stimulates expression of cell cycle regulated genes [105, 106]. Recently, clinical studies have demonstrated that CDK4/6 inhibitors can have potent single agent activity in select tumor models ostensibly addicted to kinase activity, such as liposarcoma and mantle cell lymphoma [47, 107-109]. Additionally, in breast cancer

CDK4/6 inhibitors have demonstrated highly significant activity in combination with endocrine agents [110-114]. However, it is also clear that there are features of tumor behavior that we do not fully understand, as specific diseases which frequently lose p16ink4a had minimal response to CDK4/6 inhibitors in the clinic [108, 109].

Here we find that CDK4/6 inhibition can have a potent impact on PDA models. While some models exhibit a durable response, acquired/intrinsic resistance can bypass the action of CDK4/6 inhibition in the majority of models analyzed via a novel mechanism involving induction of Cyclin E1. Drug screening reveals a complex and mechanism specific impact of CDK4/6 inhibitors on drug-sensitivity. However, specific combination therapies clearly expand the therapeutic potency of CDK4/6 inhibition for the treatment of PDA.

Results:

CDKN2A-deficient PDA models exhibit differential response to CDK4/6 inhibition:

Eight pancreatic cancer cell lines were screened for their proliferative response to CDK4/6 inhibition. In addition to multiple PDA signature mutations (e.g. KRAS, SMAD4, and TP53) these cell lines carried a non-functional CDKN2A gene (Fig. 2.1A). In order to test sensitivity to CDK4/6 inhibitors, cells were treated with increasing concentrations of PD-0332991, and proliferation was measured by 5-bromo-2-deoxyuridine (BrdU) incorporation (Fig. 2.1B). Results showed that some model experienced a complete suppression of proliferation (e.g. CAPAN2), while others were modestly or mostly resistant to CDK4/6 inhibitor (e.g. HS766T and PL5). Recognizing

that PDA cell lines display differential proliferative responses to acute treatment, long-term treatment responses were also monitored in order to evaluate if the responses are maintained over time (Fig 2.1C). CAPAN2 cells being the most sensitive to the acute treatment, also exhibited significant suppression of proliferation with long-term treatment. In contrast, cell proliferation occurred in PL45, ASPC1 and PL5, albeit at a reduced extent relative to control. These results indicate that there is differential proliferative response to CDK4/6 inhibition within CDKN2A deficient PDA cell models, and suggests that there are additional determinants of therapeutic sensitivity. A possible explanation of these results is that in resistant models the phosphorylation of RB is CDK4/6 independent. In analysis of RB phosphorylation by mobility shift and with phospho-specific antibodies, CDK4/6 inhibition did suppress the phosphorylation of RB across all models interrogated (Fig 2.1D). These results were confirmed by reverse phase protein array (RPPA) analysis, wherein RB dephosphorylation was the only consistently observed change amongst 53 phosphoproteins analyzed (not shown). Thus, from conventional assessment of the RB-pathway, CDK4/6 inhibitors should be actionable.

A.

NAME	CDKN2A
MIA PaCa-2	HD
PANC-1	HD
ASPC-1	FRAME SHIFT
HS 766T	HD
BXPC-3	HD
CAPAN-2	INSERTION
PL45	HD
PL 5	HD

B.

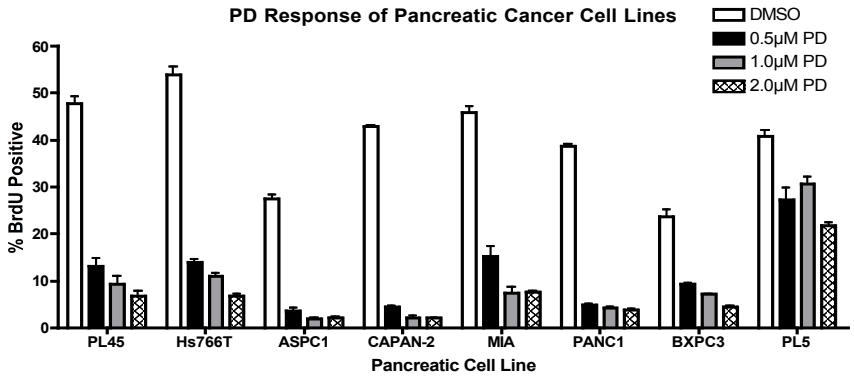

C.

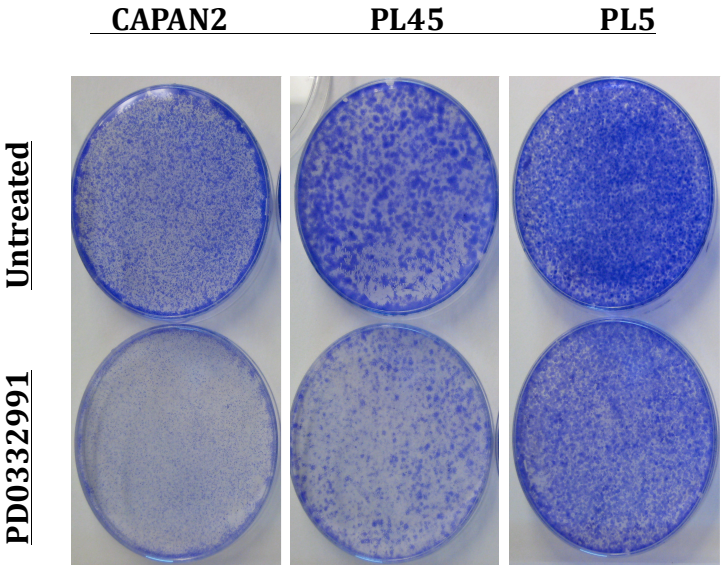

D.

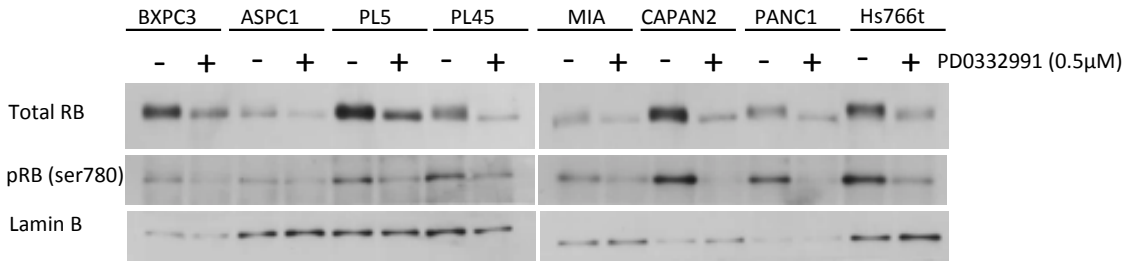

Figure 2.1 : PDA cell lines display differential responses to CDK4/6 inhibition. (A) Eight PDA cell lines were employed with documented deleterious mutations in the CDKN2A tumor suppressor. (B) Cells were treated with indicated concentrations of PD-0332991 (0.5, 1, and 2 μM) for 24 hours. Cell cycle progression was quantified by BrdU incorporation as determined by flow cytometry. Data shown is from three independent experiments. (C) CDK4/6 effects on total RB and phospho-serine 780 were evaluated by immunoblotting. (D) Long-term responses to PD-0332991 in select PDA cell lines were assessed using crystal violet staining after 10 days of treatment with drug replenishment every three days.

2.4: PDA models exhibit distinct suppression of E2F gene expression with CDK4/6 inhibition:

To interrogate the downstream signaling from CDK4/6 inhibition, we analyzed the expression of RB/E2F target genes using a high-density RBTARGET Affymetrix array (probes listed in supplemental tables). Using a 2-fold cutoff and $p<0.05$ we found that there were many RB/E2F targets genes that were repressed potently with CDK4/6 inhibition (Fig. 2.2A). Specifically, a large number of genes were repressed in CAPAN2 cells that exhibit a durable response to CDK4/6 inhibition. In contrast, the PL45 and PL5 cell lines exhibited modest suppression of such genes (Fig. 2.2B). Interestingly, by gene ontology analyses these groups of genes segregated along biological processes (Fig. 2.2C). There was potent suppression of mitotic genes across cell models with CDK4/6 inhibition; however, the suppression of DNA replication proteins was largely restricted to CAPAN2. Bar-graphs demonstrating the repression of representative genes are shown (Fig. 2.2D). One of the key determinants of mitotic gene expression is FOXM1 [106]. FOXM1 is both a transcriptional target of RB/E2F, and a direct target for protein stability by CDK4/6 [105]. By gene expression profiling FOXM1 repression was largely restricted to CAPAN2 cells; however, by RPPA analysis FOXM1 protein levels were reduced uniformly (Fig. 2.2E). These data suggest that there is a fundamental difference in the mechanisms underlying the repression of different classes of cell cycle genes, but that suppression of genes involved in DNA replication was particularly associated with durable response to CDK4/6 inhibition.

A.

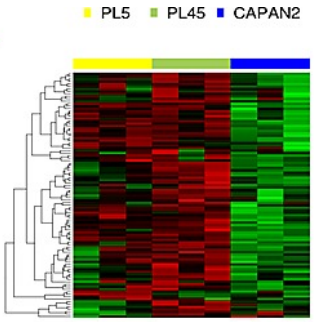

B.

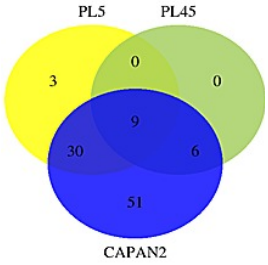

C.

Gene Ontology	Common to multiple cell lines	Repressed
Mitosis	1.99E-45	5.56E-52
M phase of mitotic cell cycle	1.81E-45	1.26E-51
M phase	1.90E-42	4.02E-54
DNA replication	0.0026	1.02E-21
DNA metabolic process	0.0259	9.53E-18

D.

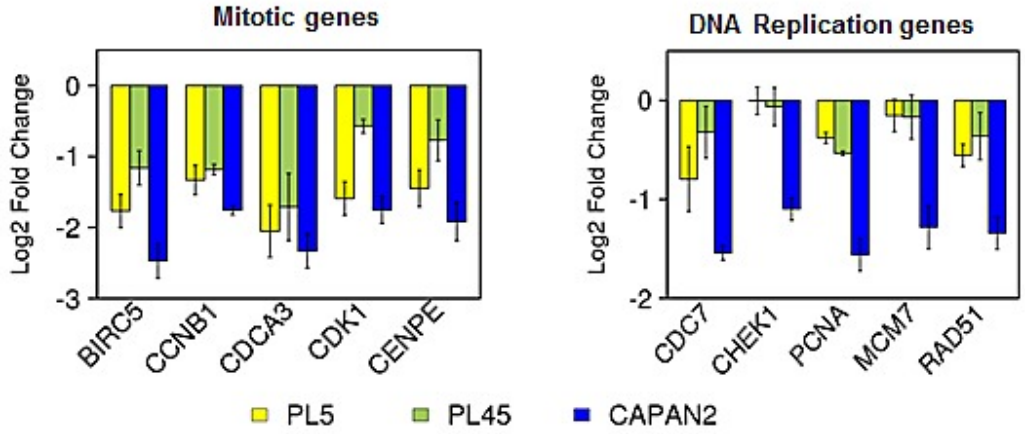

E.

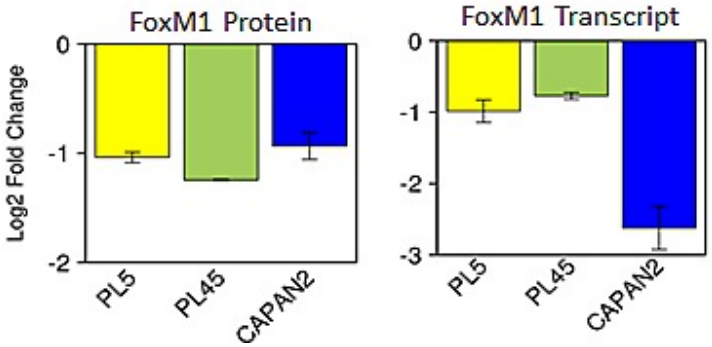

Figure 2.2: Gene expression profiling of RB/E2F target genes reveals differential transcriptional repression. (A) Heatmap analysis of transcripts that are potently repressed by PD-0332991 in at least one cell model. (B) Venn diagrams demonstrating the overlap of genes that are repressed by at least two-fold ($p<0.05$) in each cell line. (C) Gene ontology analysis of genes repressed in multiple models vs. those repressed in CAPAN2. (D) Representative gene expression of genes involved in mitotic progression (left) and DNA replication (right)

2.5: Intrinsic aberrant regulation of Cyclin E is a key determinant of resistance to CDK4/6 inhibition:

In an attempt to decipher the mechanism underlying the specific resistance to CDK4/6 inhibition, we interrogated the expression of critical CDK and Cyclins that are important for progression through G1/S. These data demonstrated that certain genes are repressed irrespectively (e.g. Cyclin A2) (Fig. 2.3A). However, there was a consistent upregulation of Cyclin D1 in all models (Fig 2.3A). Additionally in PL45 and PL5 cells that are relatively resistant to CDK4/6 inhibition there was a reproducible upregulation of Cyclin E1 transcript (Fig 2.3A). The induction of Cyclin D1 has been previously described in other models [97, 98]; however, the induction of Cyclin E1 is a unique observation in the setting of PDA. Therefore, the levels of Cyclin E1 were determined by immunoblotting across all cell lines (Fig. 2.3B). These data revealed that cyclin E1 induction was particularly apparent in multiple cell lines including PL5, MIAPACA2, PANC1 and HS766T. To determine the functional relevance of cyclin upregulation in PDA models exposed to PD-0332991, RNAi was used to knockdown Cyclin D1 and Cyclin E1. Individually, both Cyclin D1 and Cyclin E1 knockdown inhibited cell cycle progression as determined by BrdU incorporation (Fig. 2.3C/D). In the case of Cyclin D1 depletion there was an additive effect on cell cycle progression in combination with PD-0332991. In contrast, Cyclin E1 deletion prevented virtually all BrdU incorporation in combination with PD-0332991. These data indicate that Cyclin E1 upregulation contributes to the observed resistance of PDA models to CDK4/6 inhibition, and suggests a unique feature of signaling that compromises the sensitivity to CDK4/6 inhibition in PDA models.

A.

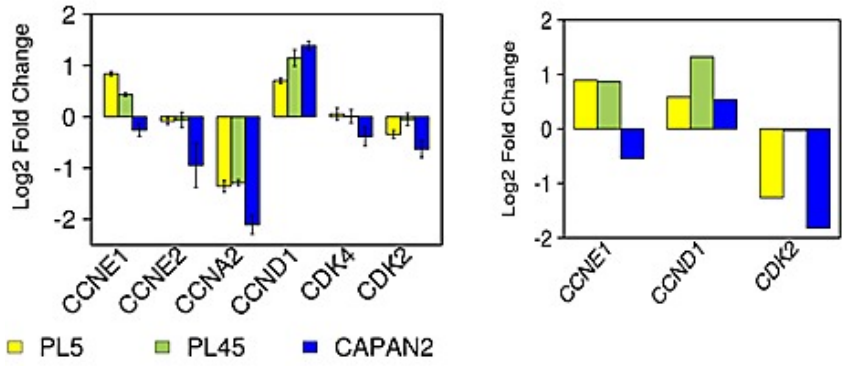
Log2 Fold Change
2
1
0
-1
-2
CCNE1
CCNE2
CCNA2
CCND1
CDK4
CDK2
PL5
PL45
CAPAN2
Log2 Fold Change
CCNE1
CCND1
CDK2

B.

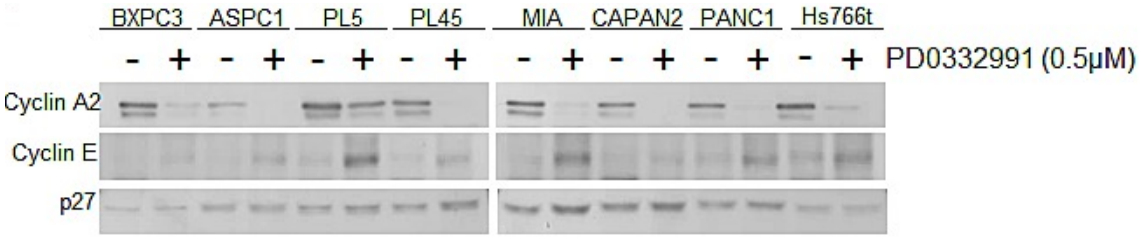
BXPC3
ASPC1
PL5
PL45
MIA
CAPAN2
PANC1
Hs766t
- + - + - + - + - + - + - + - +
PD0332991 (0.5μM)
Cyclin A2
Cyclin E
p27

C.

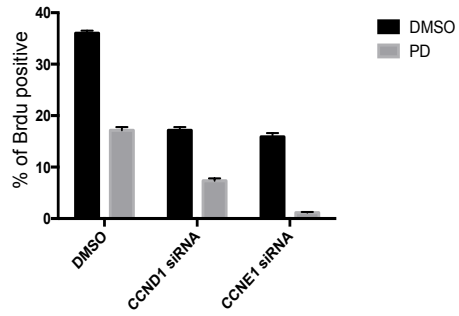
% of Brdu positive
40
30
20
10
0
DMSO
PD
DMSO
CCND1 siRNA
CCNE1 siRNA

D.

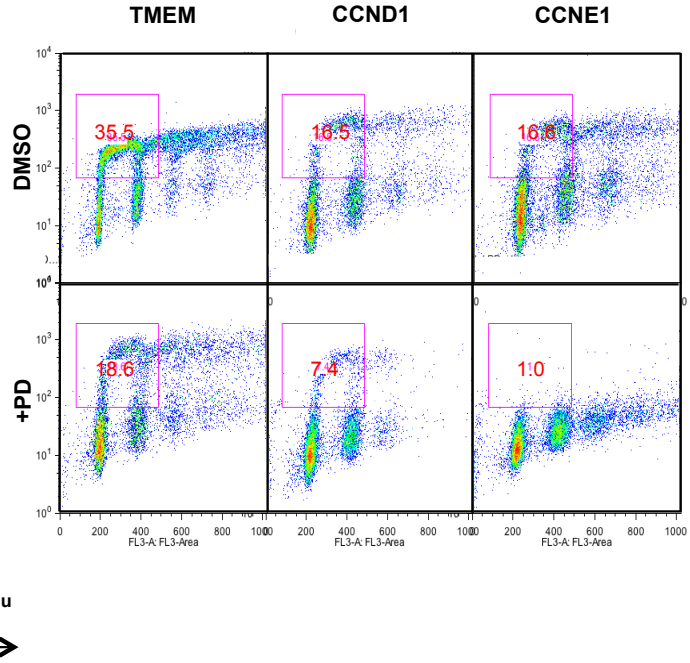
TMEM
CCND1
CCNE1
DMSO
+PD
35.5
16.5
16.6
18.6
7.4
1.0
FL3-A: FL3-Area
Brdu

Figure 2.3: CDK4/6 inhibition induces aberrant expression of CCNE1 and CCND1. (A) Analysis of gene expression related to control over G1/S regulated CDK activity is shown from two different array platforms. (B) CCNE1 expression was evaluated by immunoblotting. (C) Cell cycle progression of PL5 cells was determined following knockdown of CCND1 or CCNE1 by RNAi in the presence or absence of 1μM PD-0332991. (D) Quantification of BrdU incorporation from three independent experiments. Data is expressed as percentage of BrdU positive cells, and a significant difference ($p<0.01$) was observed between CCND1 and CCNE1 knockdown concurrent with PD-0332991 treatment versus knockdown alone in both PL-45 and PL-5.

2.6: CDK4/6 inhibition results in both antagonistic and additive responses with other anti-cancer therapies:

It is widely recognized that combination approaches to therapy will be required for the success of targeted agents in the treatment of pancreatic cancer. Given the modest response to CDK4/6 inhibitors we interrogated the impact of PD-0332991 on 304 anti-cancer compounds (supplemental tables). Drug screening was performed in PL45, PL5 and MIAPACA2 PDA models, which are relatively resistant to PD-0332991. Cells were treated singly with the drug library or with concurrent PD-0332991. Cell survival was determined by CTG analysis and representative data is depicted in the scatter plots (Fig. 2.4A). To globally evaluate the response of select classes of drugs, heatmaps were generated plotting the log fraction of surviving cells to define the relative response (Fig. 2.4B). Antagonistic responses are drug combinations where CDK4/6 inhibitor protected cells from the other agent. We observed robust antagonism of specific chemotherapeutic drugs, PLK1 inhibitors, and other drugs specifically dependent on ongoing cell cycle progression for their mechanism of action (Fig. 2.4C, left panel). In contrast, additive effects were observed for MEK across a relatively broad range of compounds (Fig. 2.4B and 2.C, middle). Similarly PI3K (e.g. GDC0941), MTOR (e.g. AZD0855), and dual PI3K/MTOR (e.g. GDC0980) inhibitors exhibited cooperative inhibition with PD-0332991 (Fig. 2.4B and C, right). In all cases the overall impact of CDK4/6 inhibition was statistically significant across the drug class selected.

A.

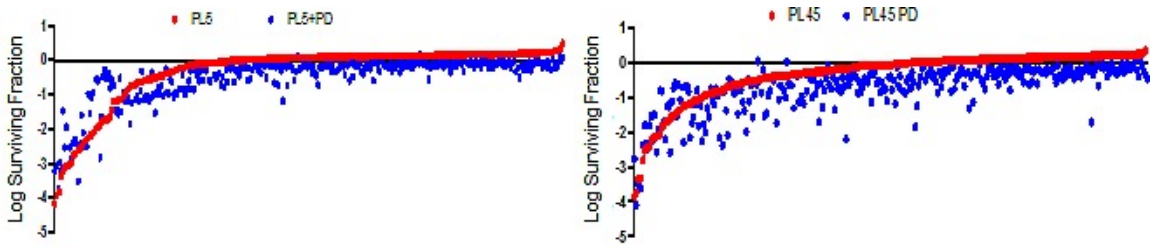
PL5
PL5+PD
Log Surviving Fraction
PL45
PL45 PD
Log Surviving Fraction

B.

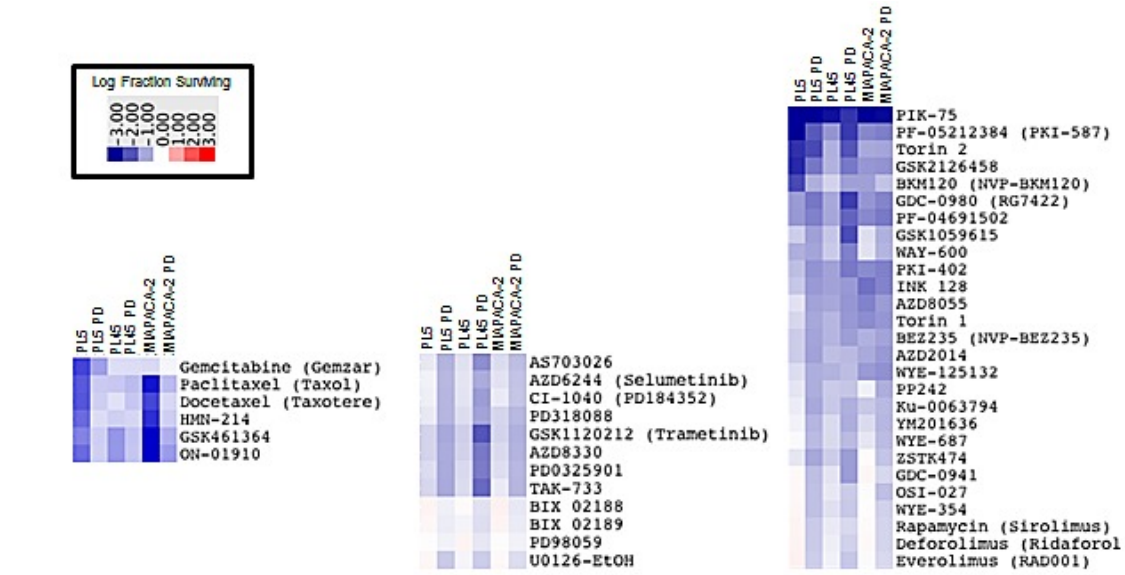
Log Fraction Surviving
-3.00
-2.00
-1.00
0.00
1.00
2.00
3.00
PL5
PL5 PD
PL45
PL45 PD
MIAPACA-2
MIAPACA-2 PD
Gemcitabine (Gemzar)
Paclitaxel (Taxol)
Docetaxel (Taxotere)
HMN-214
GSK461364
ON-01910
AS703026
AZD6244 (Selumetinib)
CI-1040 (PD184352)
PD318088
GSK1120212 (Trametinib)
AZD8330
PD0325901
TAK-733
BIX 02188
BIX 02189
PD98059
U0126-EtOH
PIK-75
PF-05212384 (PKI-587)
Torin 2
GSK2126458
BKM120 (NVP-BKM120)
GDC-0980 (RG7422)
PF-04691502
GSK1059615
WAY-600
PKI-402
INK 128
AZD8055
Torin 1
BEZ235 (NVP-BEZ235)
AZD2014
WYE-125132
PP242
Ku-0063794
YM201636
WYE-687
ZSTK474
GDC-0941
OSI-027
WYE-354
Rapamycin (Sirolimus)
Deforolimus (Ridaforol
Everolimus (RAD001)

C.

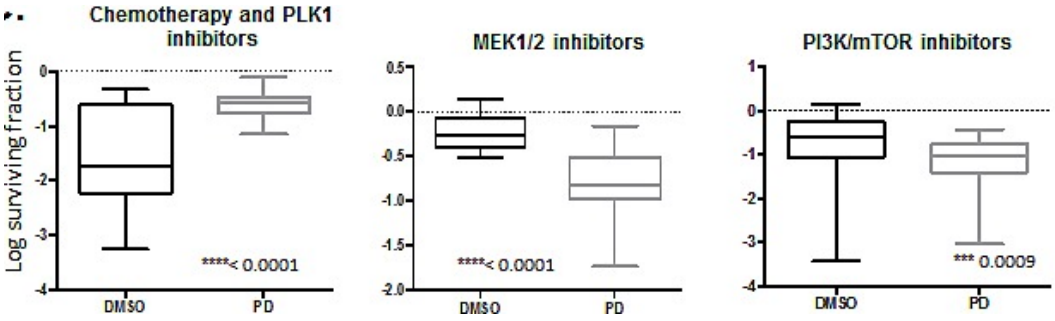
Chemotherapy and PLK1 inhibitors
MEK1/2 inhibitors
PI3K/mTOR inhibitors
Log surviving fraction
****< 0.0001
****< 0.0001
*** 0.0009
DMSO
PD
DMSO
PD
DMSO
PD

Figure 2.4: Drug screen for interaction with CDK4/6 inhibitor. (A) Scatter plots diagrams showing overall drug responses to drug screen by PL5, PL45 and MIAPACA2 in the presence or absence of 1μM PD-0332991. (B) Heatmaps displaying relative response to chemotherapy/Plk1 inhibitors (left), MEK inhibitors (middle) and PI3K/MTOR inhibitors (right) (C) Log surviving fraction chemotherapy/ Plk1 inhibitors (left), MEK inhibitors (middle) and PI3K/MTOR inhibitors (right) for all cell lines. Average, 95% confidence interval and p-value are shown.

2.7: Drug context specific effects of CDK4/6 inhibition on chemotherapies:

The drug screening indicated that CDK4/6 inhibition has the potential to antagonize the effect of various types of chemotherapies. We speculated that the cytostatic effect of CDK4/6 inhibition may represent the principle mechanism leading to a decreased efficacy of drugs targeting the mitotic machinery. As shown, PLK1 inhibitors were antagonized by co-treatment with PD-0332991 (Fig. 2.5A). Since such drugs can have off-target effects, PLK1, which is an essential kinase during mitosis, was depleted (Fig. 2.5A). In absence of CDK4/6 inhibitors, PLK inhibition led to significant reduction in viability, but in the presence of CDK4/6 inhibitor, this effect was significantly diminished. This finding suggested that even the modest cell cycle inhibition observed in PL5 and PL45 models will still impinge on the cytotoxic effects of anti-mitotic agents, such as docetaxel and paclitaxel that are present in the drug screen.

In addition to anti-mitotic drugs, PD-0332991 treatment significantly antagonized Gemcitabine activity in drug screening. Since the anti-metabolites Gemcitabine and 5-FU are both used in the treatment of PDA, we specifically evaluated response to these drugs. Initially, we simply recapitulated the antagonism of Gemcitabine-mediated toxicity (Fig. 2.5B). These short-term effects were re-affirmed in the analysis of overall cell survival by crystal violet analysis (Fig. 2.5C). In this setting, Gemcitabine effectively killed the PDA cells; however, in the presence of PD-0332991 a fraction of cells survived. These findings contrasted with the observation for 5-FU, which although having limited effect, was not antagonized by CDK4/6 inhibition and in some lines there was evidence of cooperative effects (Fig. 2.5C). A likely basis for this differential response relates to the role of E2F target genes deoxycytidine kinase (DCK) and

thymidylate synthase (TS). DCK is required to activate gemcitabine and cells exposed to PD-0332991 have reduced level of this protein (Fig. 2.5D). In contrast TS is the target for 5FU-mediated inhibition and reduced levels of TS are associated with increased drug sensitivity. In the PDA models, treatment with PD-0332991 suppressed TS levels (Fig. 2.5D). Treatment with 5FU leads to a covalent bond with TS, and thus stoichiometric inhibition of TS is ostensibly easier to achieve. Consistent with this hypothesis, we observed additive effects between PD-0332991 and 5FU and the suppression of BrdU incorporation (Fig. 2.5E). Together, these findings indicate that while combination treatments of CDK4/6 inhibitor and chemotherapy can be antagonistic, there are specific conditions where additive responses can be identified based on mechanism of action.

A.

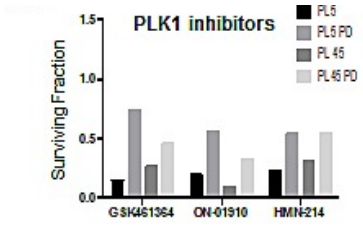
PLK1 inhibitors
PL5
PL5 PD
PL 45
PL45 PD
Surviving Fraction
1.5
1.0
0.5
0.0
GSK461364
ON-01910
HMN-214

B.

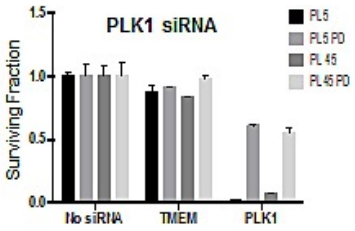
PLK1 siRNA
PL5
PL5 PD
PL 45
PL45 PD
Surviving Fraction
1.5
1.0
0.5
0.0
No siRNA
TMEM
PLK1

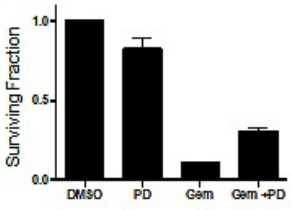
Surviving Fraction
1.0
0.5
0.0
DMSO
PD
Gem
Gem +PD

C.

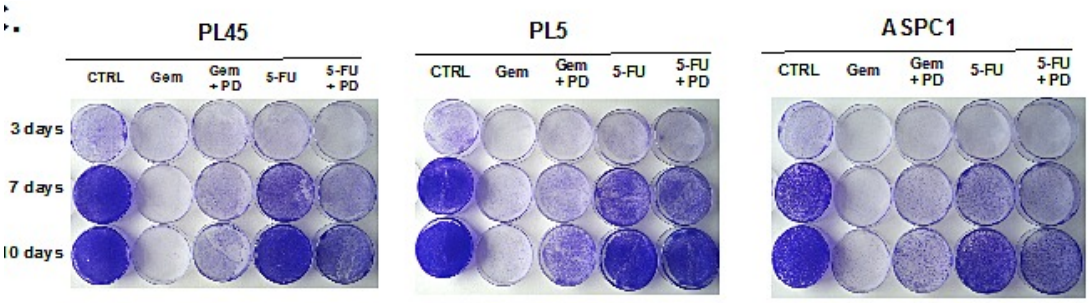
PL45
PL5
ASPC1
CTRL
Gem
Gem + PD
5-FU
5-FU + PD
3 days
7 days
10 days

D.

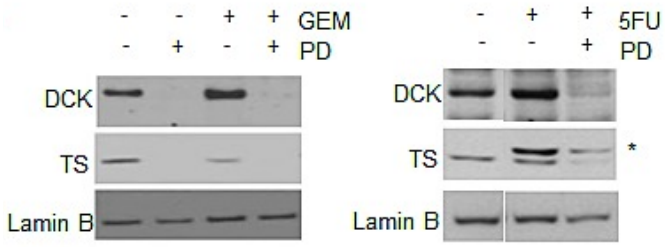
GEM
PD
5FU
PD
DCK
TS
Lamin B
*

E.

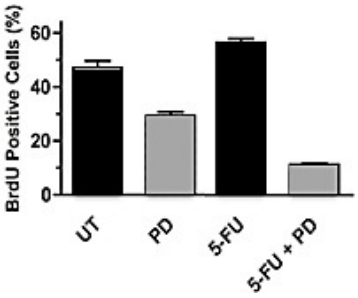
BrdU Positive Cells (%)
60
40
20
0
UT
PD
5-FU
5-FU + PD

Figure 2.5: Drug specific effect of CDK4/6 inhibition on chemotherapy. (A) PL5 cells were either treated with PLK1 inhibitors or transfected with the indicated RNAi in the presence or absence of 1 μM PD-0332991. At 72 hours post-treatment or transfection cell viability was measured by Cell-titer glow. Results are expressed as the surviving fraction, and a significant difference of $p<0.005$ was observed between co-treated with PD-0332991 compared to PLK1 inhibited alone. (B) PL-5 cells were treated with 5 μM gemcitabine as a single agent or in combination with PD-0332991 for 72 hours and viability assessed by Cell titer Glo. Results are expressed as the surviving fraction, and a significant difference of $p<0.005$ was observed between co-treated with gemcitabine and PD-0332991 compared to gemcitabine treatment alone. (C) Long-Term responses to single agent or co-treatments with Gemcitabine (1μM) and 5-FU (25 μM) in the presence or absence of 1 μM PD-0332991 was evaluated in PL-45, PL5 and ASPC1 cells by crystal violet. (D) Effects of CDK4/6 inhibition concurrent with either Gemcitabine or 5-FU on the DCK and TS protein was detected by immunoblotting. **Indicates the mobility of 5FU-TS adduct. (E) PL5 Cells were treated as indicated with PD-0332991 (1μM) or 5-FU (25 μM).

2.8: Concurrent inhibition of CDK4/6 either with PI3K/mTOR or MEK inhibitors display cooperation in suppression of PDA proliferation:

As a whole, PI3K/MTOR inhibitors showed cooperative effects in concert with CDK4/6 inhibitor treatment assessed by viability assay in drug screening. In order to examine the mechanisms, BrdU incorporation was assessed after treatment with BEZ235, GDC0980 and AZD0855 in combination with CDK4/6 inhibitor (Fig 2.6A). Results indicate that CDK4/6 inhibitor in combination with these PI3K/MTOR inhibitors has a synergistic effect in suppression of cell cycle. PL5 cells that exhibit resistance to both the CDK4/6 inhibitor and PI3K/MTOR inhibitors as single agents displayed a complete proliferative halt after treatment in both acute and long-term responses (Fig. 2.6B and C). This suppression of proliferation with co-treatment was associated with suppression of Cyclin D1 and Cyclin E1 expression that is observed with PD-0332991 (Fig. 2.6D). Additionally, there was suppression of additional critical cell cycle regulatory proteins including CDK2 and Cyclin A. In keeping with the suppression of multiple cyclins, although CDK4/6 inhibition has a profound effect on the phosphorylation of RB, there is residual phosphorylation that was further suppressed in the context of co-treatment with PI3K/MTOR inhibitors (Fig. 2.6E). These data suggest that even low levels of RB phosphorylation can facilitate cell cycle progression, and provide the emphasis for full suppression of CDK-activity through complementary mechanisms.

In addition to PI3K/MTOR, MEK inhibitors also had additive effects in concert with CDK4/6 suppression. We demonstrated the cooperation at the level of cell cycle progression by BrdU incorporation and found that similar suppression of proliferation with the combination treatment (Fig. 2.6F). The biochemical effect of MEK inhibitors on

RB phosphorylation paralleled the observation with PI3K/MTOR inhibition and revealing a similar basis for cooperation (Fig. 2.6G). Together, these findings suggest that PI3K/MTOR and MEK inhibitors could be particularly in combination with CDK4/6 inhibitors due to complementary mechanisms of action.

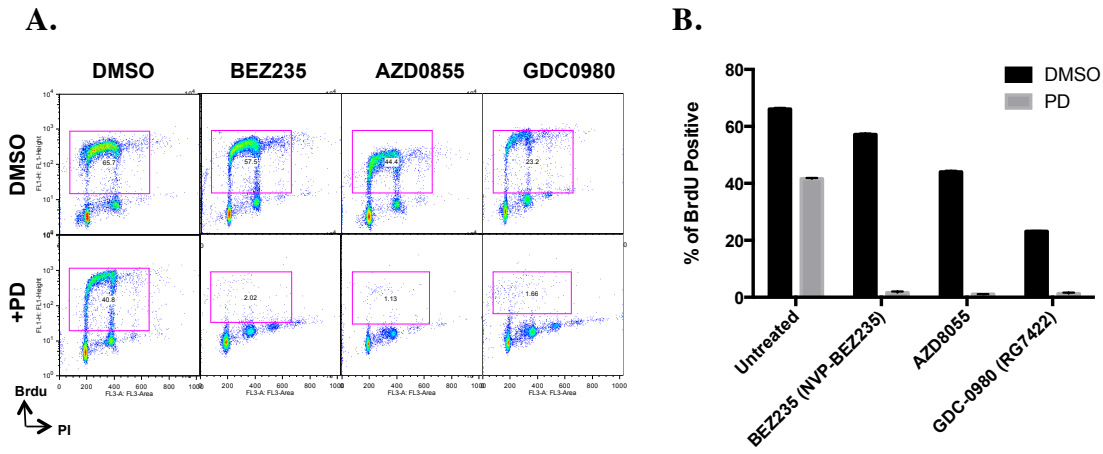
A.
DMSO
BEZ235
AZD0855
GDC0980
DMSO
+PD
Brdu
PI
B.
% of BrdU Positive
DMSO
PD
Untreated
BEZ235 (NVP-BEZ235)
AZD8055
GDC-0980 (RG7422)

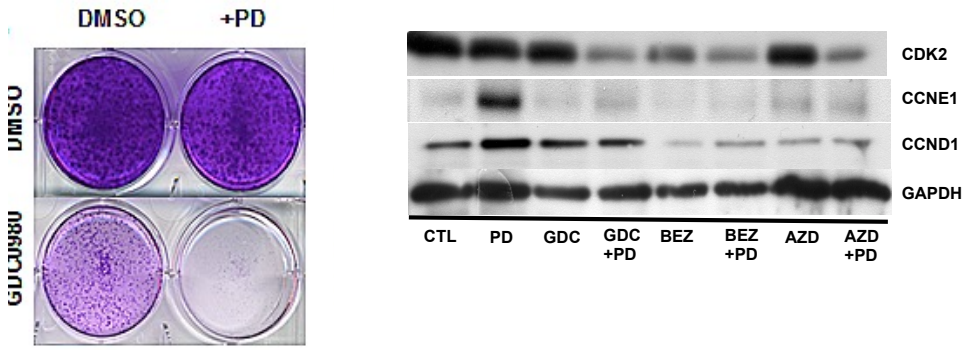
C.
DMSO
+PD
D.
CDK2
CCNE1
CCND1
GAPDH
CTL
PD
GDC
GDC +PD
BEZ
BEZ +PD
AZD
AZD +PD

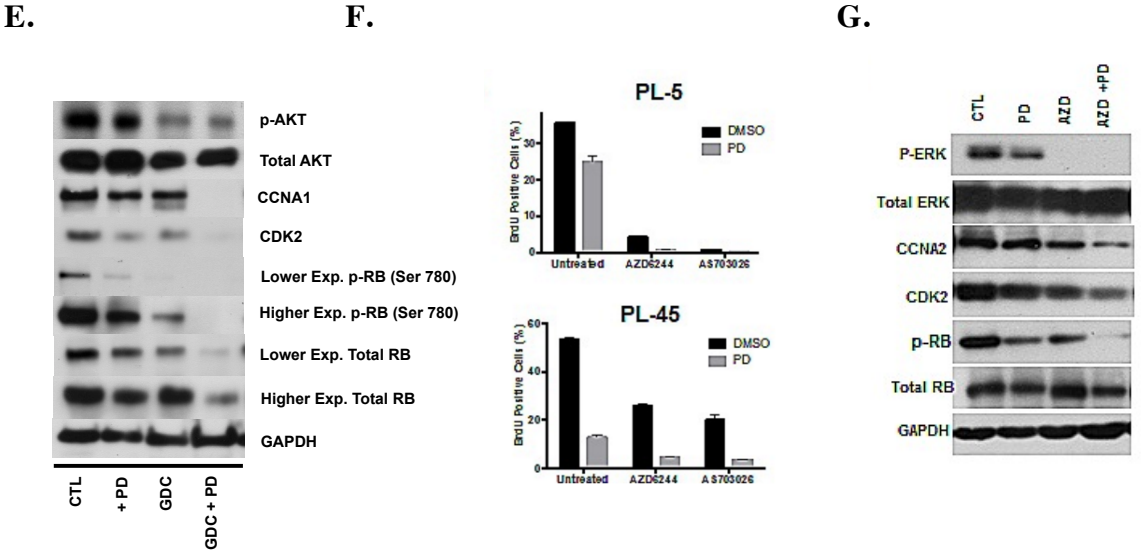
E.
p-AKT
Total AKT
CCNA1
CDK2
Lower Exp. p-RB (Ser 780)
Higher Exp. p-RB (Ser 780)
Lower Exp. Total RB
Higher Exp. Total RB
GAPDH
CTL
+ PD
GDC
GDC + PD
F.
PL-5
PL-45
DMSO
PD
BrdU Positive Cells (%)
Untreated
AZD6244
AS703026
G.
CTL
PD
AZD
AZD +PD
P-ERK
Total ERK
CCNA2
CDK2
p-RB
Total RB
GAPDH

Figure 2.6: PI3K/MTOR and MEK inhibitors synergize with CDK4/6 inhibition. (A) PDA model PL5 was treated with 1μM PI3K/MTOR inhibitors (BEZ235, AZD0855 and GDC0980) as a single agent or co-treated with 1μM PD-0332991. Cell cycle progression was determined by flow cytometry. (B) Quantification of BrdU incorporation from three independent experiments. Results are expressed as percentage of BrdU positive cells, and a significant difference of $p<0.001$ was observed between co-treated versus PI3K inhibitor treatment alone. (C) Treatment with GDC0980 as a single agent and in combination with PD-0332991 was evaluated by crystal violet. (C) Effect of treatment with the PI3K/MTOR inhibitors alone and in the presence of PD-0332991 on the expression of the indicated proteins was determined by immunoblotting. (D) Effect of treatment with the PI3K/MTOR inhibitors alone and in the presence of PD-0332991 on the expression of the indicated proteins was determined by immunoblotting. (E) Quantification of the proliferative effects by CDK4/6 inhibitor concurrent with MEK1/2 inhibitor treatment assessed by Brdu incorporation. Results are expressed as percentage of BrdU Proliferating cells, and a significant difference of $p<0.001$ was observed between co-treated and MEK1/2 inhibitor treatment alone.

2.9: Discussion:

The treatment of pancreatic cancer is a particular challenge and new therapeutic approaches are urgently needed. One appealing means of intervention is to target specific genetic features of disease, and CDKN2A loss is one of the most common genetic alterations in PDA. Ostensibly, the loss of the kinase inhibitor results in aberrant CDK4/6 activation that could be targeted through the use of CDK4/6 inhibitors. Here we challenged this simple precept in preclinical models.

Interestingly, and contrary to multiple other tumor models, PDA models exhibited disparate responses to CDK4/6 inhibition that were not dependent on the canonical RB-pathways. In breast cancer, HCC, glioma, melanoma and other models, the response to CDK4/6 inhibition is simply dependent on the presence of RB [96, 98, 115]. Such tumors generally have lost CDKN2A, which provided the rationale for the study herein. Interestingly, within PDA there was a diversity of response to CDK4/6 suppression. Particularly, there were multiple models which exhibited features associated with partial cell cycle inhibition, or relatively complete resistance. These findings are consistent with the work of others [116]. While it would be expected that there would be a full bypass of the requirement for CDK4/6 this was not observed, as RB phosphorylation remained largely dependent on CDK4/6. Additionally, there was significant suppression of a subset of E2F target genes. Interestingly, these genes are largely involved in mitosis, and are controlled by the DREAM and FOXM1 complexes that are ostensibly still effectively repressed in this setting [106]. In fact, we observed similar FOXM1 protein attenuation in all models studied, which is consistent with work demonstrating that FOXM1 protein accumulation is dependent on CDK4/6 activity [105]. However,

the control of genes involved in DNA replication has emerged as a key RB-dependent function that is associated with terminal cell cycle arrest [117]. Therefore, the data here suggest that in select tumors models there is an uncoupling of these aspects of cell cycle control. In breast cancer and additional models PD-0332991 results in robust suppression of the full spectrum of E2F target gents and therefore indicates that pancreatic cancer is somewhat unique in this aspect of cell cycle regulatory uncoupling.

The realization that such uncoupling can occur necessitated a highly focused analysis of CDK genes/proteins that drive the G1/S transition. Our group and others have shown that CDK4/6 inhibitors can lead to the accumulation of Cyclin D1 levels [97, 98]. The basis of this response remains under study, but it could reflect more potent mitogenic signaling in the G1-phase of the cell cycle to stimulate the Cyclin D1 promoter. Importantly, we have observed this response in multiple models that exhibit a profound durable response to CDK4/6 inhibition; therefore, Cyclin D1 upregulation does not appear to be associated with resistance to PD-0332991. Surprisingly, our work revealed that resistant models exhibited an aberrant upregulation of Cyclin E. To the best of our knowledge, this is the first time such a response to CDK4/6 inhibition has been observed. In general, CDK4/6 inhibition will reduce the level of Cyclin E transcripts; therefore, the upregulation in resistant models was particularly unexpected. Importantly, we could show that the "levels" of these cyclins contributes to the response and suggests that induction of such proteins will modulate the durable response to CDK4/6 inhibition in a general setting, although Cyclin E-depletion was particularly synergistic with PD-0332991. These results agree with the overall concept that Cyclin E deregulation can contribute to bypass of CDK4/6 inhibitors [118].

In recognition that many PDA models did not harbor a particularly durable response to CDK4/6 inhibition, combination treatments were interrogated. This work revealed that CDK4/6 inhibition has complex interactions on the response to multiple agents. In particular, and consistent with others [119], CDK4/6 inhibition compromised the cytotoxicities of chemotherapies that primarily act via mitotic catastrophe including PLK1 inhibitors and taxanes. This result suggests for this class of drugs it is critical to develop a rational metronomic schedule for drug treatment. In contrast, anti-metabolites are more difficult to predict as RB/E2F regulate a host of genes that are drug targets or otherwise modify dNTP pools [120]. This aspect of RB/E2F function is particularly important when evaluating anti-metabolites that would cooperate or be antagonized by CDK4/6 inhibition. It should be noted that in addition to the enzyme interrogated herein RB/E2F modulates DHFR and RNRII levels that have highly significant effect on dNTP pools.

In contrast with chemotherapy, we observed highly reproducible additive effects across a relatively large panel of MEK and PI3K/MTOR inhibitors with CDK4/6 inhibition. These findings are particularly important since MEK and PI3K/MTOR inhibitors have been considered for the treatment of pancreatic cancer [121]. As shown here CDK4/6 inhibition can have relatively subtle effects on cell cycle and suppression of proliferation. In contrast, drug combinations yielded potent cytostatic response in all models tested. In the case of PI3K/MTOR the induction of Cyclin D1 and Cyclin E that occurs with CDK4/6 inhibition was completely blocked resulting in profound de-phosphorylation of RB. These finding are consistent with the work of others showing that cyclin D1 levels are under the control of MEK or MTOR signaling [122, 123].

Presumably, these data suggest that one of the "weaknesses" of pharmacological CDK4/6 inhibitors is compensatory or alternative regulators of RB phosphorylation. In the case of MEK and PI3K/MTOR, there are well described mechanisms through which they limit the expression of Cyclins and suppress CDK activity. Ostensibly in many therapeutic contexts, these mechanisms of attenuating CDK-activity are NOT sufficient to halt cell cycle; however, due to the complementary mechanism of action such agents are particularly effective in concert with CDK4/6 inhibitors. Likely, a similar mechanism could underlie the profound clinical activity of CDK4/6 inhibitors with endocrine therapy; since in ER-positive breast cancer estrogen signaling is required for the expression of cyclin D1 and E [124, 125]. Together, the work herein provides a roadmap for considering the clinical utilization of CDK4/6 inhibitors in the treatment of PDA.

2.10:Material and Methods:

2.10.1: Cell culture, chemicals and antibodies

Human pancreatic cancer cell lines PL45, MIAPACA-2, PANC1, CAPAN2, BXPC3, HS 766T, ASPC1, PL5 were purchased from the American Type Culture Collection (ATCC). All cells except for MIAPACA2 were cultured in DMEM supplemented with 10% fetal bovine serum and antibiotics. MIAPACA2 cells were grown in DMEM with fetal bovine serum and horse serum to a final concentration of 10% and 2.5% respectively plus antibiotics. Drugs used in this study were purchased from Selleck Chemicals. Compounds were diluted in DMSO to 5 mM stock concentrations. PD- 0332991 was employed at a concentration range of 0.5-2 μM. Drugs screen was performed at 2.5 μM. Antibodies against CDK2, CCNE1, CCNA2, GAPDH, total ERK, p-ERK, lamin B, DCK, TS and p27 were purchased from Santa Cruz biotechnology. While, antibodies against total RB, p-RB(780), total Akt, p-Akt (ser473) were purchased from Cell signaling. Cyclin D1 (AB3) was from NeoMarkers.

2.10.2: Drug Screen

A library of 304 drugs from Selleck Chemicals was used for drug screening. Cells were grown in 96- well plates at 2500 cell per well. Subsequent to plating, cell were treated with 1μM PD-0332991 or DMSO for 24 hours at 37° and 5.0 CO2. The next day, cells were treated with the drug library to final concentration of 2.5 uM, and incubated at 37° and 5.0 CO2 for 72 hours. Following treatment, viability was assessed using Celltiter Glo(Promega). The relative fluorescence units were detected and analyzed by a BIOTEK plate reader and Gen5 software. Data analysis was performed using Drug-decode macro

(developed by David Haan, UT Southwestern).

2.10.3: Flow cytometry

Cell were trypsinized and fixed in 70% Ethanol post a 2 hour incubation with Brdu labeling solution(Invitrogen). Fixed cells were incubated in 2M HCl with 0.3mg/ml pepsin solution for 30 minutes followed by addition of 0.1 M sodium tetraborate solution(pH 8.5). After acid neutralization, cells were washed twice with IFA(10mM HEPES(pH 7.4), 25 mM NACI, 4% FBS) buffer. Cells were then incubated with FITC labeled anti-Brdu(BD Pharmingen) at 1:10 dilution for 30 min at room temperature. After Brdu labeling, Propidium iodine(20ug/ml) and RNAse(4ug/ml) was added and incubated for 15 minutes in Dark. BrdU incorporation was assessed using a Facscalibur Instrument and data was analyzed using FlowJo .

2.10.4: Western blot analysis and reverse phase protein array analysis

Pancreatic cell lines were lysed in RIPA buffer (10% NP-40 substitute, 1% SDS, 500mM Tris-HCI(pH 7.4), 1.5M NaCI, 5% sodium doxycholate, 10mM EDTA) containing both complete protease inhibitor cocktail tablets (Roche) and phosphatases inhibitors (Roche). Protein concentrations were subsequently measured with the BCA protein assay DCtm Protein Assay(BIO- RAD) using manufacture's protocol. These samples were separated on SDS polyacrylamide gels and electroblotted on to Immobilon-P Transfer Membrane. Membranes were washed with wash buffer (0.1% Tween- 20/1x saline). Followed by incubation with blocking solution (5% BSA, 0.1% Tween-20; saline), followed by incubation with rabbit primary antibodies (1/500 dilution) at 4°C overnight. The membranes were then washed in Wash buffer and incubated with horseradish peroxidase

conjugated secondary antibodies (Jackson ImmunoResearch) for one hour at room temperature. Antibody detection was performed with an enhanced chemiluminescence reaction (SuperSignal) as directed by manufacture.

Protein lysates were prepared from cell treated with vehicle or 1 μM PD-0332991 for 48 hours. Preparation of the lysates were as directed by the MD Anderson RPPA shared service, and the analysis of the signals were performed using their highly standardized procedures. The difference in normalized log protein values are presented in the analysis.

2.10.5: Short-term and long-term treatments of in vitro models

For short term treatments, pancreatic cell lines were seeded at 5x104 cell/well in 6 well plate and left to adhere for 3 hours at 37 °C. Cells were then treated with individual drug or drug combinations at 1uM concentrations and incubated for 24-72 hours. For long-term experiment, cell were seeded at 5x103 cell/ well and drugs were replenished every 3 days for 10 days. Following long term studies, they were assessed by cystal violet.

2.10.6: Transfection of siRNA

Pancreatic cell lines were seeded in a 6-well plate at a desity of 5x105 cells per well and transfected with siRNA against either CCND1 (Santa Cruz biotechnology), CCNE1 (SMARTpool: Accell CCNE1 siRNA; Dharmacon) and PLK1(SMARTpool: Accell PLK1 siRNA; Dharmacon) at a final concentration 50nmol/L with Lipofectamine RNAiMAX(Invitrogen) according to manufacture's instructions. Transfections with a control sRNA(TMEM) served as a negative control.

CHAPTER III: Metabolic re-programming of pancreatic cancer mediated by CDK4/6 inhibition elicits unique vulnerabilities.

3.1: Abstract:

Due to loss of p16ink4a in pancreatic ductal adenocarcinoma (PDA), pharmacological suppression of CDK4/6 could represent a potent target for treatment. In PDA models CDK4/6 inhibition had variable effect on cell cycle, but yielded accumulation of ATP and mitochondria. Pharmacological CDK4/6 inhibitors induce cyclin D1 protein levels; however, RB activation was required and sufficient for mitochondrial accumulation. CDK4/6 inhibition stimulated glycolytic and oxidative metabolism and was associated with an increase in mTORC1 activity. MTOR and MEK inhibitors potently cooperate with CDK4/6 inhibition in eliciting cell cycle exit. However, MTOR inhibition fully suppressed metabolism and yielded apoptosis and suppression of tumor growth. The metabolic state mediated by CDK4/6 inhibition increases mitochondrial number and ROS. Concordantly, the suppression of ROS scavenging or BCL2-antagonists cooperated with CDK4/6 inhibition. Together, these data define the impact of therapeutics on PDA metabolism and provide strategies for converting cytostatic response to tumor cell killing.

3.2: Introduction: Pancreatic ductal adenocarcinoma (PDA) has a five year survival of only ~6%[126, 127]. This dire prognosis is due to multiple clinical features of the disease, including diagnosis at late stage and ineffective systemic therapies [68]. Therefore, there is significant energy directed at delineating biological features of PDA that could be exploited for therapeutic intervention.

One of the hallmark genetic events in PDA is loss of the CDKN2A/2B tumor suppressor locus[128]. This locus encodes endogenous CDK4/6 inhibitors that are particularly relevant in the context of KRAS driven tumors, such as PDA[75, 129]. Oncogenic KRAS can induce a senescent-like growth arrest state in cells[77, 80]. The execution of this phenotype is mediated by p16ink4a encoded by CDKN2A that blocks the activity of CDK4/Cyclin D and CDK6/Cyclin D complexes[75, 80]. This leads to the suppression of RB phosphorylation and concomitant inhibition of cell cycle progression through the suppression of E2F-mediated transcription[117]. Highly selective drugs that phenocopy features of p16ink4a function would be expected to have potency in PDA[44]. While such drugs have some degree of effect in established PDA cell lines[116, 130-132], resistance can develop quickly, thereby necessitating the use of combination therapeutic approaches.

Although the underlying mechanisms remain unclear, cell division is coordinated with metabolic functions. First observed in yeast, cell cycle entry is associated with increased cellular mass and the accumulation of energetic metabolites required for cell division[133]. In PDA, much of the metabolic circuitry is subservient to mutant KRAS, which drives a complex reprogramming of glycolytic, oxidative and non-canonical (e.g. macropinocytosis) metabolic pathways in concert with tumorigenic proliferation[62, 134]. Key downstream effectors include MEK and MTOR signaling pathways that engage multiple distal features of metabolism through transcriptional and translational regulatory programs[61, 135-137]. The interface of cell cycle regulatory factors with metabolism is similarly complex and varied [138]. For example, Cyclin D1, which is a requisite activator of CDK4/6, has been shown to act in a transcriptional role to

coordinate metabolism/mitochondrial function [139]. Additionally, at a cellular and organismal level CDK4/6 activity plays important roles in controlling gluconeogenesis and responsiveness to insulin [138]. RB has been shown to bind to mitochondria and regulate apoptotic functions[140], while E2F has been shown to drive mitochondrial-dependent apoptosis in Drosophila[141, 142]. Interestingly, in fibroblastic models RB loss is associated with increased glutamine utilization [143, 144], and loss of RBF has been associated with altered glutamine catabolism in drosophila [145]. Recent studies have shown that loss of RB can lead to decreased oxidative phosphorylation and more dependency on glycolytic metabolism [146, 147]. Consonantly, E2F1 and RB in tissue can provide a critical node of regulation between proliferation and metabolic activity [138, 148]. Since metabolic features of cancer are progressively emerging as a target for therapeutic intervention, these findings supported a direct interrogation of how pharmaceutical CDK4/6 inhibitors impinge on tumor metabolism and the ability to selectively target that metabolic state.

3.3: CDK4/6 inhibition yields increased mitochondrial mass via RB*:*

In order to address the role of CDK4/6 inhibition in PDA, three cell models were utilized. These models contain classic features of PDA [130], but exhibit differing cell cycle inhibition with pharmacological suppression of CDK4/6 activity (Figure S1). While many therapeutic agents that target KRAS signaling suppress metabolism, we observed that CDK4/6 inhibition with PD-0332991, resulted in increased cellular complexity, which is an indirect surrogate of increased organelles and metabolic functions within the cytoplasm (Figure 1A). Concordantly, CDK4/6 inhibition was accompanied by an increase in ATP levels (Figure 1B) and an increase in mitochondrial

mass in multiple cell lines (Figure 1C, 1D and Figure S1). Since these effects could represent a specific feature of PD-0332991 as opposed to CDK4/6 inhibition, two other specific CDK4/6 inhibitors (LEE-11 and LY2853219) were employed, and exhibited similar increased mitotracker staining (Figure S1). Transmission electron microscopy confirmed the numerical increase in mitochondria in cells treated with CDK4/6 inhibitors (Figure 1E).

CDK4/6 inhibitors are known to inhibit cell cycle [44] but also exert two biochemical effects that are potentially germane to tumor metabolism. Notably, CDK4/6 inhibitors will lead to the accumulation of Cyclin D1 that has the capacity to impact cell biology through non-catalytic functions[149], and CDK4/6 inhibition results in the suppression of RB phosphorylation [45, 98] (Figure S1). Using RNA-i mediated knockdown (Figure S1), Cyclin D1 depletion had little effect on mitochondrial accumulation (Figure 1F). In contrast, the knockdown of RB1 partially reverted the accumulation of mitochondria (Figure 1F) and decreased cellular complexity (Figure S1). Additionally, we defined rare cases of PDA that exhibit endogenous RB loss[150]. Using a cell line derived from such a case (EMC7310) we observed that the increase in mitochondrial mass was dependent on RB (Figure S1). Furthermore, employing constitutively active RB allele refractory to phosphorylation (PSM.7-LP)[151], indicated RB activity was sufficient to induce the accumulation of mitochondria in a manner comparable to PD-0332991 (Figure 1G). It has recently been shown that RB can associate with mitochondria [140]. However, in the presence of the CDK4/6 inhibitor RB was solely nuclear as determined by immunofluorescence microscopy (Figure S1). In parallel with these established cell lines, PD-0332991 treatment of a low passage

patient-derived PDA cell line elicited a similar increase in mitotracker (Figure 1H). To determine whether these effects were observed *in vivo*, the matched xenograft model derived from the same patient was treated with PD-0332991 for 8 days. This treatment elicited potent suppression of Ki67, consistent with the established role for CDK4/6; and as observed in cell lines, there was an increase in mitochondria (Figure 1I).

A.

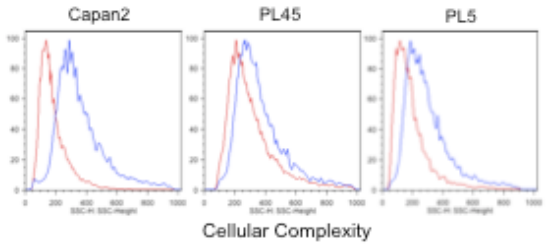
Capan2
PL45
PL5
Cellular Complexity

B.

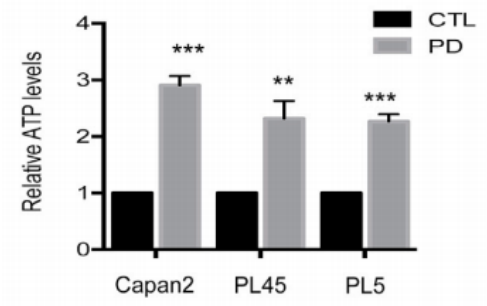
CTL
PD
Relative ATP levels
0
1
2
3
4
***
**
***
Capan2
PL45
PL5

C.

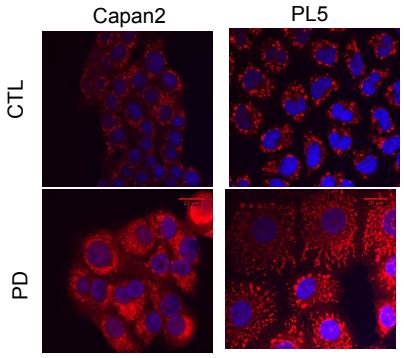
Capan2
PL5
CTL
PD

D.

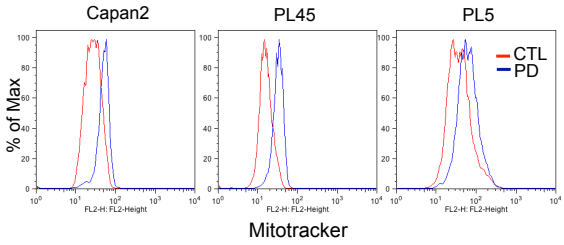
Capan2
PL45
PL5
CTL
PD
% of Max
Mitotracker

E.

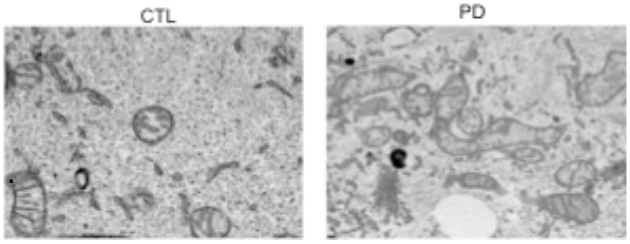
CTL
PD

F.

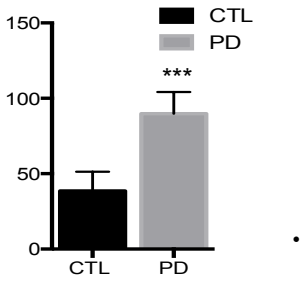
CTL
PD
150
100
50
0
***
CTL
PD

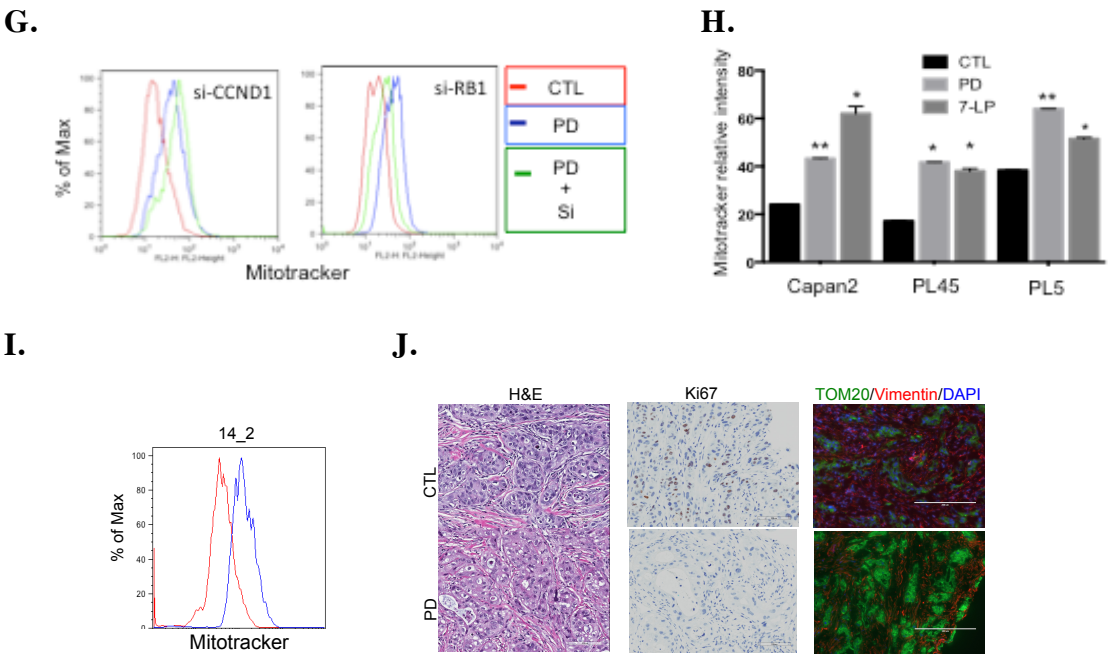

Figure 3.1: CDK4/6 inhibition leads to mitochondria accumulation in an RB-dependent fashion.

(A) Representative flow cytometry histogram displaying cellular complexity on the x-axis for cells treated with PD-0332991 for 120 hours. (B) Relative ATP levels from cells treated with control or PD-0332991 for 120 hours. The average and standard deviation are shown, statistical comparison to vehicle control was determined by t-test (**p<0.01, ***p<0.001). (C) Confocal fluorescence imaging of mitochondria (62.5x) in the indicated cells treated with PD-0332991 for 120 hours (scale bar 20 μm). (D) Flow cytometry histograms showing comparison of mitotracker red fluorescence of the control vs. PD-0332991 treated. (E) Representative transmission electron microscope micrograph of PL5 cells control and treated with PD-0332991 (scale bar 1 μm). Quantification of mitochondria from counting high-power fields, the average and standard deviation are shown. Statistical comparison to vehicle control was determined by t-test (***p<0.001).

(F) Flow cytometry histograms showing comparison of mitotracker red fluorescence of the control vs. PD-0332991 treated following CCND1 or RB knockdown. (G) Quantitation of mitotracker red intensity treatment with PD-0332991 or transduction of the constitutively active RB allele 7-LP. The average and standard deviation are shown. Statistical comparison to vehicle control was determined by t-test (*$p<0.05$, **$p<0.01$). (H) Flow cytometry histograms showing comparison of mitotracker red fluorescence of the control vs. PD-0332991 treated in the EMC43 cell model. (I) Hematoxylin and eosin staining, immunohistochemistry for(Ki67) (scale bar 100 μm), and fluorescence (scale bar 200 μm) imaging (TOM20/Vimentin/DAPI) of patient-derived xenograft EMC43. See also figure S1.

3.4: Reprogramming of metabolism with CDK4/6 inhibition:

To determine the effect of increased mitochondria number on metabolism, oxygen consumption was evaluated as a measure of increased oxidative phosphorylation. As shown in Figure 2A, there was a substantial increase in oxidative phosphorylation with CDK4/6 inhibition. Analysis of metabolite levels in culture media indicated that PD-0332991 treatment resulted in a significant increase in glucose and glutamine consumption. Correspondingly, there was enhanced glutamate secretion as a product of glutamine metabolism, and increased lactate efflux as a measure of the end product of glycolysis (Figure 2B). Consistent with the increase in lactate production, there was a significant increase in media acidification (Figure 2C). These features were recapitulated with LEE-011 and LY2853219, indicating that increased metabolism is a general feature of CDK4/6 inhibition (Figure S2). Metabolomic analysis was performed in conjunction with universally labeled 13C-glucose and 13C-glutamine to monitor

metabolic flux. These analyses showed increase in glycolytic intermediates (ie. glucose 6-phosphate, fructose 1,6-bisphosphate, pyruvate, and lactate) that were predominantly derived from glucose as expected (Figure 2E). For TCA metabolites (ie. malate, fumarate, succinate, and alpha-ketoglutarate), there were also significant increases in metabolite levels (Figure 2F). Flux analysis indicated that these metabolites were principally derived from glutamine; therefore, the majority of mitochondrial-derived metabolism is fueled by glutamine in these models (Figure 2G). Starving cells of either glutamine or glucose significantly reduced viability (Figure 2H-I). However, pre-treatment with CDK4/6 inhibitors protected selectively against the effect of acute glucose withdrawal, suggesting that enhanced glutamine metabolism was sufficient to rescue the reliance on glucose. Similarly, CDK4/6 inhibition limited the acute toxicity of mitochondrial inhibitors phenformin and rotenone (Figure S2). These findings underscore the possibility that the metabolic status of CDK4/6-treated cells could impact on tumor biology and therapeutic sensitivities.

A.

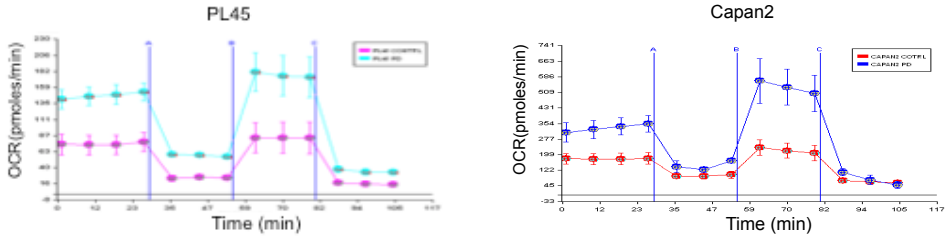
PL45
OCR(pmoles/min)
Time (min)
Capan2
OCR(pmoles/min)
Time (min)

B.

C.

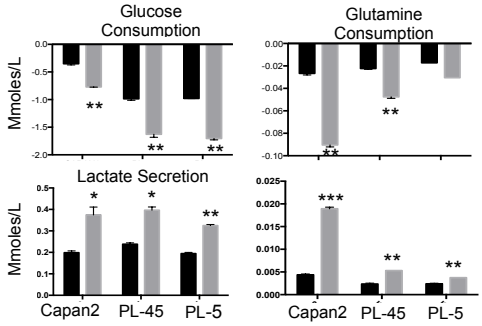
Glucose Consumption
Glutamine Consumption
Mmoles/L
Lactate Secretion
Capan2
PL-45
PL-5

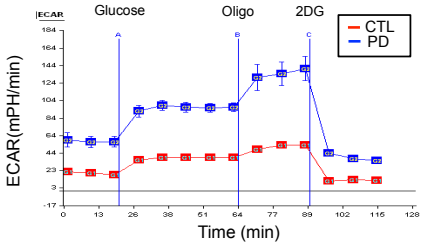
ECAR
Glucose
Oligo
2DG
CTL
PD
ECAR(mPH/min)
Time (min)

D.

E.

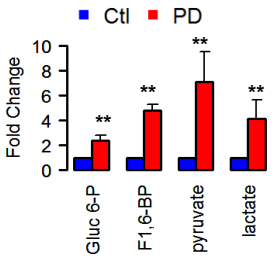
Ctl
PD
Fold Change
Gluc 6-P
F1,6-BP
pyruvate
lactate

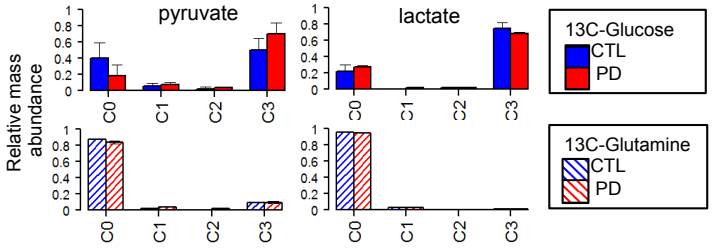
pyruvate
lactate
Relative mass abundance
C0
C1
C2
C3
13C-Glucose
CTL
PD
13C-Glutamine
CTL
PD

F.

G.

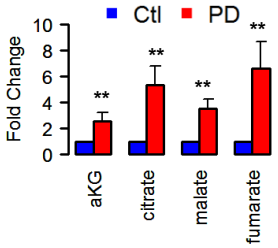
Ctl
PD
Fold Change
aKG
citrate
malate
fumarate

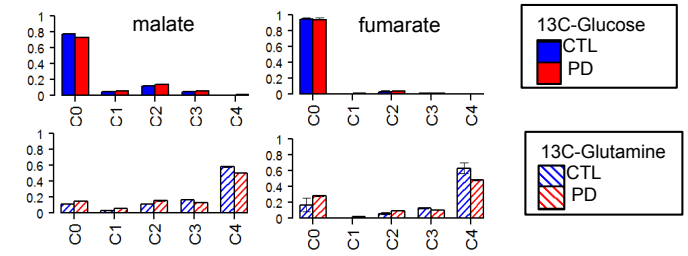
malate
fumarate
C0
C1
C2
C3
C4
13C-Glucose
CTL
PD
13C-Glutamine
CTL
PD

H.

I.

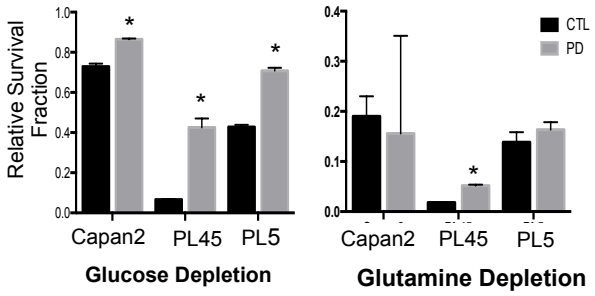
Relative Survival Fraction
Capan2
PL45
PL5
Glucose Depletion
CTL
PD
Capan2
PL45
PL5
Glutamine Depletion

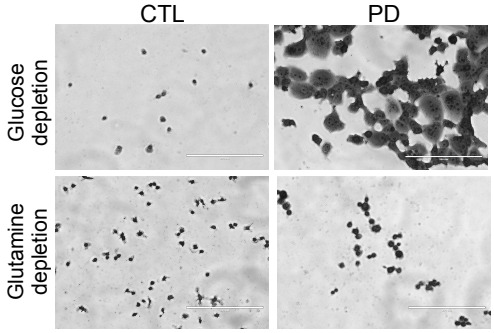
CTL
PD
Glucose depletion
Glutamine depletion

Figure 3.2: CDK4/6 inhibition leads to metabolic reprogramming.

(A) Oxygen Consumption Rate (OCR) of PL45 and Capan2 cell lines either control or treated with PD-0332991. (B) Quantification of media glucose and glutamine uptake, and glutamate and lactate production from the indicated cell lines with or without PD-0332991 treatment. The average and standard deviation are shown. Statistical comparison to vehicle control was determined by t-test (*p<0.05, **p<0.01,***p<0.001). (C) Extracellular acidification rate (ECAR) in cells treated with or without PD-0332991 treatment. (D) Relative fold change of glycolytic intermediates Glucose 6P, Fructose 1,6BP, pyruvate and lactate as determined by mass-spectrometry. The average and standard deviation are shown. Statistical comparison to vehicle control was determined by t-test. (E) Flux analysis of cell populations treated with universally labeled 13C-glucose (solid bars) or universally labeled 13C-glutamine (stippled bars). Bars show the relative average abundance and standard deviation of differing mass species. (F) Relative fold change of TCA intermediates alphaketoglutare, citrate, malate and fumarate. The average and standard deviation are shown. Statistical comparison to vehicle control was determined by t-test (**p<0.01). (G) Flux analysis of cell populations treated with universally labeled 13C-glucose (solid bars) or universally labeled 13C-glutamine (stippled bars). Bars show the relative average abundance and standard deviation of differing mass species. (H) Quantification of cell viability following acute glucose or glutamine withdrawal. The average and standard deviation are shown. Statistical comparison to vehicle control was determined by t-test (*p<0.05). (I) Representative images of crystal violet stained cells following either glutamine or glucose withdrawal (scale bar is 200 μm). See also figure S2.

3.5 CDK4/6 inhibition drives MTOR pathway activation:

Given the significance of signaling pathways in regulating metabolism, we assessed how CDK4/6 inhibition influences the levels of 217 protein and phospho-proteins by reverse phase protein array (RPPA) analysis [152] (Figure 3A). Interestingly, there were very few significant changes in protein abundance mediated by CDK4/6 inhibition. In terms of down-regulated proteins, phosphorylated RB and E2F targets (e.g. Cyclin B1) were downregulated as expected (Figure 3A). In contrast, the phosphorylation of ribosomal protein S6 at Ser235/236 was uniquely observed to be significantly increased with CDK4/6 inhibition (Figure 3A). Immunoblotting confirmed the increased phosphorylation of S6, an MTOR complex 1 (TORC1) substrate, and also increased phosphorylation of RSK at Ser 389 (Figure 3B). In contrast, there was no increase in either ERK or AKT phosphorylation (Figure 3B). To determine if this signaling feature of CDK4/6 inhibition is observed *in vivo*, tumor sections from xenografts treated with PD-0332991 were stained for Ki67 and phosphorylated S6, and showed the expected reduction in Ki67 and a significant increase in S6 phosphorylation (Figure 3C). Similar results were observed in PDX models (Figure S3). Together, these data indicate that MTOR signaling is activated with the inhibition of CDK4/6. Parallel analysis of transcriptional pathways was performed on cells treated with PD-0332991 for five days. This treatment resulted in the down-regulation of multiple genes involved in cell cycle control, consistent with the expected suppression of RB phosphorylation (Figure 3D and S3). However, a large number of genes were significantly up-regulated (Figure 3D), and gene set enrichment analysis identified the induction of genes associated with glycolysis, lysosome, pyruvate metabolism, fatty acid metabolism, and PPAR

signaling (Figure 3D and S3). Importantly, many of these processes are activated downstream of MTOR [136] suggesting this signaling pathway is associated with CDK4/6-inhibition mediated metabolic effects.

Canonically, the activation state of MTOR is regulated by PI3K/AKT/TSC pathway, amino acid availability, lysosomes, and the appropriate milieu of regulatory proteins [137]. In the analysis of gene expression data and RPPA, there was no evidence for the activation of PI3K/AKT or the abundance of TORC1 or TORC2 subunits or regulatory proteins (not shown). However, there was a rapid (24 hr) increase in lysosomes that preceded the increase in mitochondria (Figure S3). Immunofluorescence analysis demonstrated that the majority of MTOR in PDA models is associated with lysosomal structures, and treatment with CDK4/6 inhibitors increased lysosome-associated MTOR (Figure S3). These data suggest that TORC1 complex activation is occurring. Additionally, there was an accumulation of amino acids as determined by mass-spectrometry (Figure S3). Consistent with the supposition that amino acids play an important role downstream from RB, depletion of amino acids blocked the induction of MTOR activity with CDK4/6 inhibition (Figure S3). Together, these data suggest that CDK4/6 inhibition triggers an energetic feed-forward loop that engages MTOR signaling for metabolic reprogramming.

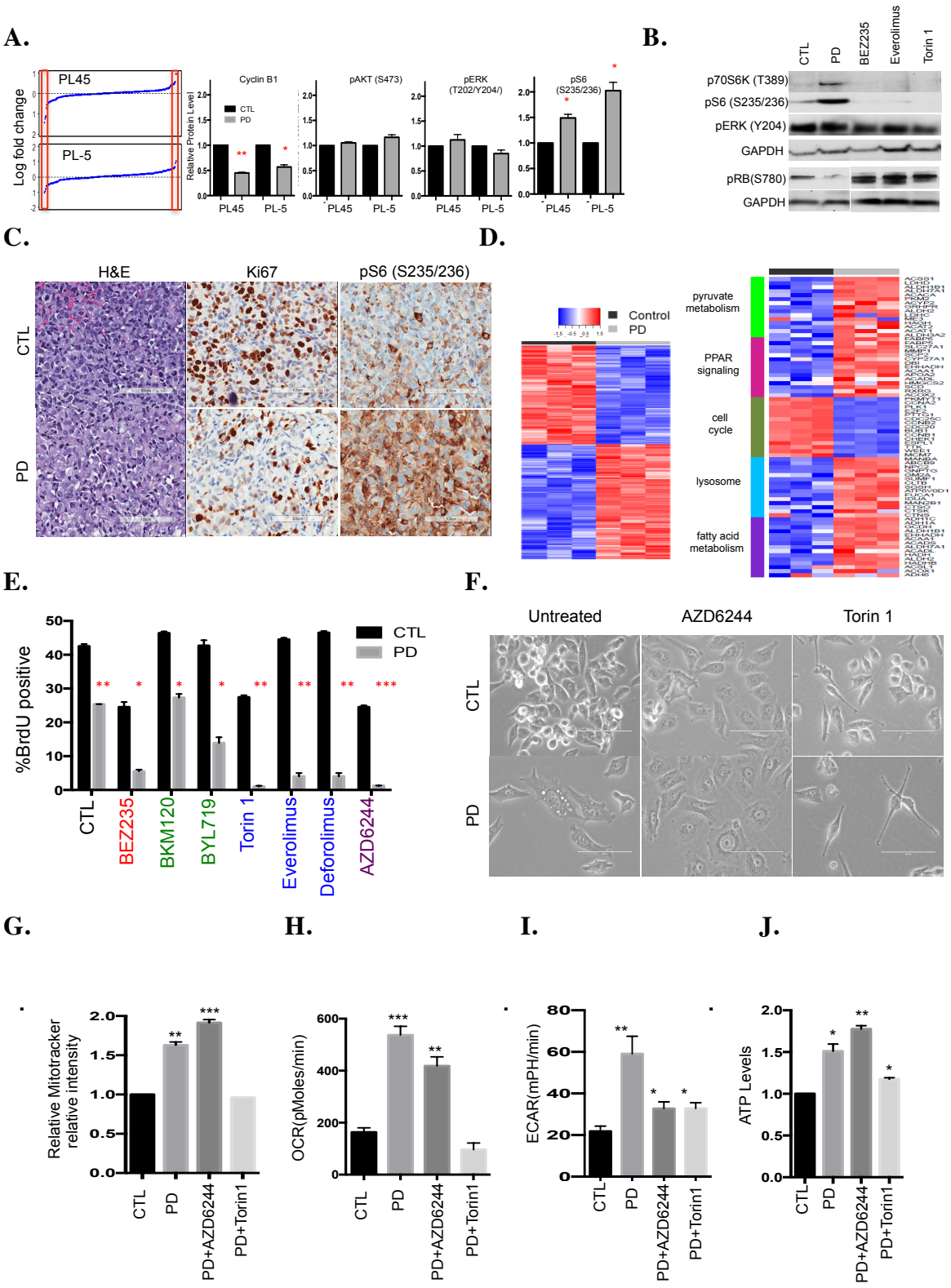
A.
PL45
PL-5
Log fold change
Cyclin B1
pAKT (S473)
pERK (T202/Y204/)
pS6 (S235/236)
Relative Protein Level
CTL
PD
PL45
PL-5
B.
CTL
PD
BEZ235
Everolimus
Torin 1
p70S6K (T389)
pS6 (S235/236)
pERK (Y204)
GAPDH
pRB(S780)
GAPDH
C.
H&E
Ki67
pS6 (S235/236)
CTL
PD
D.
Control
PD
pyruvate metabolism
PPAR signaling
cell cycle
lysosome
fatty acid metabolism
E.
%BrdU positive
CTL
PD
CTL
BEZ235
BKM120
BYL719
Torin 1
Everolimus
Deforolimus
AZD6244
F.
Untreated
AZD6244
Torin 1
CTL
PD
G.
Relative Mitotracker relative intensity
CTL
PD
PD+AZD6244
PD+Torin1
H.
OCR(pMoles/min)
CTL
PD
PD+AZD6244
PD+Torin1
I.
ECAR(mPH/min)
CTL
PD
PD+AZD6244
PD+Torin1
J.
ATP Levels
CTL
PD
PD+AZD6244
PD+Torin1

Figure 3.3: CDK4/6 inhibition leads to the induction of MTOR activity and downstream effects on metabolism.

(A) Quantification of reverse phase protein array (RPPA) data. The log-fold change of proteins abundance with PD-0332991 treatment is displayed as a function of the 217 protein species detected on the array. RPPA data for selected proteins and phosphoproteins is shown, with the average abundance and standard deviation. Statistical comparison to vehicle control was determined by t-test (*p<0.05, **p<0.01). (B) Immunoblotting was performed for the indicated proteins in cells treated with the indicated pathway selective inhibitors. (C) Immunohistochemical analysis of xenograft tumors treated with lactate control or PD-0332991 for 8 days. Representative images of Ki67 and pS6 (S235/236) are shown (scale bar is 100 μm). (D) Gene expression profiling was performed on Capan 2 cells treated with control or PD-0332991 for 120 hours. Heatmap shows genes passing a 1.5-fold p<0.05 cutoff. Representative genes falling into selected gene set enrichment categories are shown in the heatmap. (E) Quantification of BrdU positive cells following 24 hour treatment with dual PI3K/MTOR (BEZ235), PI3K (BKM120, BYL719), mTOR (Torin, Everolimus and Deforolimus) and MEK (AZD-6244) inhibitors alone and in combination with PD-0332991 treatment. Average BrdU incorporation and standard deviations are shown. Statistical comparison to single agent treatment was determined by t-test (*p<0.05, **p<0.01,***p<0.001). (F) Bright filed images of PD-0332991, AZD-6244 and Torin 1 and combination treated cells (scale bar is 100 μm). (G-J) Quantification of mitochondria, OCAR, ECAR, and ATP levels from cells treated with the indicated drugs and

combinations. Average signals and standard deviations are shown. Statistical comparison to control was determined by t-test (*p<0.05, **p<0.01, ***p<0.001). See also figure S3.

3.6: MTOR and MEK inhibitors exhibit distinct endpoints with CDK4/6 inhibition:

To determine the functional interaction between CDK4/6 inhibition and signaling pathways, a panel of agents that inhibit PI3K, MTOR, and MEK was employed. Consistent with prior work[130], we observed potent cooperation between MTOR and MEK inhibitors with CDK4/6 inhibitors; however, there was little influence of PI3K selective inhibitors (Figure 3E). Interestingly, there were significant differences in the morphology of cells treated with MEK vs. MTOR inhibitors (Figure 3F). Since both MTOR and MEK inhibitors cooperated to invoke similar levels of cell cycle inhibition, the associated influence on metabolism was evaluated. MEK inhibition further augmented the impact of CDK4/6 inhibition on oxidative metabolism including increased mitochondrial mass, cellular complexity and enhanced OCAR (Figure 3G and 3H and S3). However, MEK inhibition selectively inhibited glycolysis (Figure 3I). In contrast, combined CDK4/6 and MTOR inhibition resulted in the suppression of both glycolytic and oxidative functions, as was most evident in terms of the mitochondrial accumulation that was completely suppressed (Figure 3G-I and S3). These combined findings suggest a pathway through which the selective activation of RB in the presence of oncogenic signals enables the further accumulation of MTOR signaling and resultant stimulation of metabolism, while MEK is predominantly required for the maintenance of glycolytic metabolism.

3.7: Combination treatments with CDK4/6 inhibitors result in durable therapeutic response:

The distal effects of the combination of CDK4/6 inhibition with MTOR or MEK inhibition were evaluated. MEK in combination with CDK4/6 inhibition enforced a profound effect on cell cycle inhibition (Figure S4), and a potent cytostatic effect with evidence of induced senescence (SA-ß-Gal) (Figure 4A). In contrast, MTOR inhibition suppressed senescence, but resulted in the induction of cell death (Figure 4B). This apoptotic cell death could not be reversed by supplementation with methyl-pyruvate or alpha-ketoglutarate which directly support mitochondrial metabolism (Figure S4). The endpoints of combination treatment yielded suppression of tumor cell proliferation over >2 weeks in culture (Figure 4C). Importantly, in PL5 xenograft models while both PD-0332991 and the PI3K/MTOR inhibitor BEZ235 exhibit some single agent activity, the combination was significantly more potent for the suppression of tumor cell growth and proliferative index (Figure 4D, E, and S4). These data were further confirmed through the use of an independent orthotopic model (PL45), where the combined treatment both suppressed tumor growth and reduced metastatic burden in this highly aggressive model (Figure 4E and S4).

3.8: Selectively targeting ROS and mitochondria in the presence of CDK4/6 inhibition:

A high level of oxidative phosphorylation is believed to represent a liability to tumor cells, due to the role of mitochondria in apoptosis and generation of reactive oxygen species (ROS). Indeed, treatment of the PDA models with CDK4/6 inhibitor

resulted in increased total ROS and mitochondria-derived ROS (Figure 4F and S4). However, one of the key transcriptional responses to CDK4/6 inhibition includes the accumulation of genes involved in peroxisome biosynthesis and the expression of ROS scavengers including hemeoxygenase 1 (HO-1) and catalase (CAT) (Figure S4). The knockdown of either HO-1 or CAT elicited a significant reduction in PDA cell growth and cooperated with CDK4/6 inhibition (Figure 4G, 4H, S4). These findings suggest that increased utilization of mitochondria is balanced by antioxidant pathways in the context of CDK4/6 inhibition. Interestingly, not all perturbations of ROS regulatory processes cooperated with CDK4/6 inhibition. Notably, the glutathione inhibitor BSO failed to further increase ROS levels above CDK4/6 inhibition, and similarly did not cooperate with CDK4/6 inhibition (Figure S4).

An alternative means to exploit mitochondria is through mobilization of BH3-containing proteins. It is known that ROS and other stresses, including CDK inhibition, can effectively limit the expression of MCL1 or modify its activity [153, 154]. Cells treated with PD-0332991 exhibited a marked suppression of the high-mobility form of MCL1 (Figure S4). To determine if this was related to increased sensitivity to mitochondrial-mediated apoptosis, the BCL2 inhibitor ABT-737 was employed [155]. Cells that had been pretreated with PD-0332991 and exhibited an accumulation of mitochondria were selectively sensitive to ABT-737 that elicited apoptotic cell death (Figure 4 J-L and S4). Importantly, the pretreatment with CDK4/6 inhibition also elicited long-term suppression of proliferation in combination with ABT-737 (Figure 4L). Together, these data indicate that the mitochondria/metabolic features of CDK4/6 treated cells could be selectively exploited to yield a synthetic approach to cancer treatment.

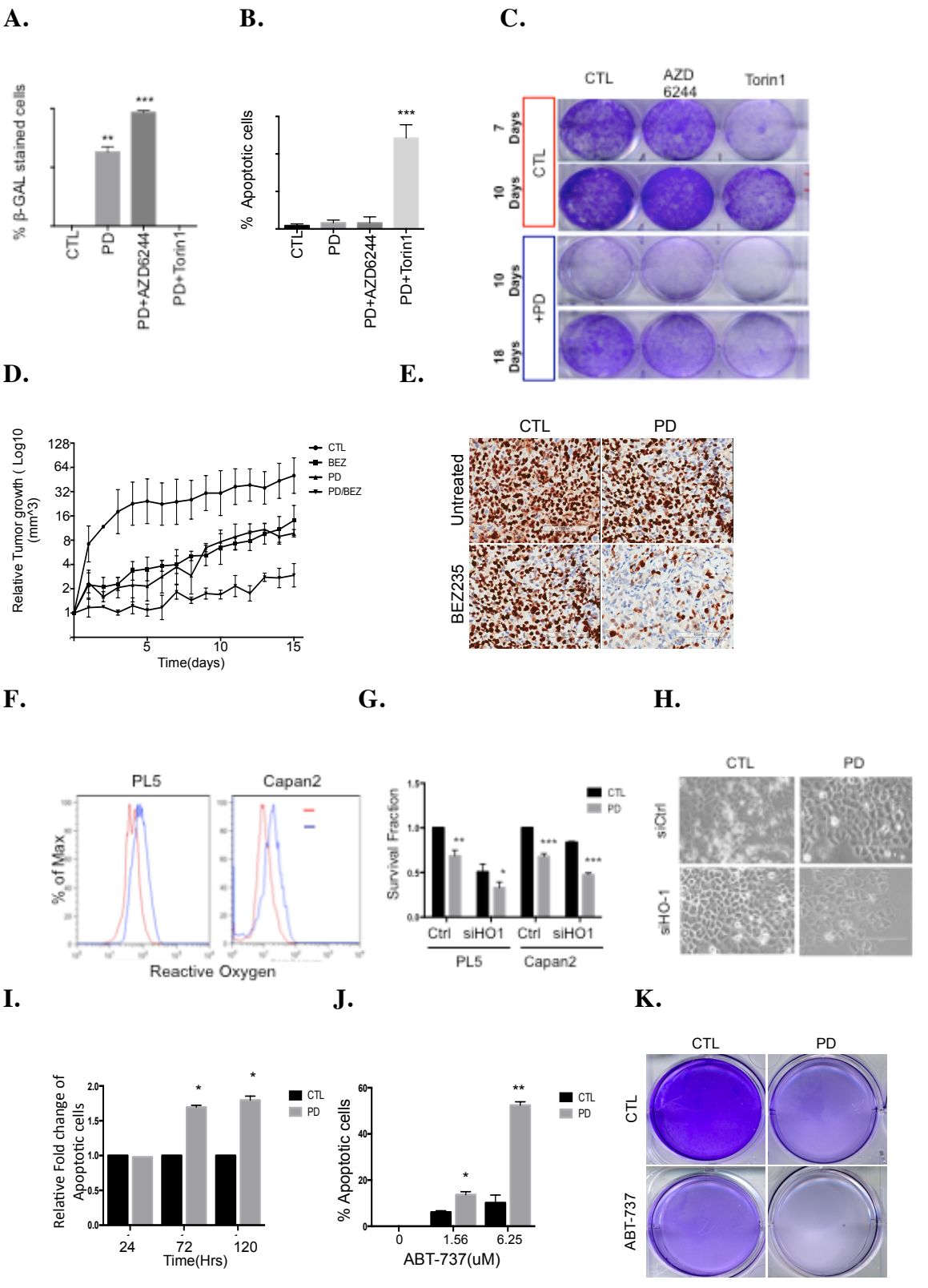
A.
B.
C.
% β-GAL stained cells
CTL
PD
PD+AZD6244
PD+Torin1
% Apoptotic cells
CTL
AZD 6244
Torin1
7 Days
10 Days
10 Days
18 Days
CTL
+PD
D.
E.
Relative Tumor growth (Log10 (mm^3)
Time(days)
CTL
BEZ
PD
PD/BEZ
CTL
PD
Untreated
BEZ235
F.
G.
H.
PL5
Capan2
% of Max
Reactive Oxygen
Survival Fraction
Ctrl
siHO1
PL5
Capan2
CTL
PD
siCtrl
siHO-1
I.
J.
K.
Relative Fold change of Apoptotic cells
Time(Hrs)
% Apoptotic cells
ABT-737(uM)
CTL
PD
ABT-737

Figure 3.4: Selective cooperation with CDK4/6 inhibition for enhancing therapeutic effect.

(A) Quantification of SA-β-gal positive cells following the indicated treatments. Average number of senescent cells and standard deviations are shown. Statistical comparison to control was determined by t-test (**p<0.01, ***p<0.001). (B) Quantification of apoptotic cells following the indicated treatments. Average apoptotic cells and standard deviations are shown. Statistical comparison to control was determined by t-test (***p<0.001). (C) Colony-formation was assessed at the indicated times by crystal violet staining. Representative images are shown (D) Tumor volume of PL5 xenografts following treatment with BEZ235, PD-0332991, and the combination was measured as a function of time The average volume and standard deviation are plotted, the statistical comparison vs. vehicle treated control is shown by t-test (*p<0.05, **p<0.01). (E) Representative Ki-67 immunohistochemistry of the PL5 treated xenografts (scale bar is 100 μm). (F) Tumor volume of orthotopically implanted PL45 cells that were treated with the indicated agents. The average volume and standard deviation are shown, statistical comparison to the vehicle treated control is shown. (G) Representative histograms showing fluorescence of total ROS in the presence vs. absence of PD-0332991. (H) Surviving cells following HO-1 or CAT knockdown in the absence or presence of PD-0332991 was determined. Bars show average surviving fraction relative to control transfected controls. Statistical analyses to the RNAi control was determined by t-test (*p<0.05, **p<0.01, ***p<0.001). (I) Colony outgrowth of knockdown cells alone or in combination with PD-0332991. Representative images shown. (J) Fold change in fraction of apoptotic cells pre-treated with PD-0332991 for the indicated period of time, followed by acute treatment with

ABT-737. The average number of apoptotic cells and standard deviation is shown. Statistical analysis was by t-test to single agent vs. combination with PD-0332991 (*$p<0.05$). (K) Impact of PD-0332991 pretreatment on sensitivity to ABT-737 Average and standard deviations are shown. Statistical comparison to control was determined by t-test (*$p<0.05$, **$p<0.01$) (L) Prolonged treatment with ABT-737 of control or PD-0332991 pretreated and stained for crystal violet. See also figure S4.

3.9: Discussion:

There has been an ever-increasing appreciation of the importance of metabolism in cancer and as a target for therapeutic intervention[134, 156]. In parallel, it is becoming evident that the class of CDK4/6 inhibitors will be utilized in multiple clinical settings either singly or in combination[44, 113].

The impact of CDK4/6 inhibition on tumor metabolism is distinct from other targeted agents that have been evaluated in PDA models. In general, therapeutic agents against the KRAS signaling pathway suppress features of mitogenic signaling and result in attenuation of specific facets of metabolic activity[61, 135, 156, 157]. This can occur either through the attenuation of glycolysis as observed with MEK inhibitors, or a general diminution of metabolic function as reported with MTOR inhibitors. Increased metabolic activity observed in PDA models with CDK4/6 inhibition was surprising, since in different settings CDK4 and Cyclin D1 expression or RB loss enhance metabolic functions associated with proliferation [138, 143, 144]. For example, in *Drosophila* CDK4 is well-established to drive cellular growth by activating metabolic pathways [158]. In spite of these prior studies, recent work has shown that RB loss is selectively associated with a diminution of oxidative phosphorylation, and increased sensitivity to mitochondrial poisons [146]. Therefore, our findings suggest that RB activation by CDK4/6 inhibition essentially drives this process in reverse and activates mitochondrial function. Correspondingly, such treated cells are actually less sensitive to glucose withdrawal and mitochondrial poisons.

The finding that tumors treated with CDK4/6 inhibitors maintain a high metabolic rate has significant clinical implications. Such a state could represent a potential liability

as the treated tumor cells are metabolically charged for cell division, and cessation of the CDK4/6 inhibition could elicit rapid cell cycle progression. In yeast models the accumulation of cell mass and energetics can drive subsequent rounds of proliferation under non-ideal conditions[133]. This could also explain in part why single agent treatment with CDK4/6 inhibitors (ie. PD-0332991) has not proved effective in most solid tumors. Importantly, the metabolic features observed here in preclinical models are consistent with imaging from clinical trials. In the analysis of single agent PD-0332991 in mantle cell lymphoma FLT-PET signal which measures thymidine utilization was suppressed, while the signal for FDG-PET was maintained suggesting the tumors treated in this fashion maintain significant metabolic activity[46].

Mechanistically, CDK4/6 inhibitors are unique as they suppress proliferation downstream from many of the oncogenic signaling pathways that stimulate both metabolism and cellular proliferation[44, 113]. As shown here, the activity of effectors distal to KRAS is maintained following the exposure to CDK4/6 inhibitor. Additionally, we find MTOR signaling is stimulated with suppression of CDK4/6 activity in the PDA cells and tumor models studied. MTOR engages a signaling program downstream from nutrient availability to stimulate metabolism leading to cell cycle progression[136, 137], and therefore is generally antagonistic to the cytostatic effect of CDK4/6 inhibition. We observe the induction of multiple gene expression programs known to be downstream of MTOR including glycolysis, lysosome biogenesis, fatty acid metabolism and PPAR signaling [136]. Presumably this elevated MTOR signaling in concert with a suppression of cell cycle progression is sufficient to enhance the metabolic features observed in the PDA cultures and tumors observed. One of the key questions is how

CDK4/6 impacts MTOR. MTOR activation occurs as a consequence amino acid availability and lysosomal localization[159]. Interestingly, CDK4/6 inhibition yielded a rapid accumulation of lysosomes, and metabolomics analysis showed increased amino acid pools. These data suggest an energetic feed-forward loop, wherein CDK4/6 inhibition yields increased metabolic activity that is further exaggerated by MTOR activation that mediates downstream effects on metabolism/mitochondria. Critically, MTOR inhibition can suppress effects of CDK4/6 inhibitor on metabolism, thus mTOR activity is required for metabolic reprogramming induced by CDK4/6 inhibition. In spite of these findings, the exact signaling through which CDK4/6 and RB controls metabolism remains under study, as does the potential context dependence beyond the PDA models studied here.

In pancreatic cancer and in other solid tumor models, CDK4/6 inhibitors as single agents do not appear to be very effective [44]. Thus defining means to selectively capitalize on the metabolic status imparted by CDK4/6 inhibition is particularly pertinent. Due to the withdrawal from the cell cycle, CDK4/6 inhibitors have an antagonistic function related to select chemotherapies, further underscoring the need for rational combinatorial approaches. In breast cancer models, PI3K inhibitors potently cooperate with CDK4/6 inhibition[160]. However, this combination has a relatively modest effect in PDA models. In contrast, MEK and MTOR inhibition potently cooperates with CDK4/6 inhibition [130, 131]. In spite of similar effects on cell cycle suppression, MEK and MTOR inhibition have distinct effects on metabolism and biology. As has been previously published, MEK activity is particularly relevant for maintaining glycolytic function in PDA models[61]. MEK inhibitors function in concert with CDK4/6 inhibition

to enhance the accumulation of mitochondria and oxidative phosphorylation, eliciting a pronounced cell cycle arrest with features of senescence. In contrast, MTOR inhibitors restricted glycolytic metabolism and oxidative phosphorylation induced by CDK4/6 inhibition and yielded cell death and suppression of tumor growth. While potent cooperation is observed in several cell and xenograft models, a concerted effort across multiple patient-derived models will be required to determine the fraction of tumors that would be expected to be sensitive to such interventions in the clinic.

Targeting metabolism or other conserved features of cell biology represents a challenge in establishing a therapeutic index[161]. In contrast with other agents, the increase in tumor associated mitochondria and ROS could represent a unique target for tumors treated with CDK4/6 inhibitors [162]. Inhibitors of antioxidants are being considered as cancer therapies due to the established increase in ROS production by many tumors[163]. We observed that both depletion of catalase or hemoxygenase-1 cooperated with CDK4/6 inhibition. Similarly the high levels of mitochondria in principle could yield increased sensitivity to mitochondrial driven cell death mediated by agents such as ABT-737. Thus these studies provide potential avenues for considering converting the cytostatic nature of CDK4/6 inhibitors to cytotoxicity.

Given the recent FDA approval of CDK4/6 inhibitors, their use will become progressively common-place. Understanding both canonical cell cycle and metabolic features of treatment exposure will be important for defining preferred combination strategies and capitalizing on tumor biology.

A.

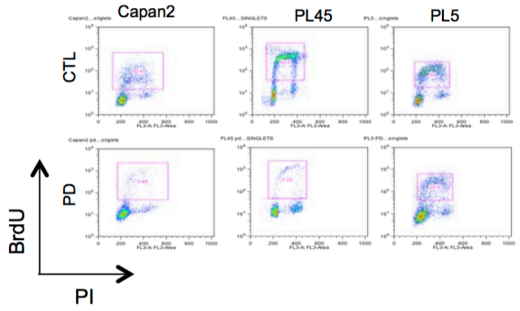
Capan2
PL45
PL5
CTL
PD
BrdU
PI

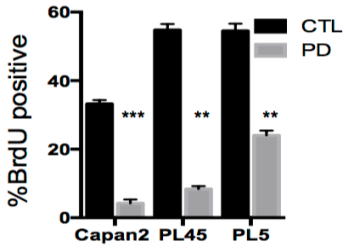
%BrdU positive
CTL
PD
***
**
**
Capan2
PL45
PL5

B.

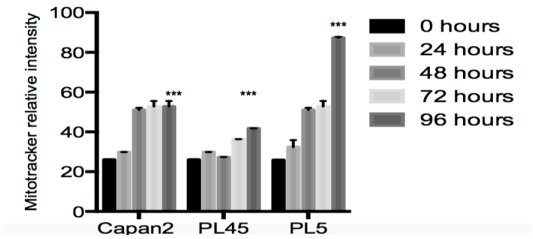
Mitotracker relative intensity
0 hours
24 hours
48 hours
72 hours
96 hours
***
***
***
Capan2
PL45
PL5

C.

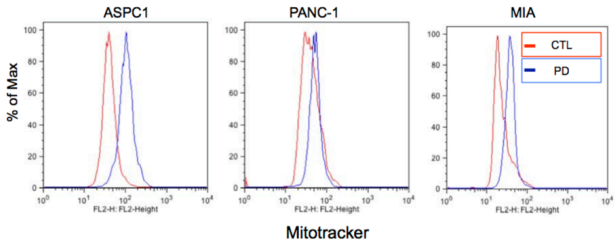
ASPC1
PANC-1
MIA
CTL
PD
% of Max
Mitotracker

D.

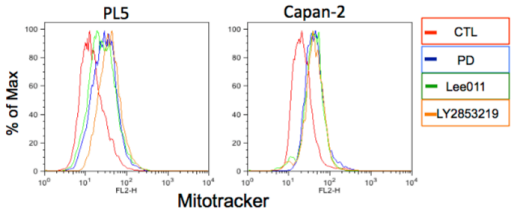
PL5
Capan-2
CTL
PD
Lee011
LY2853219
% of Max
Mitotracker

E.

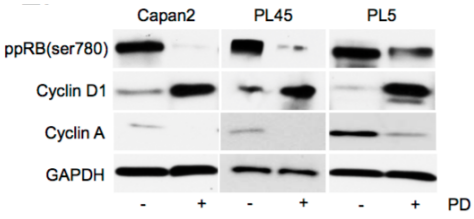
Capan2
PL45
PL5
ppRB(ser780)
Cyclin D1
Cyclin A
GAPDH
- + - + - +
PD

F.

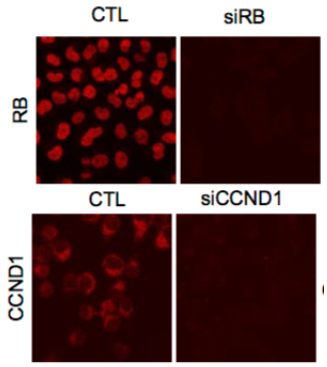
CTL
siRB
RB
CTL
siCCND1
CCND1

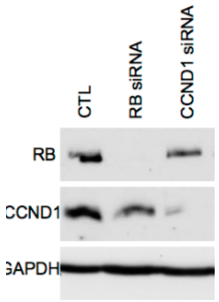
CTL
RB siRNA
CCND1 siRNA
RB
CCND1
GAPDH

G.

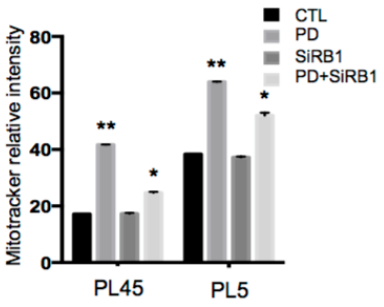
CTL
PD
SiRB1
PD+SiRB1
Mitotracker relative intensity
**
*
**
*
PL45
PL5

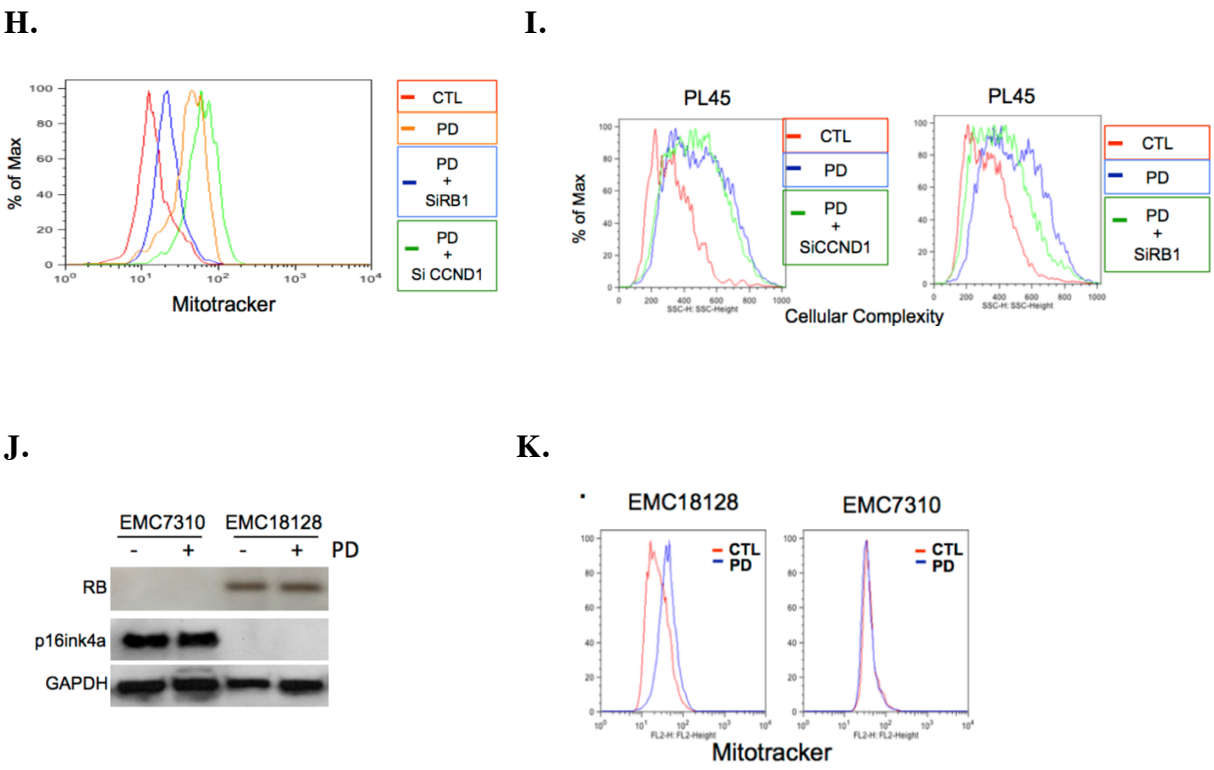

Figure 3.5: Supplemental Figure 1: (A) The indicated cell lines were treated with DMSO or PD- 0332991 and BrdU was determined at 24 hours post treatment. Data shown is from three independent experiments. Bars demonstrate the average and standard deviation. Statistical comparisons relative to the control were determined by t-test (**p<0.01, ***p<0.001). (B) The indicated cell lines were treated with PD-0332991 for

the indicated time. Mitotracker signal was determined as a function of time. The average signal and standard deviation are shown. Statistical comparisons relative to the control were determined by t-test (***$p<0.001$). (C) Representative histograms of mitotracker signal from the indicated cell lines cultured in the presence of DMSO or PD-0332991. (D) The indicated cell lines were treated with CDK4/6 inhibitors PD-0332991, Lee011, and LY2853219 for 120 hours. Representative histograms of mitotracker signal are shown. (E) Immunoblots of Cyclin D1, Cyclin A, ppRB (Ser780) following 120 hour treatment with PD-0332991 are shown from the indicated cell lines. (F) Immunofluorescence (scale bar is 20 μm) and immunoblots of RB and Cyclin D1 following transfection with pooled RNAi against RB and CCND1 in PD-0332991 pre-treated cells. (G) Mitochondria accumulation following RB knockdown was quantified in the indicated cell lines. The average and standard deviation are shown. Statistical comparisons relative to the control were determined by t-test (*$p<0.05$, **$p<0.01$). (H) Confirmation of effects on mitonchondria accumulation with independent RNAi molecules against CCND1 and RB1. Representative histograms are shown. (I) Cellular complexity changes with PD-0332991 in the presence of pooled RNAi mediated knockdown of cyclin D1 or RB. (J) Immunoblotting for the indicated proteins in the indicated cell lines. The EMC7310 cell line is RB deficient and expresses high-levels of p16ink4a, while EMC18128 is RB- proficient. (K) Mitocondrial accumulation was evaluated in the indicated cell lines by mitotracker staining. Representative histograms are shown. (L) The localization of RB and mitochondria were determined by immunofluorescence staining in the presence of PD-0332991 (scale bar is 20 μm).

A.

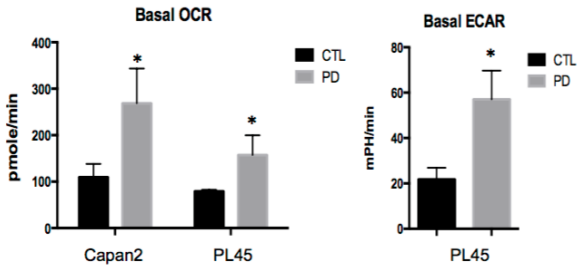
Basal OCR
pmole/min
400
300
200
100
0
CTL
PD
Capan2
PL45
Basal ECAR
mPH/min
80
60
40
20
0
CTL
PD
PL45

B.

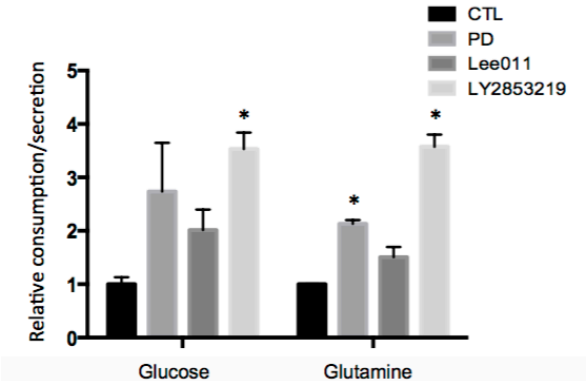
CTL
PD
Lee011
LY2853219
Relative consumption/secretion
5
4
3
2
1
0
Glucose
Glutamine

C,

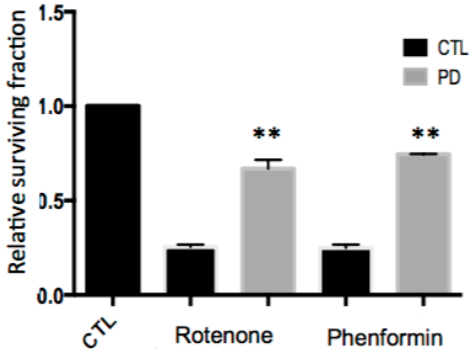
Relative surviving fraction
1.5
1.0
0.5
0.0
CTL
PD
CTL
Rotenone
Phenformin

Figure 3.5: Supplemental Figure 2: (A) The effect of PD-0332991 treatment on basal OCR and ECAR was determined in the indicated cell lines. Average and standard deviation are shown. Statistical comparisons relative to the control were determined by t-test (*$p<0.05$) (B) The impact of the indicated PD-0332991, Lee011 and LY2853219 on glucose consumption and lactate secretion were determined in Capan2 cells. Average and standard deviation are shown. Statistical comparisons relative to the control were determined by t-test (*$p<0.05$). (C) Cells were treated with Rotenone or Phenformin in the presence of vehicle control or PD-0332991. Surviving fraction was determined average and standard deviation are shown. Statistical comparisons relative to the vehicle control were determined by t-test (**$p<0.01$).

A.

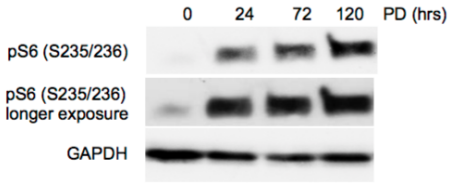

B.

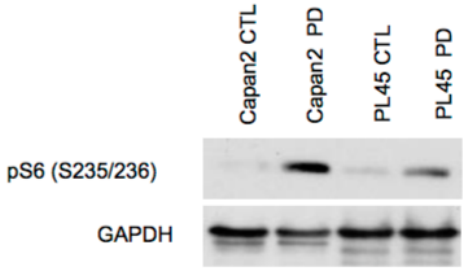

C.

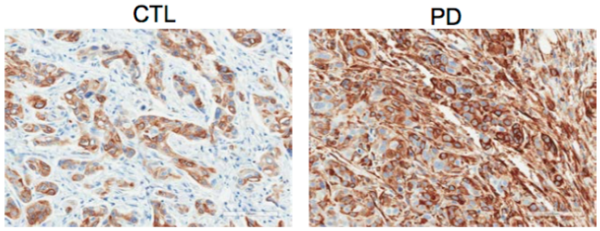

pS6 (S235/236)

D.

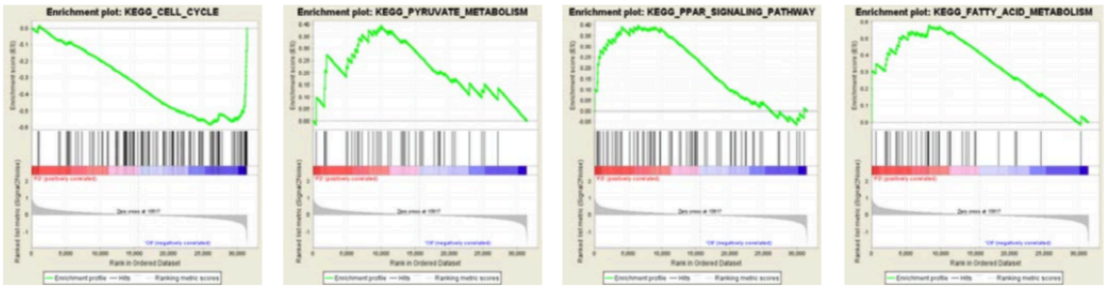

E.

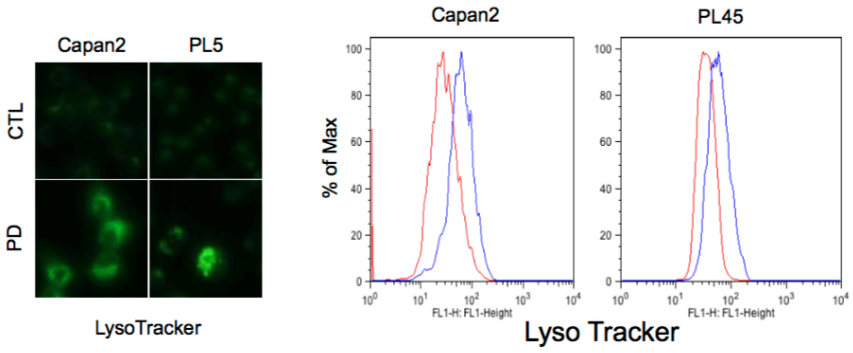

F.

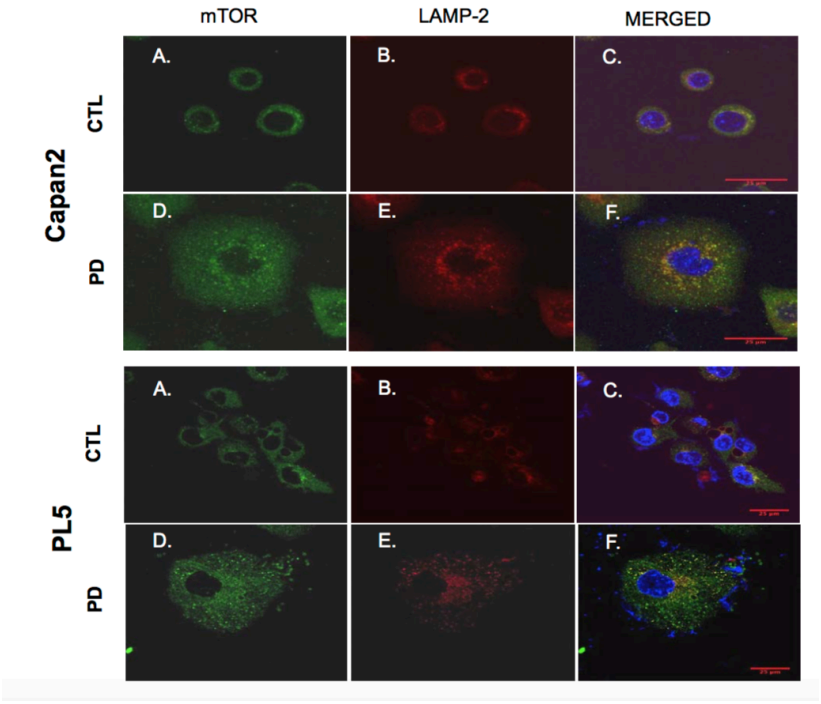
mTOR
LAMP-2
MERGED
Capan2
PL5
CTL
PD
A.
B.
C.
D.
E.
F.

G.

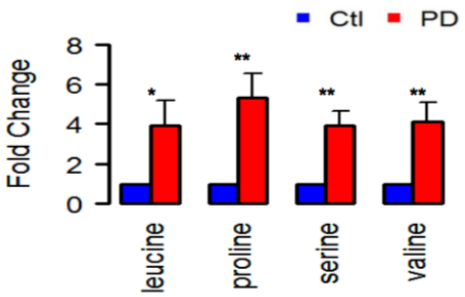
Ctl
PD
Fold Change
0
2
4
6
8
*
**
**
**
leucine
proline
serine
valine

H.

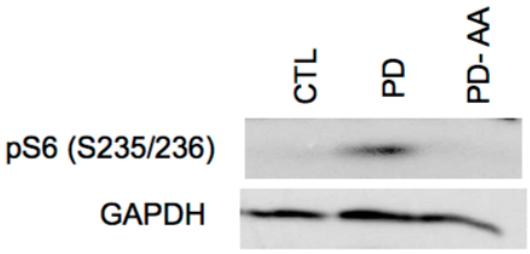
CTL
PD
PD- AA
pS6 (S235/236)
GAPDH

Figure 3.5: Supplemental Figure 3: (A) Immunoblotting for the phosphorylation of ribosomal protein S6 (Ser235/236) over time. (B) Immunoblots showing S6 phosphorylation (Ser235/236) following treatment with PD-0332991. (C) Representative immunohistochemical staining for phosphorylated ribosomal protein S6 (Ser 235/236) following 8 days of PD-0332991 treatment is shown for the patient- derived xenograft model EMC43 (scale bars 100 μm). (D) Gene set enrichment data for KEGG terms CELL CYCLE, PYRUVATE METABOLISM, PPAR SIGNALING, and FATTY ACID METABOLISM. (E) Histograms and representative images of LysoTracker staining following 24 hour PD-332991 treatment in Capan2 and PL45 cell lines (scale bars 50 μm). (F) Immunostaining for MTOR and LAMP2 was performed in the indicated cell lines treated with DMSO or PD-0332991. Representative images showing the accumulation of MTOR in the lysomal compartment are shown (scale bars 25 μm). (G) Amino acid levels as determined by mass-spectrometry from cells treated with PD-0332991. The average and standard deviation are shown. Statistical comparisons relative to the vehicle control were determined by t-test (*$p<0.05$, **$p<0.01$). (H) Immunoblot of phosphorylated S6 (Ser235/236) following treatment with PD-0332991 alone or with concurrent amino acid withdrawal.

A.

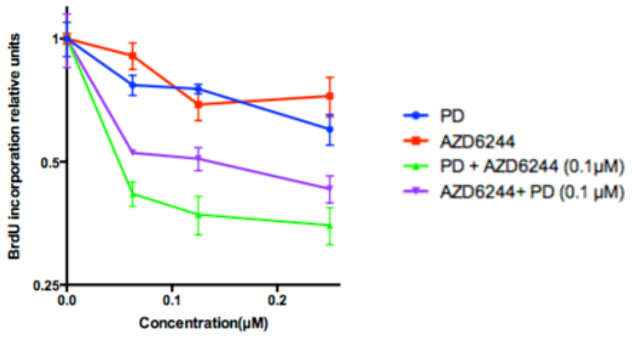
BrdU incorporation relative units
1
0.5
0.25
0.0
0.1
0.2
Concentration(μM)
PD
AZD6244
PD + AZD6244 (0.1μM)
AZD6244+ PD (0.1 μM)

B.

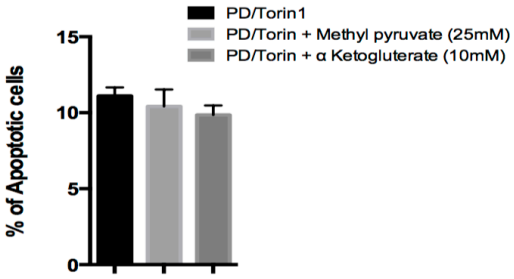
PD/Torin1
PD/Torin + Methyl pyruvate (25mM)
PD/Torin + α Ketogluterate (10mM)
% of Apoptotic cells
15
10
5
0

C.

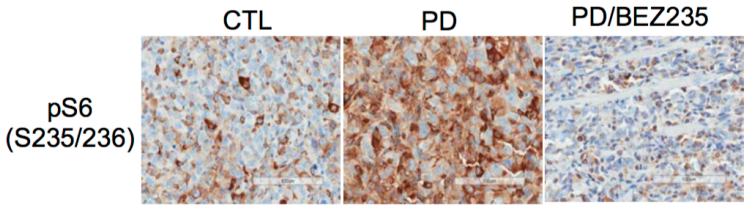
CTL
PD
PD/BEZ235
pS6
(S235/236)

D.

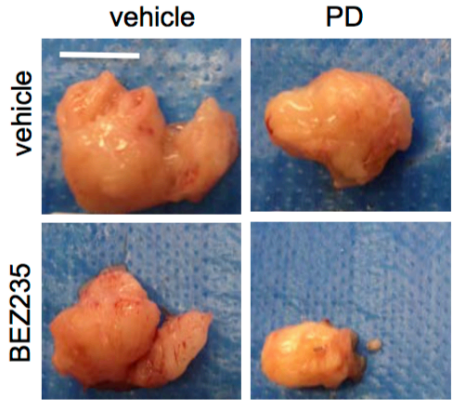
vehicle
PD
vehicle
BEZ235

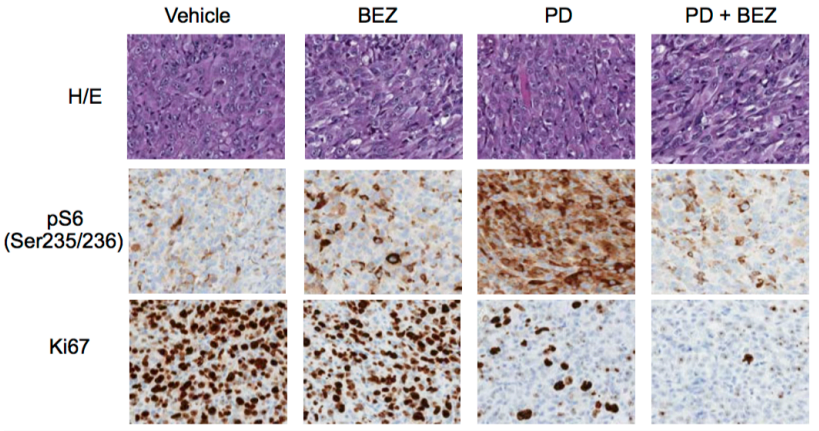
Vehicle
BEZ
PD
PD + BEZ
H/E
pS6
(Ser235/236)
Ki67

E.

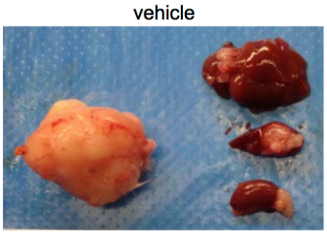
vehicle

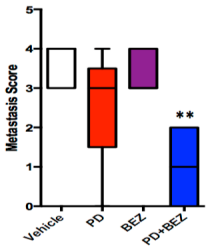
Metastasis Score
5
4
3
2
1
0
**
Vehicle
PD
BEZ
PD+BEZ

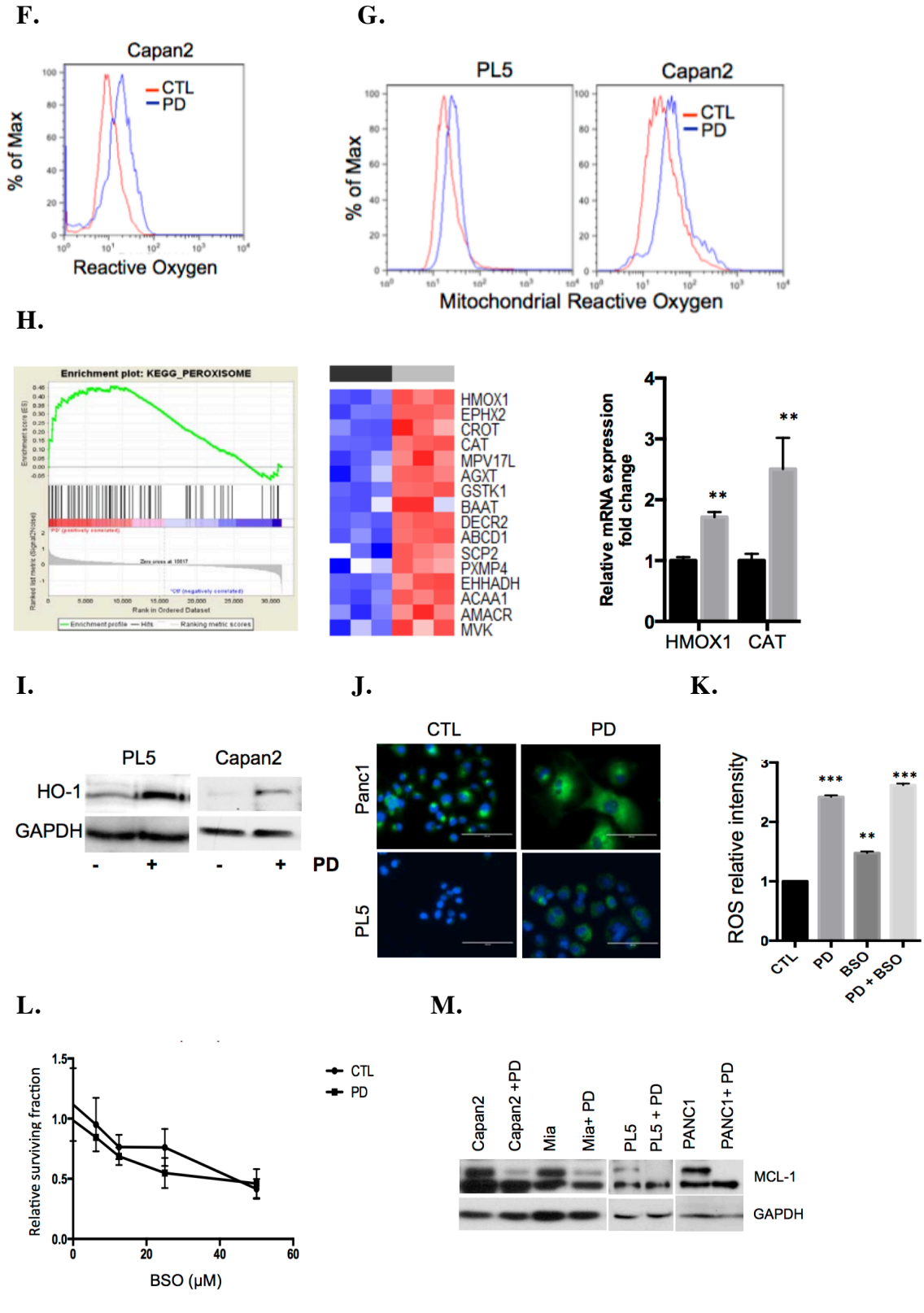
F.
Capan2
CTL
PD
% of Max
Reactive Oxygen
G.
PL5
Capan2
CTL
PD
% of Max
Mitochondrial Reactive Oxygen
H.
Enrichment plot: KEGG_PEROXISOME
HMOX1
EPHX2
CROT
CAT
MPV17L
AGXT
GSTK1
BAAT
DECR2
ABCD1
SCP2
PXMP4
EHHADH
ACAA1
AMACR
MVK
Relative mRNA expression fold change
HMOX1
CAT
I.
PL5
Capan2
HO-1
GAPDH
PD
J.
CTL
PD
Panc1
PL5
K.
ROS relative intensity
CTL
PD
BSO
PD + BSO
L.
Relative surviving fraction
BSO (μM)
CTL
PD
M.
Capan2
Capan2 +PD
Mia
Mia+ PD
PL5
PL5 + PD
PANC1
PANC1+ PD
MCL-1
GAPDH

Figure 3.5: Supplemental Figure 4: (A) Cells were treated with the indicated doses of PD-0332991 and AZD6244. BrdU incorporation was quantified and the average and standard deviation are shown. Data show significant cooperation between the agents. (B) Cells were treated with PD-0332991 and Torin1 alone or in conjunction with methylpyruvate or alpha-ketogluturate. Average number of apoptotic cells and standard deviation is shown. (C) Representative immuhistochemical staining of phosphorylated S6 (Ser235/236) in PL45 xenograft following 8 days treatment with vehicle control, PD-0332991 or combined treatment with PD-0332991 and BEZ235 (scale bars 100 μm). (D) Representative images of orthotopic xenografts (scale bar 1 cm). Immunohistochemical staining of tumors treated with the indicated agents was performed. Representative images of pS6 (Ser235/236) and Ki67 staining are shown (scale bars 100 μm). (E) Representative images of vehicle treated tumors and metastasis to spleen and liver (scale bar 1 cm), quantification of metastatic burden was determined by visual examination of all animals. Statistical comparison of the combined treatment relative to the vehicle control were determined by t-test (**$p<0.01$). (F) Flow cytometric analysis of reactive oxygen species from the indicated cell line. Representative histogram is shown. (G) Flow cytometric analysis of mitochondria-derived reactive species from the indicated cell lines treated with PD-0332991. Representative histogram are shown (H) Gene set enrichment analysis for KEGG term PEROXISOME, heatmap of select peroxisome associated genes, expression level of HMOX and CAT genes (**$p<0.01$). (I) Immunoblotting of HO-1 protein following treatment with PD-0332991 in the indicated cell lines. (J) Immunostaining for catalase in the presence of DMSO or PD-0332991 treatment (scale bar 100 μm). (K) Analysis of ROS levels from cells treated with vehicle, PD- 0332991,

25 μM BSO, or 25 μM BSO+PD-0332991. The mean and standard deviation is shown. Statistical comparisons of treatments relative to the vehicle control were determined by t-test (**p<0.01, p<0.001). (L) Cells were treated with increasing concentrations of BSO in the absence or presence of PD-0332991.

are shown. (M) Immunoblot analysis of MCL1 in the indicated cell lines treated with vehicle (DMSO) or PD-0332991.

3.10.1: Mitochondria Staining:

Mitochondria were assessed with MitoTracker®Red CMXRos 540/604 (50nM) (Live technologies). Cells were incubated under normal culture conditions for 30 minutes and fixed with 70% ice-cold ethanol. Mitochondria were subsequently visualized by fluorescence confocal microscopy using a Zeiss LSM 510 META NLO at magnification 62.5x or quantified by Flow cytometry using BD FACSCaliburTM (measured at 530 [FL-1, green] and 590 [FL-2, red] nm).

3.10. 2: Transfection:

Cells were cultured in 96 well plates then transfected with ON-TARGETplus siRNA (100nM) specific for CCND1 or RB or HO-1 (All purchased from Dharmacon), using RNAiMAX Lipofectamine according to the manufacturer's specifications.

3.10. 3: Quantification of ATP levels:

Cells were seeded in 24 well plates and treated with PD-0332991 and/or combination (AZD- 6244 and Torin 1) for 120 hours. Following treatment, cells were counted and assessed by CellTiter-Glo Reagent (Promega), luminescent signal is proportional to the amount of Adenosine triphosphate (ATP) present. Results were analyzed by dividing Relative Luminescence Units (RLUs) by cell number.

3.10. 4: Immunofluorescence:

Cells were plated onto cover slips and staining was conducted after finalization of treatment. Cells were first washed twice with PBS and then fixed with ice-cold methanol for 15 min. Following fixation, cell were washed with PBS and blocked in IF buffer

(PBS, 05% NP40 substitute, and 5% BSA) for 10 min at room temperature (RT). Primary antibodies were subsequently added, diluted in blocking buffer, and incubated for 1 hr at 37 °C in humidifying chamber. Following incubation, cover slips were washed with PBS and incubated in fluorescent-conjugated secondary antibodies, dilluted in blocking buffer, for 30 min at RT. Cells were washed and counter stained with DAPI and subsequently mounted onto slides using mounting agent. Subsequent to staining, cell were images by fluorescence confocal microscopy using a Zeiss 510 at magnification (62x).

3.10. 5: Transmission Electron Microscopy:

Cells were fixed on MatTek dishes with 2.5% (v/v) glutaraldehyde in 0.1M sodium cacodylate buffer. After three rinses in 0.1 M sodium cacodylate buffer, they were post-fixed in 1% osmium tetroxide and 0.8 % K3[Fe(CN6)] in 0.1 M sodium cacodylate buffer for 1 h at room temperature. Cells were rinsed with water and en bloc stained with 2% aqueous uranyl acetate overnight. After three rinses with water, specimens were dehydrated with increasing concentration of ethanol, infiltrated with Embed-812 resin and polymerized in a 60oC oven overnight. Blocks were sectioned with a diamond knife (Diatome) on a Leica Ultracut ultramicrotome (Leica Microsystems) and collected onto copper grids, post stained with 2% Uranyl acetate in water and lead citrate. Images were acquired on a Tecnai G2 spirit transmission electron microscope (FEI) equipped with a LaB6 source using a voltage of 120

kV.

3.10. 6: Metabolite deprivation:

PD-0332991 pre-treated (96 hours) and control cell populations were acutely deprived of glutamine and/or glucose. Cells were seeded and cultured in Glutamine-free DMEM

and/or Glucose-free DMEM media (Corning) with 10% dialyzed FBS (Sigma). Bright field images (10x) were taken following 48 hours incubation under glucose deprivation or 72 hours when deprived of glutamine. For amino acid deprivation experiment, cells were pre-treated with PD- 0332991 followed by Amino Acid deprivation using DMEM w/o amino acids (US biological) supplemented with 10% dialyzed FBS and antibiotics for 8 hours.

3.10. 7: Biochemical analyzer:

Glucose and glutamine uptake and lactate and glutamate production was assessed using a biochemistry analyzer (BioProfile Basic-4 Analyzer; NOVA). Cell were plated in 6-well plates and exposed to drugs as indicated. Twelve hours before analysis, media was changed. Media was collected and glucose/glutamine and lactate/glutamate levels were evaluated, and results were reported in mmoles/mL normalized to cells number (Baek et al., 2014).

3.10. 8: Oxygen consumption and extracellular acidification rates

OCR and ECAR measurement were conducted using Seahorse Bioscience XF24 Extracellular FLUX analyzer according to manufacturing's protocol. Cells were first plated XF24 polystyrene cell culture plates to 60-80% confluence (20,000 cell per well) 12 hours at 37° with 5.0 CO2 before ECAR or OCR analysis. Following incubation and before conduction of assay, growth

medium was replaced with the appropriate assay medium (DMEM with 1.85g/L NaCI, 3 mg/L phenol red, 2 mM L-glutamine). During assay, glucose, oligomicin, and 2-DG for ECAR, and oligomycin, FCCP, and rotenone for OCR were sequentially injected into each wells in accordance with standard protocols. OCR and ECAR were graphed as

absolute rates (pmoles/min for OCR and mpH/min for ECAR) and normalized against cell number.

3.10.9: LC/MS-based metabolite profiling:

LC/MS analyses were conducted on a QExactive benchtop orbitrap mass spectrometer equipped with an Ion Max source and a HESI II probe, which was coupled to a Dionex UltiMate 3000 UPLC system (Thermo Fisher Scientific, San Jose, CA). External mass calibration was performed using the standard calibration mixture every 7 days.

Dried metabolite samples were stored at -80°C and then resuspended in 100 µL water; 1 µl of each sample was injected onto a ZIC-pHILIC 2.1 x 150 mm (5 µm particle size) column (EMD Millipore). Buffer A was 20 mM ammonium carbonate, 0.1% ammonium hydroxide; buffer B was acetonitrile. The chromatographic gradient was run at a flow rate of 0.150 ml/min as follows: 0-20 min.: linear gradient from 80% to 20% B; 20-20.5 min.: linear gradient from 20% to 80% B; 20.5-28 min.: hold at 80% B. The column was held at 25°C. The mass spectrometer was operated in full-scan, polarity switching mode with the spray voltage set to 3.0 kV, the heated capillary held at 275°C, and the HESI probe held at 350°C. The sheath gas flow was set to 40 units, the auxiliary gas flow was set to 15 units, and the sweep gas flow was set to 1 unit. The MS data acquisition was performed in a range of 70-1000 m/z, with the resolution set at 70,000, the AGC target at 106, and the maximum injection time at 80 msec. Relative quantitation of polar metabolites was performed with XCalibur QuanBrowser 2.(Thermo Fisher Scientific) using a 5 ppm mass tolerance and referencing an in-house library of chemical standards.Cell number was utilized to normalize the data obtained from mass spectrometry analysis. Change in metabolites levels in PD-0332991 treated cells were

calculated relative to control. A two tailed t-test was used to obtain significance value. Ratio of labeled to total metabolite were calculated in both 13C-glucose and 13C-glutamine for the flux analysis data. All plots were obtained using functions implemented in gplots package in R.

3.10. 10: SA-β-Gal and Apoptotic staining:

Senescence was measured with the senescence-associated β-galactosides (SA- β-Gal) activity assay (Cell Signaling) following manufacture's standard protocol. Apoptotic cell death was assessed by incubating growing cells with propidium iodide solution for 30 minutes, and then quantifying positive cell staining using flow cytometry.

3.10. 11: Microarray Analysis:

Microarray was performed on Illumina HumanHT-12 V4.0 expression beadchip array. The data was normalized using the robust multi-array average method (RMA) implemented in the limma1 Bioconductor package in R2. For genes with multiple probe sets, the median expression level was used. A two tailed t-test was calculated to identify differentially expressed genes. Genes with absolute fold change > 1.5 and p-value < 0.05 were identified as differentially expressed. Gene set enrichment analysis (GSEA) was used to identify signaling and metabolic pathways that were enriched for the microarray dataset (Subramanian et al.,

http://www.genome.jp/kegg/pathway.html

2005). KEGG gene sets ( ) from the molecular signature database (MSigDB) was used as the gene set of interest.

3.10. 12: Xenografts and PDX Studies:

Patient-derived tumors were engrafted subcutaneously into the flanks of

immunocompromised NOD-SCID IL2Rgammanull (NSG) mice and expanded and passaged over time as described previously(Witkiewicz et al., 2015). PDXs were treated with PD (125mg/kg) or with DMSO diluted in sodium lactate buffer (50 mM, pH 4.0) by oral route for 8 days. For established cell line derived xenografts, 5 million cells were injected subcutaneously with matrigel (1:1 volume) and treated with PD-0332991 (125 mg/kg), BEZ235 (25 mg/kg) and the combination when tumors reached ~200mm3 . All animal experiments were carried out under protocols approved by the University of Texas Southwestern Medical Center Animal Care. At the end of the treatment period mice were sacrificed, tumors were excised from mice, weighed and then fixed overnight in formalin or flash frozen using liquid nitrogen. Formalin fixed tissue was embedded in paraffin; while, frozen tissue was embedded in optimal cutting temperature (OCT). Immunohistochemical staining for Ki-67 and pS6 (Ser235/236) was performed on paraffin embedded sections. The Ki67 staining was performed as previously reported(Witkiewicz et al., 2015). For the pS6 (Ser235/236) staining was performed on a DAKO autostainer. Antigen retrieval was performed low pH for twenty minutes at 97C and the peroxidase block was for 5 minutes. pS6 (Ser235/236) antibody was used at a 1:400 dilution for 20 minutes. A rabbit linker and HRP secondary antibody were sequentially applied for 15 and 20 minutes respectively. DAB developing was for 10 minutes, and Hematoxylin staining was for 5minutes.

Immunofluorescence staining for Tom20 and vimentin was performed on frozen sections, using methanol fixation and the same protocol as described above for cells on cover slips.

CHAPTER IV: Discussion and Future Directions

4.1: Overall Findings: CDK4/6 Inhibitors Have Potent Activity in Combination with Pathway Selective Therapeutic Agents in Models of Pancreatic Cancer.

We initiated our study by investigating the sensitivity of PDA to CDK4/6 inhibitor PD0332991 using a panel of established cell lines. Our results demonstrated that PDA cells exhibit variable responses to CDK4/6 inhibition; these responses range from very sensitive to highly resistant. Interestingly, those models that were highly resistant, such as PL5, maintained residual RB suppression even after CDK4/6 inhibition thus alluding to a compensatory mechanism responsible for sustaining RB in a hyper-phosphorylated state. These responses were consistent with the results obtained from gene expression profiling where resistant models displayed a decrease in transcriptional suppression of cell cycle genes compared to more sensitive models.

Surprisingly, unlike most other cell cycle related genes, which expression decreased following CDK4/6 inhibition, Cyclin D1 and Cyclin E1 were up-regulated, but only Cyclin E1 was deregulated in resistant models. Later, we found that indeed Cyclin E1 induction was responsible for resistance. Cyclin D1 up-regulation have been previously reported by other groups, but to our knowledge, we were the first group to report that Cyclin E1 deregulation could be a mechanism that PDA cells can utilize to bypass CDK4/6 inhibition. This mechanism of resistance has been furthered confirmed since we published this study by another group showing similar results in ovarian

cancer[164]. So far, resistance to CDK4/6 inhibitors had only been noted in models that were RB-deficient, which fortunately is a low occurrence in PDA where it occurs in less than 6% of cases[165].

This alternative mechanism of resistance by aberrant cyclin induction may be potentially involved in PDA rapid resistance to CDK4/6 inhibitors, which we observed while investigating durable responses to CDK4/6 inhibitor PD0332991. We learned that PDA established cell lines quickly overcome CDK4/6 inhibition. This was true even in models that initially displayed high sensitivity such as Capan2 (Appendix A). We suspect that cyclin deregulation may be playing an active role in this process. To date, only RB loss is associated with resistance in the clinical setting, it remains to be ascertain if CDK4/6 inhibition leads to aberrant cyclin expression and if this is associated with resistance in PDA tumors.

While testing CDK4/6 inhibitors, we encountered various unwanted drug combinations that could be potentially be used in the clinic. We found that CDK4/6 inhibition was consistently protected from the cytotoxicity exerted by several targeted therapies (PLK1, AURIKA, CHEK) and chemotherapies (Gemcitabine). Even though antagonistic responses to chemotherapies have been discovered, we were the first to report antagonist responses to targeted therapies [166]. We speculate that CDK4/6 antagonism results from CDK4/6-induced cell cycle arrest, which state protects cells from the DNA damage elicited by these agents, thus diminishing their cytotoxicity.

Lastly, we uncovered that this aberrant cyclin expression is directly associated with MTOR activity. We found that impinging on MTOR signaling by pharmacological means was sufficient to block aberrant cyclin E and D1 induction, thus leading to

furthered RB de-phosphorylation and cell cycle blockade. Both MTOR and MEK inhibitors, in combination with CDK4/6 inhibition, had a comparable effect on the proliferation of resistant cell models. This suggests that MEK signaling may be carrying out an equivalent role but this remains to be determined.

Even though, we found that Cyclin D1 is uncoupled to responses by resistant models, future experiments will investigate the mechanism by which CDK4/6 stabilizes Cyclin D1 expression. Previous studies have shown that Cyclin D1 expression is dynamic, actively being shuttled from the nucleus to the cytoplasm and the other way around. This shuttling is associated with the phosphorylation of Cyclin D1. When phosphorylated at Thr 286, Cyclin D1 is located in the cytoplasm, where it can be degraded by proteolysis; while, in the nucleus it is protected from degradation and can fully exert its activity. Unlike other cyclins with oscillating expression, Cyclin D1 expression does not suggest the transport from and out of the nucleus is the major mechanism to regulate its activity[167].

4.2: Overall Findings: Metabolic Reprogramming of Pancreatic Cancer Mediated by CDK4/6 Inhibition Elicits Unique Vulnerabilities

There is a growing appreciation that cell cycle control is associated with cellular metabolism. Several components of the cell cycle machinery have already been linked to several metabolic processes. For instance, CDK4/6, RB, and E2F have been presumably found to be active regulators of glycolysis, oxidative respiration and lipid metabolism but these effects are context dependent [143, 168]. Hence, we decided to investigate if CDK4/6 inhibitors had any influence on the metabolic state of PDA.

Surprisingly, we uncovered that PDA cells treated with CDK4/6 inhibitors exhibited an altered metabolic state with both an increase in oxidative respiration and glycolysis; this phenotype was dependent on RB expression. This altered metabolic state was associated with an accumulation of mitochondria and changes in cellular complexity. The increase in mitochondria was not mutually exclusive to our *in vitro* studies. After treating patient-derived Xenografts (PDXs) with PD-03332991 for 8 days, we noticed an accumulation of mitochondria in tumor tissue, thus making mitochondria accumulation a possible biomarker for responses to CDK4/6 inhibitors.

These effects on metabolism led to a robust accumulation of ATP, metabolism intermediates (pyruvate, citrate, malate, etc..), and amino acids. This metabolic charged phenotype protected PDA cells from acute glucose deprivation, but not from glutamine deprivation, thus emphasizing the importance of glutamine for PDA survival. Acknowledging that these metabolic effects are attributed to cross-talk with other signaling pathways, we decided to performed Reverse phase protein array (RPPA), which is a high-throughput assay that assesses the expression levels of more than 200 phosphorylated proteins, many of which are downstream targets of multiple signaling pathways. Results indicated that for the most part, CDK4/6 inhibition had a minimal impact on most signaling pathways except for MTOR signaling, which exhibited heighten activity. MTOR hyperactivity was further confirmed by gene expression profiles that showed many genes involved in MTOR-regulated processes being up regulated. Expectedly, enhanced MTOR signaling was also corroborated by xenografts experiments.

Subsequent findings uncovered that CDK4/6-enhanced MTOR activity was caused by an accumulation of amino acids and increased induction of lysosome, which

mechanism has been recently discovered [169, 170] [171]. The role of amino acids in MTOR induction was evaluated by depriving cell of exogenous amino acid, which prevented CDK4/6 induced MTOR activity. Also, we found that this increase in MTOR signaling was responsible for the altered metabolism state of CDK4/6 treated cells. Unexpectedly, even though impinging on MTOR and MEK signaling had similar effect on proliferation when combined with CDK4/6 inhibitors, they exerted a differential effect on metabolism. Disrupting MEK signaling using AZD6244 inhibited suppressed glycolysis; while, impinging of MTOR signaling with Torin 1 led to both suppression of glycolysis and oxidative respiration. Furthermore, we discovered that they led to distinct endpoints; MEK inhibition reinforced senescence while MTOR inhibition led to death. It remains to be determined if their differential effects on metabolism are leading to their distinct endpoints.

Lastly, we decided to investigate if CDK4/6 induced altered metabolism could become a liability for PDA cells. Acknowledging that CDK4/6 inhibition led to an accumulation of mitochondria, we decided to assess if this accumulation lead to an increase in ROS production. Results showed that CDK4/6 inhibition did indeed elicit an increase in ROS production, but this was accompanied with induction of ROS scavenging genes (HMOX1 and catalase), which we found to participate in protecting cells from ROS accumulation. Moreover, we uncovered that CDK4/6 inhibition could also sensitize cells to drugs such as ABT-737, which target pro-survival BCL-2, because it reduces that expression of MCL-1, which is known to compensate for BCL-2 activity loss.

Future experiments will investigate if PDXs become more metabolically active after treatment with PD-0332991 using FDG-PET, which uses fluorine-18 (F-18)

fluorodeoxyglucose (FDG) as tracer to detect glycolysis. In the clinic, it has already been noted that tumors treated with CDK4/6 inhibitors significantly reduced FLT-PET, which measures proliferation by detecting thymidine incorporation, but no changes in PDG-PET, thus suggesting that tumors remain metabolically active.

4.3: Future Directions Of Present Study

4.3.1: CDK4/6 Inhibition Effects on Stromal Compartment

The major focus of this study has been to uncover the effects elicited by CDK4/6 on the growth and biology of PDA epithelium cells. We purposely disregarded a main component of PDA, which is its stroma, due to its cellular complexity. A feature of PDA is the presence of a dense stroma, which could account for more than 90% tumor weight, consisting largely of fibroblasts, endothelium cells, and immune cells[172]. The stroma is thought to contribute to the aggressive nature of PDA by promoting tumor growth and metastasis while also enhancing drug resistance[172, 173]. Interestingly, CDK4/6 activity has been implicated in regulating all of these stromal components, which we will discuss in greater detail in the section bellow. Future studies will focus on uncovering the effects of CDK4/6 inhibition on these stromal components in the context of PDA, which may expose new therapeutic avenues for combination therapies.

4.3.2: Cancer-Associated Fibroblasts

In healthy tissue, fibroblasts are responsible for facilitating tissue repair, especially during inflammation. The main function of fibroblasts is to produce components of the extracellular matrix, which assist in maintaining the structural integrity within the

connective tissue which are often damaged during inflammation[174]. Fibroblasts are recruited by chemoattractants that direct them to the site of injury. Interestingly, cancer highjacks this system and recruits fibroblasts to form its stroma using a similar mechanism to the one discussed above [175]. Once in the tumor environment, fibroblasts are referred to as Cancer-Associated Fibroblasts (CAFs) [176]. It has been reported that CAFs enhance cancer cell proliferation, angiogenesis, invasion, and metastasis[177]. It was also discovered that CAFs could protect cancer cells from therapeutic agents[178]. The aforementioned finding leads us to speculate if a similar outcome would be observed after treatment with CDK4/6 inhibition. Furthermore, no one has fully studied the direct effects of CDK4/6 inhibition on PDA CAFs, and how these effects may influence the microenvironment. CDK4/6 activity has already been reported in CAFs in the context cancer. CDK activity has previously been shown to play a pivotal role in the secretion of certain extracellular matrix components, which aids in metastasis of cancer cells[179, 180]. Thus, this emphasizes the need to elucidate the impact of CDK4/6 inhibitor on CAFs to uncover how this may change the tumor microenvironment in PDA and if this could be furthered targeted in future therapies.

4.3.3: Role of CDK4/6 in Angiogenesis in PDA

Angiogenesis is the processes by which new vessels form from pre-existing ones. These new vessels are responsible for feeding the tumor with nutrients and other essential molecules required for growth and overall tumor maintenance. In the context of PDA, angiogenesis is thought to promote PDA growth and metastasis, which is regulated by angiogenic signals provided by both tumor cells and stroma [181]. The transcription of vascular endothelial growth factor A (VEGFA) is an important factor that stimulates

vascular endothelial growth and is highly expressed by PDA[182]. VEGF ligands mediate their angiogenic effects by binding to VEGF receptors, leading to subsequent signal transduction and promoting vascularization. Unexpectedly, a study found that CDK6 promotes formation of blood vessels in lymphoid malignancies[183]. While another group showed that CDK4 inhibition can directly prevent endothelium proliferation[184]. Interestingly, both groups showed that CDK4/6 inhibition had a detrimental effect on VEGF expression by cancer cells, which may be potentially having an effect on the tumor microenvironment. However, it remains to be determined whether CDK4/6 also plays a role in angiogenesis in PDA tumors and if this process could be altered by CDK4/6 inhibition.

4.3.4: CDK4/6 effects on Stromal Immune Component

Immune cells are a significant part of pancreatic tumor associated stroma and the accumulation of certain immune subtypes has been associated with poorer prognosis[54]. Normally, immune effector cells carry out surveillance in the blood for cancer cells and destroy them when recognized. However, in established tumors including PDA, it is often found that immune cells are either inactive or are actively cooperating with tumor. A large number of these cells are highjacked immune cells, referred to as regulatory immune cells, which are involved in dampening effector immune cell function and preventing tumor clearance[185, 186]. Multiple studies have also implicated these infiltrates in cancer processes such as growth and metastasis. [187]. As a result, there is a current emphasis in developing new therapeutic approaches that could target this suppressive environment, thus helping effector cells penetrate to elicit their anti-tumor effector function. Interestingly, CDK4/6 activity plays an active role in immune cell

development and function[188-190]. Hence, I suspect that the immune component of PDA stroma will be the most effected by CDK4/6 inhibition. However, it will be difficult to anticipate if this will be beneficiary to either tumor clearance or tumor survival, as both may be actively regulated by CDK4/6 activity.

4.4: Significance

PDA has presently no therapeutic options outside of surgery and chemotherapy and these therapies only have a marginal effect on the overall survival of these patients. However, we are optimistic that the current focus in discovering more directed approaches targeting the biology of PDA could lead to better treatments. In this study we sought to investigate if PDA could benefit from RB reactivation using CDK4/6 inhibitors. Results indicated that CDK4/6 inhibitors may be a good option, but not as a single-agents due to the rapid development of resistance seen in PDA established models. However, combination therapy with MTOR exerted significant suppressive effect on proliferation of PDA cells compared to single agent in both *in vivo* and *in vitro* systems, thus emphasizing that this combination therapy may a good alternative treatment options. From our studies, we believe this synergism comes from the fact that MTOR signaling is necessary for aberrant cyclin E1 resistance and also to that fact that MTOR plays an active role in the altered metabolism of CDK4/6 arrested cells, however the mechanism by which MTOR couples metabolism and cell cycle deregulation remains to identified. Together, these findings suggest that PDA may benefit from CDK4/6 inhibition in combination with agents that target MTOR. This remains to be seen in the clinic, but based on what has been observed *in vitro* and *in vivo* models, we are hopeful that results will be recapitulated. Future

experiments will uncover new combination therapies with CDK4/6 inhibitors against PDA, targeting both the tumor and stromal compartment, which may lead to more effective and durable treatment against PDA.

APPENDIX A: Rapid acquired resistance to CDK4/6 inhibitor displayed by PDA established models.

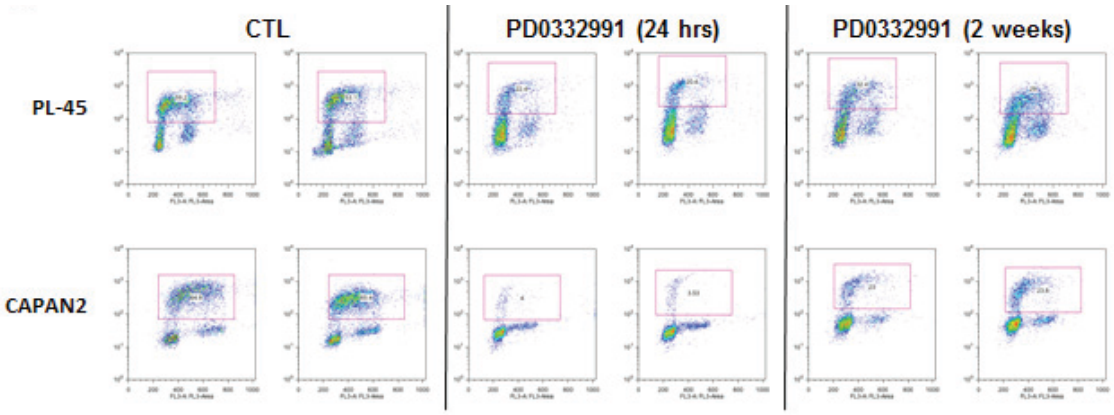

Representative BrdU incorporation after 24 hours and after 2 weeks of treatment with PD-0332991.

APPENDIX B: RB loss sensitizes to Gemcitabine, PLK1, CHK1/2 and Taxanes.

Introduction

Triple negative breast cancer (TNBC) is distinguished from other breast cancers types due to the lack of expression of estrogen receptor (ER), progesterone receptor (PR) and human epidermal growth factor receptor 2 (HER2)[191]. Accounting for approximately 30% of all breast cancers, the incidence of this type of cancer is often associated with a younger demographics[192, 193]. TNBC has a poor prognosis as compared to estrogen receptor positive (ER^+) breast cancer, due to both its aggressive nature as well as the lack of targeted therapies[194, 195]. Because TNBC is believed to be a heterogeneous disease consisting of a collection of several molecularly diverse tumors, it is thus extremely difficult to find adequate targets[196].

Current therapies for TNBC include: surgery, radiation and chemotherapy[197]. While it frequently exhibits higher chemo-sensitivity as compared to ER+ breast cancers, a large proportion of TNBC tumors quickly become resistant to chemotherapy[197, 198]. This feature of the disease demonstrates the critical importance of finding more effective and targeted treatments for TNBC.

A common feature in TNBC is the frequent loss of Retinoblastoma tumor suppressor (RB1)[191]. Occurring in approximately 40% of cases, RB1 disruption is due to gene deletion/mutation or gene silencing presumably leading to the deregulation of E2F activity and aberrant cell cycle progression[199-201]. This is supported by various studies that noted very high levels of RB/E2F signature genes in TNBC[201].

Interestingly, it has been reported that RB loss is associated with increase in tumor aggressiveness and chemo-sensitivity, however, the exact mechanism of these changes remains unknown[202]. Previous studies attempting to uncover novel selective therapies against TNBC using several large non-targeted drug libraries, but failed to yield drugs that selectively target TNBC cells based on RB-status[202, 203].

Here, we took an alternative approach, where we utilized pharmacological activation of RB with CDK4/6 inhibitors, vs. matched RB-deficient models to define agents that were reproducibly regulated by RB function We found that RB-status had a major impact on the selective sensitivity to targeted therapies.

Results

Primary Screen for RB-Selective Therapeutic Agents: We initiated this study by conducting a unbiased high throughput drug screen on MDA-MB 231 in the presence or absence of CDK4/6 inhibitor, PD0332991. This inhibitor results in the activation of RB by preventing the inhibitory phosphorylation events that occur with cell cyce progression. Cells either untreated or pre-treated with PD-0332991, were exposed to the Prestwick Chemical Library. This library contain 1,280 that are all FDA approved and cover diverse areas of medicine including oncology. The primary results for the drug screen are shown in a dot-plot diagram where each point signifies a single compound from the library in the presence or absence of CDK4/6 inhibitors (Figure 5.1A) . This screen showed antagonistic effects of CDK4/6 inhibition (ie. RB activation suppressed sensitivity) for a large number of compounds, yet there were very few cooperative combinations. CDK4/6 inhibition exerted antagonism against a number of

chemotherapies (e.g. Docetaxel and Gemcitabine), and, intriguingly, several anti-helminthic medications (e.g. Parbendazole, Oxibendazol, Mebendazole, Albendazole) which had not been previously reported (Figure 5.1B-C).

Since activating RB by CDK4/6 inhibitors leads to resistance, we hypothesized that the loss of RB might lead to sensitivity. Thus, we utilized the same compound library to investigate if RB-deficient MDA-MB 468 might display differential responses to these compounds as compared to RB-proficient MDA-MB 231 (Data not shown). Results indicated that some of the compounds that were antagonized by RB reactivation, also exerted greater potency in the RB-deficient model. For instance, Gemcitabine cytotoxicity was partly mitigated by CDK4/6 inhibition in MDA-MB 231 and also exerted greater potency in RB-deficient model MDA-MB 468 (Figure 5.1D). These results were furthered validated by dose response curves using MDA-MB 231 and several RB-deficient models including two models that are derivatives of MDA-MB 231 (miRB and Crispr RB) but where RB expression was depleted by different approaches (Figure 5.1E).

Not surprisingly, RB-deficient and proficient models differential responses to Gemcitabine were not exclusive to the *in vitro* screens as results were also recapitulated *in vivo* (Figure 5.1F). Herein, MDA-MB 231 and Crispr RB, RB-deficient MDA-MB 231 derivatives, were injected subcutaneously on opposite flanks of female NSG mice. When the tumor reached 200mm^3, mice were treated with gemcitabine (10ug/kg) weekly for 4 weeks. Results indicated that RB loss did indeed sensitize RB-deficient cells to Gemcitabine as indicated by a reduction in tumor growth that consequently led to smaller tumors (Figure 5.1G-H).

RB1 Loss Sensitizes to PLK, CHK Inhibitors and Taxanes: In recognition that targeted therapies will be important for the treatment of TNBC we investigated if loss of RB could potentially sensitize cells to targeted therapies. A high throughput drug screen using a custom library of, array pharmacological agents that target multiple signaling pathways as well as some chemotherapies was employed. Similarly to what we observed with the Prestwick library, CDK4/6 inhibition led to antagonistic responses to several classes of inhibitors including those that targeted PLK1 and CHK1/2, as well as some chemotherapies such as taxanes (Figure 5.2A-C). RB's role was furthered confirmed when RB-deficient miRB cells were protected from these agents when transduced with constitutively active RB (Figure 5.2D). Acknowledging that the antagonism effects elicited by CDK4/6 inhibitors may be coupled with augmented cytotoxicity to RB-deficient models, we performed this same screen on MDA-MB 231 and a number of RB-deficient models (miRB, MDA-MB468, and BT 549). Results from the screen confirmed that RB-deficient models were indeed hyper-sensitized to PLK, CHK inhibitors and taxanes (Figure 5.3A). These results were further corroborated by dose response curves, where RB-proficient model MDA-MB 231 and RB-deficient cell models (mIRB, MDA-MB468 and BT-549) were treated with decreasing concentrations of compounds (Figure 5.3B). These findings suggest that RB1 loss was actively involved in protecting RB-proficient cells from the cytotoxicity of these DNA damaging agents.

We further confirmed the previous findings by targeting PLK and CHK using siRNAs in both RB-deficient and proficient models. First, we noted that RB-deficient cells did truly exhibit greater sensitivity to PLK and CHK depletion. Also, similar to what

was observed using therapeutic agents, RB reactivation via CDK4/6 inhibition protected from the cytotoxic effects of PLK and CHEK depletion in RB-proficient models and not in RB1-deficient models. Also, when RB was depleted concurrently with PLK or CHEK, the antagonistic effect of CDK4/6 inhibition was mitigated (Figure 5.3C-D). Together, these results suggest that RB loss does sensitize cells to chemotherapies or chemo-like targeted therapies like PLK and CHEK inhibitors.

Knowing that RB-deficient cells are sensitive to PLK inhibitors, we decided to test the effects of combination therapy with Gemcitabine, which we previously determined to be more effective in RB-deficient models. We found that combining PLK inhibitors and Gemcitabine led to an accumulative effect in cytotoxicity in RB-deficient cells, which was less obvious in RB-proficient cells *in vitro* (Figure 5.3E). We speculated that the differential responses to these compounds were caused by RB-induced cell cycle arrest, which may protect cells from DNA damage elicited by these agents. This was supported by subsequent findings that showed that PLK inhibitors led to RB activation as evidenced by a decrease in its hyper-phosphorylated state, and also by the fact that RB-deficient cells displayed a significant decrease in proliferation compared to RB deficient cells following treatment with PLK and CHEK inhibitors (Figure 5.3F).

Differential Dependencies in TNBC Based on RB-status: Lastly, we decided to test if impinging on either MTOR or MEK pathways had differential effect on TNBC based on RB-status as these are major signaling pathways known to drive TNBC. First, we characterized MTOR and MEK signaling in both RB-proficient and RB-deficient cells. Results confirmed that RB loss led to differential signaling; RB-deficient cells displayed enhanced MTOR signaling and a reduction in MEK signaling based on pS6 and pERK

expression, respectively (Figure 5.4A). These results suggest a possible differential signaling dependency. In order to test if they possessed distinct dependencies, we impinged on either the MTOR or MEK pathways by pharmacological means. After treating cells with MTOR or MEK inhibitors, we found that not only did RB-proficient cells arrest more readily than their RB-deficient cells counterparts, but unexpectedly this occurred when both MTOR or MEK were inhibited (Figure 5.4B-C). We also observed that inhibition of both MTOR and/or MEK led to higher proportions of cell death in RB-proficient cells (Figure 5.4D). Based on both of these results, we can conclude that RB-status in TNBC could also dictate how TNBC may respond to therapies targeting signal transduction pathways due to differential dependencies exhibited by RB-deficient and proficient tumors.

Materials and Methods:

Cell lines:

MDA-MB 231 and MDA-MB 468, BT549, MCF7 human breast carcinoma cell lines were growth in DMEM supplemented with 10 % FBS and antibiotics.

High Throughput Screens:

Prestwick and Selleckchem screens were performed by. All libraries were diluted in DMSO to 2.5 μM. Preceding drug screen breast cancer cells MDA-MB-231, miRB, MDA-MB 468, BT 549, AW23, MCF7 were seeded with their corresponding media in 384 well plates at a density of 800 cells/well in a total volume of 60ul/well and incubated for 3 hours at 37°C and 5 % CO_2. Following incubation, plates were treated with drug

libraries to reach a final concentration of 2.5 μM and incubated for 72 hours at 37°C and 5 % CO_2.

CTG viability and BRDU Cell Proliferation ELISA, BrdU *(*chemiluminescent*):*

Cells were seeded in 96 well plates at a density of $5x10^3$ cell/well and treated with indicated drug and concentration to a total volume of 100μl for 72 hours at 37°C and 5 % CO_2. Following treatment, plates were incubated at RT for 15 min and then 15 μl of CellTiter-Glo® Luminescent Cell Viability Assay reagent was added to each well. After gently agitation to ensure even mixture of the dye, a 96-well microplate reader was used to determine the luminesent of each well. Cell Proliferation ELISA, *BrdU* (*chemiluminescent*), was performed using manufactory protocol.

Transfections:

First, $5 x10^3$ cells were seeded in 96 well plates then they were s transfected with PLK1, CHK1 and RB siRNA using SIRNAMAX as indicated by manufacture protocol. All pool siRNAs was obtain from Dharmacon.

Immunoblotting:

Breast cancer cells were lysed in RIPA buffer (10% NP-40 substitute, 1% SDS, 500mM Tris-HCI(pH 7.4), 1.5M NaCI, 5% sodium doxycholate, 10mM EDTA) containing both complete protease inhibitor cocktail tablets (Roche) and phosphatases inhibitors (Roche). Following lysis, protein concentration was measured with the BCA protein assay DC^{tm} Protein Assay(BIO-RAD) using manufacture's protocol. These samples were then separated on on SDS polyacrylamide gels and electroblotted on PVDF membranes.

Membranes were washed with wash buffer (0.1% Tween-20/1x saline), and subsequently blocked for 1 h in 5% nonfat dry milk in wash buffer and probed overnight with primary antibodies diluted in wash buffer/5% nonfat dry milk. Membranes were then washed with wash × 3 (5min) and incubated for 1 h with horseradish peroxidase-labeled secondary antibodies in in wash buffer/5% nonfat dry milk. Following an additional 3 washes, blots were visualized by chemiluminescence.

Xenografts:

NOD scid gamma(NSG) mice were purchased from. Six week old female mice were injected subcutaneously with $1.0x10^6$ cells in 100µl in 50:50 Media/Matrigel. Tumor growth was monitored weekly using vernier calipers till they reached $200mm^3$. After tumors reached the aforementioned volume, mice were treated weekly with Gemcitabine at 10 mg/kg in PBS or PBS i.p. After 30 days, these mice were sacrificed and their tumors were extracted measured and weighted.

A.

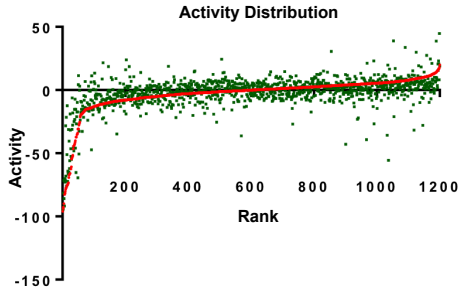

B.

SWID	Drug	Untreated	PD-0332991
SW102861	Nocodazole	-77.2666	-21.6085
SW196847	Colchicine	-75.3187	-12.3807
SW197324	Parbendazole	-73.3751	-31.1753
SW199074	Oxibendazol	-65.8477	-18.9115
SW197493	Docetaxel	-53.8238	-31.1174
SW196606	Mebendazole	-51.6073	-18.0764
SW199649	Gemcitabine	-43.2493	-15.1713
SW196830	Albendazole	-42.5959	-23.2638
SW197228	Methiazole	-35.1779	-17.4065
SW199522	Trifluridine	-34.953	-9.66761
SW197039	Antimycin A	-33.9177	-17.2974
SW196680	Thioguanosine	-30.9506	4.291153
SW198560	Azathioprine	-26.032	-0.24344
SW199090	Mercaptopurine	-25.3139	3.148936
SW197081	Indoprofen	5.942555	-35.8057

C.

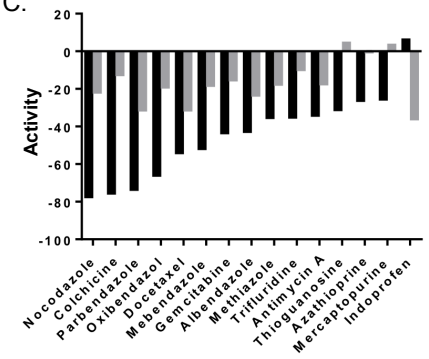

D.

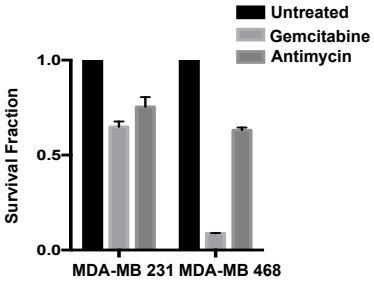

E.

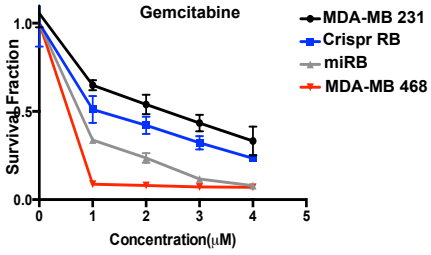

F.

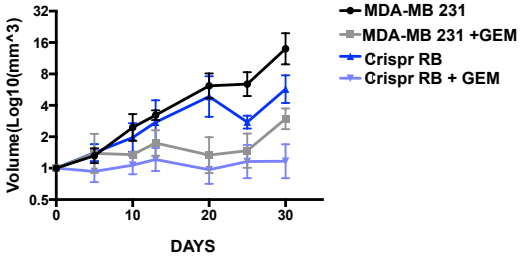

G.

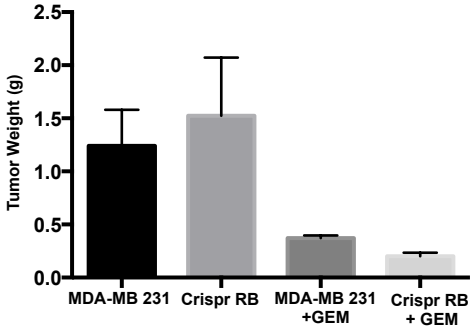

H.

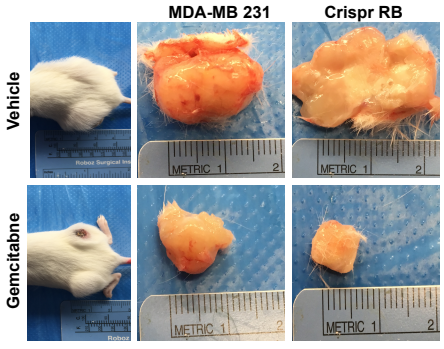

Figure 5.1. Therapeutic antagonism by CDK4/6 inhibitors and RB-loss sensitization to Gemcitabine in TNBC. (A) Overall responses to Prestwick screen in the presence or absence of CDK4/6 inhibitor in MDA-MB 231 TNBC model after 72 hour treatment. (B) Chart displaying top most antagonized Prestwick drugs by CDK4/6 inhibition. (C) Graphical representation of screen results showing top agents that were antagonized by CDK4/6 inhibitors. (D) Testing Gemcitabine (50nM) and Antimycin A (100nM) activity on RB-proficient MDA-MB 231 and MDA-MB 468 after 72 hour treatments. (E) Gemcitabine dose curves comparing RB-proficient and RB-deficient sensitivity. (F) Graphical representation of tumor growth over time using RB-proficient MDA-MB 231 and RB-deficient derivative Crispr RB xenografts. (G) Tumor weights after finalization of treatment. (H) Images of tumor size following treatment with Gemcitabine.

A.

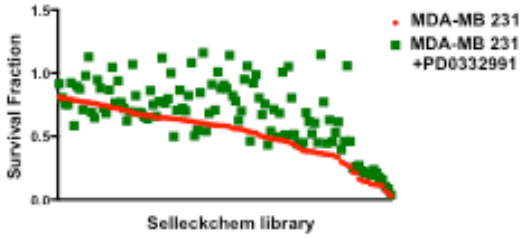

B.

Targeted Therapies

Drug name	Drug Class	Target
BI 6727	PLK Inhibitor	PLK
BI 2536	PLK Inhibitor	PLK
HMN-214	PLK Inhibitor	PLK
Chir-124	Chk1 inhibitor	Chk1
LY2603618	Chk1 inhibitor	Chk1

Chemotherapies

Drug name	Drug Class	Target
Paclitaxel	Taxanes	microtubules
Docetaxel	Taxenes	microtubules

C.

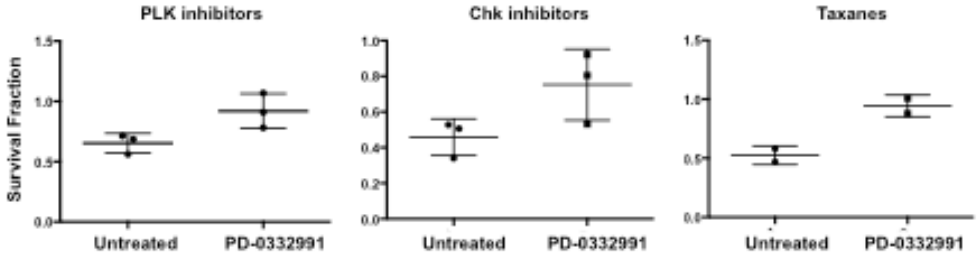

D.

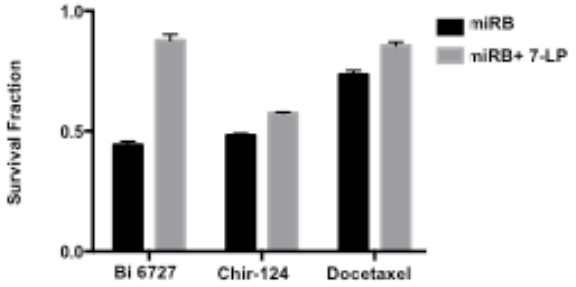

Figure 5.2. Therapeutic antagonism by CDK4/6 inhibition to PLK1, CHK inhibitors and taxanes in TNBC. (A) Dot-plot representation of overall responses to targeted – therapeutic screen in the presence or absence or CDK4/6 inhibitor 1μM using TNBC model MDA-MB 231. (B) Chart displaying top targeted therapies from Sellectchem screen antagonized by CDK4/6 inhibitor. (C) Overall graphical representation of results from PLK inhibitor, CHK ½ inhibitors and taxanes in the presence or absence of CDK4/6 inhibitor PD-0332991. (D) Graphical representation of RB reactivation by 7LP in the presence of Bi 6727 or Chir-124 or Docetaxel.

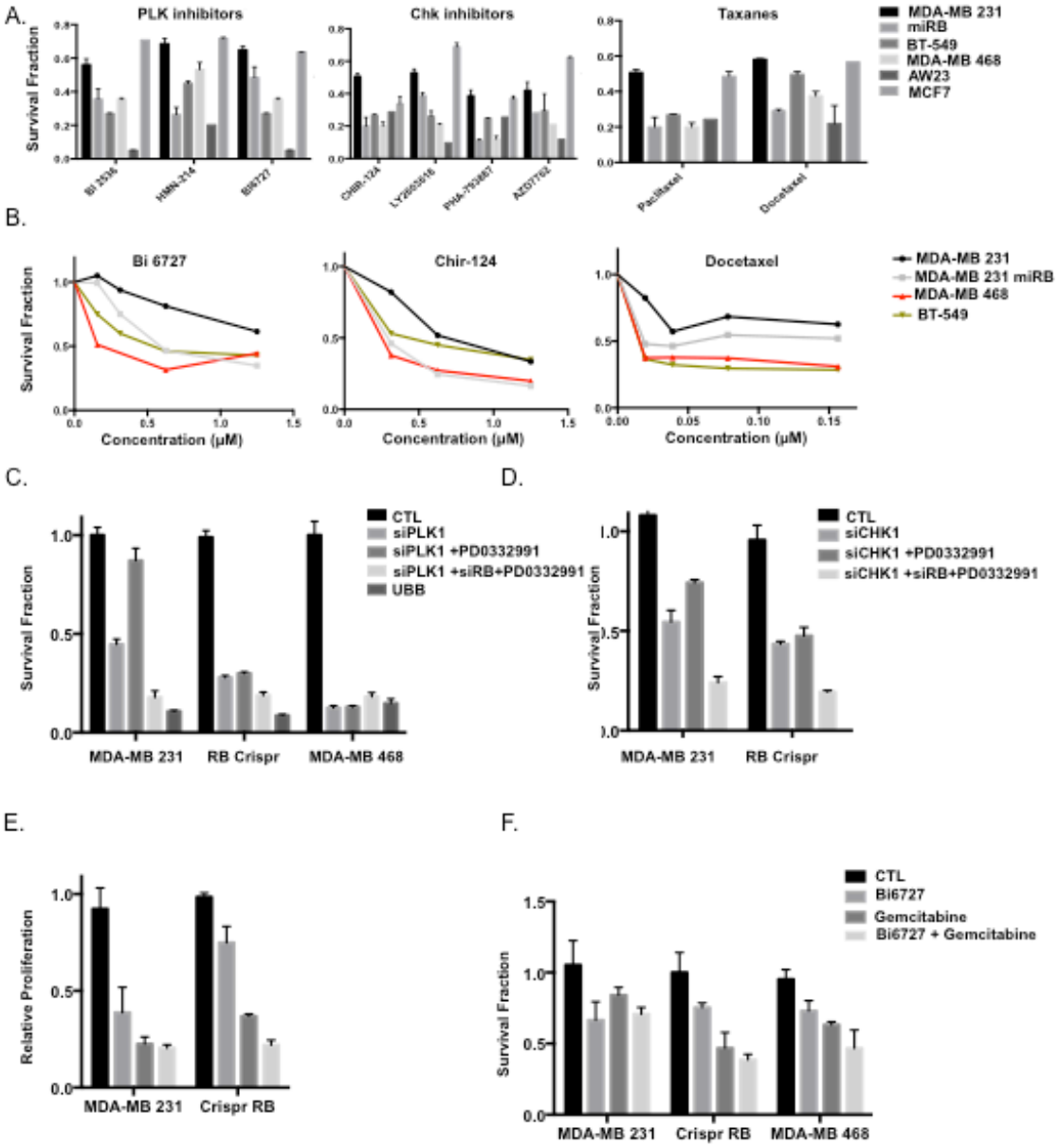
A.
PLK inhibitors
Chk inhibitors
Taxanes
Survival Fraction
MDA-MB 231
miRB
BT-549
MDA-MB 468
AW23
MCF7
BI 2536
HMN-214
BI6727
CHIR-124
LY2603618
PHA-793887
AZD7762
Paclitaxel
Docetaxel
B.
Bi 6727
Chir-124
Docetaxel
Survival Fraction
Concentration (μM)
MDA-MB 231
MDA-MB 231 miRB
MDA-MB 468
BT-549
C.
D.
CTL
siPLK1
siPLK1 +PD0332991
siPLK1 +siRB+PD0332991
UBB
siCHK1
siCHK1 +PD0332991
siCHK1 +siRB+PD0332991
Survival Fraction
MDA-MB 231
RB Crispr
MDA-MB 468
E.
F.
Relative Proliferation
Crispr RB
CTL
Bi6727
Gemcitabine
Bi6727 + Gemcitabine

Figure 5.3. RB-loss sensitizes cells to PLK, CHK inhibitors and Taxanes. (A) Screen results for PLK1, CHK inhibitors and taxanes against various TNBC models. (B) Graphical representation of Bi-6727, Chir-124 and Docetaxel dose curves. (C-D) Effects of CDK4/6 inhibitor on PLK1 or CHK siRNA cytotoxicity in the presence or absence of RB using RB-proficient MDA-MB 231. (E) Graphical representation of relative BRDU incorporation or (F) cytotoxicity after treatment with Gemcitabine or BI-6727 or in combination, respectively.

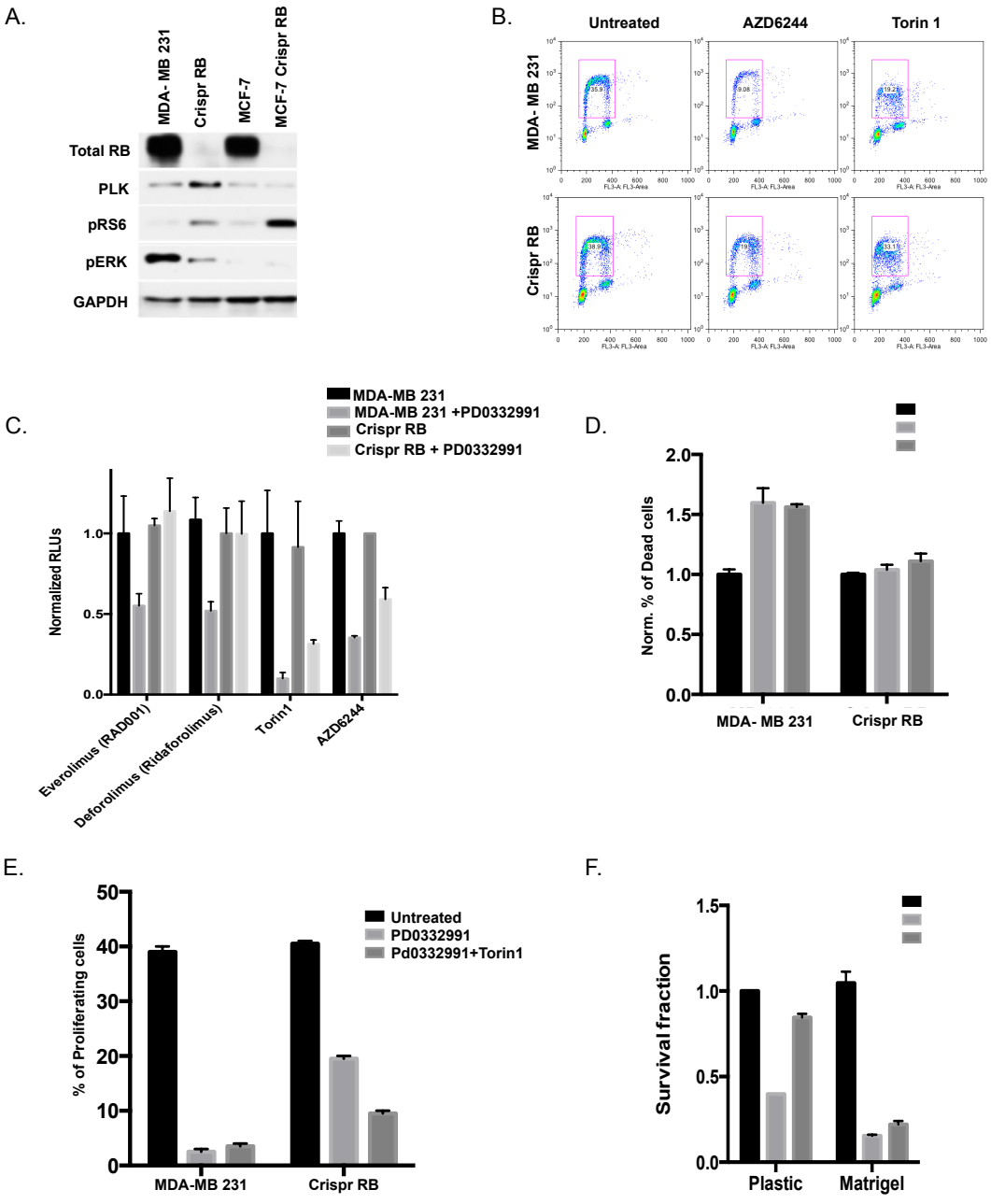
A.
MDA- MB 231
Crispr RB
MCF-7
MCF-7 Crispr RB
Total RB
PLK
pRS6
pERK
GAPDH
B.
Untreated
AZD6244
Torin 1
MDA- MB 231
Crispr RB
C.
MDA-MB 231
MDA-MB 231 +PD0332991
Crispr RB
Crispr RB + PD0332991
Normalized RLUs
Everolimus (RAD001)
Deforolimus (Ridaforolimus)
Torin1
AZD6244
D.
Norm. % of Dead cells
MDA- MB 231
Crispr RB
E.
Untreated
PD0332991
Pd0332991+Torin1
% of Proliferating cells
MDA-MB 231
Crispr RB
F.
Survival fraction
Plastic
Matrigel

Figure 5.4. RB-loss protects from MTOR and MEK inhibitors. (A) Immunioblots of PLK, prs6 (Ser235/6) and pERK. (B) Dot-plot diagrams displaying BRDU incorporation following treatment with indicated therapies. (C) Graphical representation of BRDU incorporation after treatment with indicated treatment. (D) Death was measured by flow cytometry using PI staining after treating cells for 72 hours with indicated inhibitor.

References

1. Bardeesy, N. & DePinho, R. A. (2002) Pancreatic cancer biology and genetics, *Nature reviews Cancer.* **2**, 897-909.
2. Rahib, L., Smith, B. D., Aizenberg, R., Rosenzweig, A. B., Fleshman, J. M. & Matrisian, L. M. (2014) Projecting cancer incidence and deaths to 2030: the unexpected burden of thyroid, liver, and pancreas cancers in the United States, *Cancer research.* **74**, 2913-21.
3. Ryan, D. P., Hong, T. S. & Bardeesy, N. (2014) Pancreatic adenocarcinoma, *The New England journal of medicine.* **371**, 1039-49.
4. Helgadottir, H., Hoiom, V., Jonsson, G., Tuominen, R., Ingvar, C., Borg, A., Olsson, H. & Hansson, J. (2014) High risk of tobacco-related cancers in CDKN2A mutation-positive melanoma families, *Journal of medical genetics.* **51**, 545-52.
5. Wang, W., Liao, Z., Li, G., Li, Z. S., Chen, J., Zhan, X. B., Wang, L. W., Liu, F., Hu, L. H., Guo, Y., Zou, D. W. & Jin, Z. D. (2011) Incidence of pancreatic cancer in chinese patients with chronic pancreatitis, *Pancreatology.* **11**, 16-23.
6. Brand, R. E., Greer, J. B., Zolotarevsky, E., Brand, R., Du, H., Simeone, D., Zisman, A., Gorchow, A., Lee, S. Y., Roy, H. K. & Anderson, M. A. (2009) Pancreatic cancer patients who smoke and drink are diagnosed at younger ages, *Clinical gastroenterology and hepatology : the official clinical practice journal of the American Gastroenterological Association.* **7**, 1007-12.
7. Munigala, S., Kanwal, F., Xian, H. & Agarwal, B. (2014) New diagnosis of chronic pancreatitis: risk of missing an underlying pancreatic cancer, *The American journal of gastroenterology.* **109**, 1824-30.
8. Solomon, S., Das, S., Brand, R. & Whitcomb, D. C. (2012) Inherited pancreatic cancer syndromes, *Cancer J.* **18**, 485-91.
9. McWilliams, R. R., Wieben, E. D., Rabe, K. G., Pedersen, K. S., Wu, Y., Sicotte, H. & Petersen, G. M. (2011) Prevalence of CDKN2A mutations in pancreatic cancer patients: implications for genetic counseling, *European journal of human genetics : EJHG.* **19**, 472-8.
10. Hruban, R. H., Goggins, M., Parsons, J. & Kern, S. E. (2000) Progression model for pancreatic cancer, *Clinical cancer research : an official journal of the American Association for Cancer Research.* **6**, 2969-72.
11. Yachida, S., Jones, S., Bozic, I., Antal, T., Leary, R., Fu, B., Kamiyama, M., Hruban, R. H., Eshleman, J. R., Nowak, M. A., Velculescu, V. E., Kinzler, K. W., Vogelstein, B. & Iacobuzio-Donahue, C. A. (2010) Distant metastasis occurs late during the genetic evolution of pancreatic cancer, *Nature.* **467**, 1114-7.
12. Casper, E. S., Green, M. R., Kelsen, D. P., Heelan, R. T., Brown, T. D., Flombaum, C. D., Trochanowski, B. & Tarassoff, P. G. (1994) Phase II trial of gemcitabine (2,2'-difluorodeoxycytidine) in patients with adenocarcinoma of the pancreas, *Investigational new drugs.* **12**, 29-34.
13. Vaccaro, V., Sperduti, I. & Milella, M. (2011) FOLFIRINOX versus gemcitabine for metastatic pancreatic cancer, *The New England journal of medicine.* **365**, 768-9; author reply 769.

14. Von Hoff, D. D., Ervin, T., Arena, F. P., Chiorean, E. G., Infante, J., Moore, M., Seay, T., Tjulandin, S. A., Ma, W. W., Saleh, M. N., Harris, M., Reni, M., Dowden, S., Laheru, D., Bahary, N., Ramanathan, R. K., Tabernero, J., Hidalgo, M., Goldstein, D., Van Cutsem, E., Wei, X., Iglesias, J. & Renschler, M. F. (2013) Increased survival in pancreatic cancer with nab-paclitaxel plus gemcitabine, *The New England journal of medicine.* **369**, 1691-703.
15. Troiani, T., Martinelli, E., Capasso, A., Morgillo, F., Orditura, M., De Vita, F. & Ciardiello, F. (2012) Targeting EGFR in pancreatic cancer treatment, *Current drug targets.* **13**, 802-10.
16. Kelley, R. K. & Ko, A. H. (2008) Erlotinib in the treatment of advanced pancreatic cancer, *Biologics : targets & therapy.* **2**, 83-95.
17. Senderowicz, A. M., Johnson, J. R., Sridhara, R., Zimmerman, P., Justice, R. & Pazdur, R. (2007) Erlotinib/gemcitabine for first-line treatment of locally advanced or metastatic adenocarcinoma of the pancreas, *Oncology (Williston Park).* **21**, 1696-706; discussion 1706-9, 1712, 1715.
18. Moore, M. J., Goldstein, D., Hamm, J., Figer, A., Hecht, J. R., Gallinger, S., Au, H. J., Murawa, P., Walde, D., Wolff, R. A., Campos, D., Lim, R., Ding, K., Clark, G., Voskoglou-Nomikos, T., Ptasynski, M. & Parulekar, W. (2007) Erlotinib plus gemcitabine compared with gemcitabine alone in patients with advanced pancreatic cancer: a phase III trial of the National Cancer Institute of Canada Clinical Trials Group, *Journal of clinical oncology : official journal of the American Society of Clinical Oncology.* **25**, 1960-6.
19. Macdonald, J. S., McCoy, S., Whitehead, R. P., Iqbal, S., Wade, J. L., 3rd, Giguere, J. K. & Abbruzzese, J. L. (2005) A phase II study of farnesyl transferase inhibitor R115777 in pancreatic cancer: a Southwest oncology group (SWOG 9924) study, *Investigational new drugs.* **23**, 485-7.
20. Murray, A. (1995) Cyclin ubiquitination: the destructive end of mitosis, *Cell.* **81**, 149-52.
21. Obaya, A. J. & Sedivy, J. M. (2002) Regulation of cyclin-Cdk activity in mammalian cells, *Cellular and molecular life sciences : CMLS.* **59**, 126-42.
22. Morgan, D. O., Fisher, R. P., Espinoza, F. H., Farrell, A., Nourse, J., Chamberlin, H. & Jin, P. (1998) Control of eukaryotic cell cycle progression by phosphorylation of cyclin-dependent kinases, *The cancer journal from Scientific American.* **4 Suppl 1**, S77-83.
23. Malumbres, M. & Barbacid, M. (2009) Cell cycle, CDKs and cancer: a changing paradigm, *Nature reviews Cancer.* **9**, 153-66.
24. Johnson, D. G. & Walker, C. L. (1999) Cyclins and cell cycle checkpoints, *Annual review of pharmacology and toxicology.* **39**, 295-312.
25. Giono, L. E. & Manfredi, J. J. (2006) The p53 tumor suppressor participates in multiple cell cycle checkpoints, *Journal of cellular physiology.* **209**, 13-20.
26. Bertoli, C., Skotheim, J. M. & de Bruin, R. A. (2013) Control of cell cycle transcription during G1 and S phases, *Nature reviews Molecular cell biology.* **14**, 518-28.
27. Zhou, B. B. & Elledge, S. J. (2000) The DNA damage response: putting checkpoints in perspective, *Nature.* **408**, 433-9.

28. Sherr, C. J. & McCormick, F. (2002) The RB and p53 pathways in cancer, *Cancer cell.* **2**, 103-12.
29. Hruban, R. H., Offerhaus, G. J., Kern, S. E., Goggins, M., Wilentz, R. E. & Yeo, C. J. (1998) Tumor-suppressor genes in pancreatic cancer, *Journal of hepato-biliary-pancreatic surgery.* **5**, 383-91.
30. Furukawa, T. & Horii, A. (2004) Molecular pathology of pancreatic cancer: in quest of tumor suppressor genes, *Pancreas.* **28**, 253-6.
31. Barton, C. M., Staddon, S. L., Hughes, C. M., Hall, P. A., O'Sullivan, C., Kloppel, G., Theis, B., Russell, R. C., Neoptolemos, J., Williamson, R. C. & et al. (1991) Abnormalities of the p53 tumour suppressor gene in human pancreatic cancer, *British journal of cancer.* **64**, 1076-82.
32. Moskaluk, C. A., Hruban, R. H. & Kern, S. E. (1997) p16 and K-ras gene mutations in the intraductal precursors of human pancreatic adenocarcinoma, *Cancer research.* **57**, 2140-3.
33. Wilentz, R. E., Iacobuzio-Donahue, C. A., Argani, P., McCarthy, D. M., Parsons, J. L., Yeo, C. J., Kern, S. E. & Hruban, R. H. (2000) Loss of expression of Dpc4 in pancreatic intraepithelial neoplasia: evidence that DPC4 inactivation occurs late in neoplastic progression, *Cancer research.* **60**, 2002-6.
34. Goldstein, A. M., Fraser, M. C., Struewing, J. P., Hussussian, C. J., Ranade, K., Zametkin, D. P., Fontaine, L. S., Organic, S. M., Dracopoli, N. C., Clark, W. H., Jr. & et al. (1995) Increased risk of pancreatic cancer in melanoma-prone kindreds with p16INK4 mutations, *The New England journal of medicine.* **333**, 970-4.
35. Sherr, C. J. (2001) The INK4a/ARF network in tumour suppression, *Nature reviews Molecular cell biology.* **2**, 731-7.
36. Sherman, M. Y., Meng, L., Stampfer, M., Gabai, V. L. & Yaglom, J. A. (2011) Oncogenes induce senescence with incomplete growth arrest and suppress the DNA damage response in immortalized cells, *Aging cell.* **10**, 949-61.
37. Qiu, W., Sahin, F., Iacobuzio-Donahue, C. A., Garcia-Carracedo, D., Wang, W. M., Kuo, C. Y., Chen, D., Arking, D. E., Lowy, A. M., Hruban, R. H., Remotti, H. E. & Su, G. H. (2011) Disruption of p16 and activation of Kras in pancreas increase ductal adenocarcinoma formation and metastasis in vivo, *Oncotarget.* **2**, 862-73.
38. Lundberg, A. S. & Weinberg, R. A. (1998) Functional inactivation of the retinoblastoma protein requires sequential modification by at least two distinct cyclin-cdk complexes, *Molecular and cellular biology.* **18**, 753-61.
39. Roskoski, R., Jr. (2016) Cyclin-dependent protein kinase inhibitors including palbociclib as anticancer drugs, *Pharmacological research.* **107**, 249-275.
40. Trimarchi, J. M. & Lees, J. A. (2002) Sibling rivalry in the E2F family, *Nature reviews Molecular cell biology.* **3**, 11-20.
41. Gore, A. J., Deitz, S. L., Palam, L. R., Craven, K. E. & Korc, M. (2014) Pancreatic cancer-associated retinoblastoma 1 dysfunction enables TGF-beta to promote proliferation, *The Journal of clinical investigation.* **124**, 338-52.
42. Gansauge, S., Gansauge, F., Ramadani, M., Stobbe, H., Rau, B., Harada, N. & Beger, H. G. (1997) Overexpression of cyclin D1 in human pancreatic carcinoma is associated with poor prognosis, *Cancer research.* **57**, 1634-7.
43. Knockaert, M., Greengard, P. & Meijer, L. (2002) Pharmacological inhibitors of cyclin-dependent kinases, *Trends in pharmacological sciences.* **23**, 417-25.

44. Asghar, U., Witkiewicz, A. K., Turner, N. C. & Knudsen, E. S. (2015) The history and future of targeting cyclin-dependent kinases in cancer therapy, *Nature reviews Drug discovery.* **14**, 130-46.
45. Fry, D. W., Harvey, P. J., Keller, P. R., Elliott, W. L., Meade, M., Trachet, E., Albassam, M., Zheng, X., Leopold, W. R., Pryer, N. K. & Toogood, P. L. (2004) Specific inhibition of cyclin-dependent kinase 4/6 by PD 0332991 and associated antitumor activity in human tumor xenografts, *Molecular cancer therapeutics.* **3**, 1427-38.
46. Leonard, J. P., LaCasce, A. S., Smith, M. R., Noy, A., Chirieac, L. R., Rodig, S. J., Yu, J. Q., Vallabhajosula, S., Schoder, H., English, P., Neuberg, D. S., Martin, P., Millenson, M. M., Ely, S. A., Courtney, R., Shaik, N., Wilner, K. D., Randolph, S., Van den Abbeele, A. D., Chen-Kiang, S. Y., Yap, J. T. & Shapiro, G. I. (2012) Selective CDK4/6 inhibition with tumor responses by PD0332991 in patients with mantle cell lymphoma, *Blood.* **119**, 4597-607.
47. Dickson, M. A., Tap, W. D., Keohan, M. L., D'Angelo, S. P., Gounder, M. M., Antonescu, C. R., Landa, J., Qin, L. X., Rathbone, D. D., Condy, M. M., Ustoyev, Y., Crago, A. M., Singer, S. & Schwartz, G. K. (2013) Phase II trial of the CDK4 inhibitor PD0332991 in patients with advanced CDK4-amplified well-differentiated or dedifferentiated liposarcoma, *Journal of clinical oncology : official journal of the American Society of Clinical Oncology.* **31**, 2024-8.
48. Finn, R. S., Crown, J. P., Lang, I., Boer, K., Bondarenko, I. M., Kulyk, S. O., Ettl, J., Patel, R., Pinter, T., Schmidt, M., Shparyk, Y., Thummala, A. R., Voytko, N. L., Fowst, C., Huang, X., Kim, S. T., Randolph, S. & Slamon, D. J. (2015) The cyclin-dependent kinase 4/6 inhibitor palbociclib in combination with letrozole versus letrozole alone as first-line treatment of oestrogen receptor-positive, HER2-negative, advanced breast cancer (PALOMA-1/TRIO-18): a randomised phase 2 study, *The Lancet Oncology.* **16**, 25-35.
49. Kanda, M., Matthaei, H., Wu, J., Hong, S. M., Yu, J., Borges, M., Hruban, R. H., Maitra, A., Kinzler, K., Vogelstein, B. & Goggins, M. (2012) Presence of somatic mutations in most early-stage pancreatic intraepithelial neoplasia, *Gastroenterology.* **142**, 730-733 e9.
50. Pylayeva-Gupta, Y., Grabocka, E. & Bar-Sagi, D. (2011) RAS oncogenes: weaving a tumorigenic web, *Nature reviews Cancer.* **11**, 761-74.
51. Lu, S., Jang, H., Nussinov, R. & Zhang, J. (2016) The Structural Basis of Oncogenic Mutations G12, G13 and Q61 in Small GTPase K-Ras4B, *Scientific reports.* **6**, 21949.
52. Prior, I. A., Lewis, P. D. & Mattos, C. (2012) A comprehensive survey of Ras mutations in cancer, *Cancer research.* **72**, 2457-67.
53. Eser, S., Schnieke, A., Schneider, G. & Saur, D. (2014) Oncogenic KRAS signalling in pancreatic cancer, *British journal of cancer.* **111**, 817-22.
54. Hruban, R. H., Adsay, N. V., Albores-Saavedra, J., Anver, M. R., Biankin, A. V., Boivin, G. P., Furth, E. E., Furukawa, T., Klein, A., Klimstra, D. S., Kloppel, G., Lauwers, G. Y., Longnecker, D. S., Luttges, J., Maitra, A., Offerhaus, G. J., Perez-Gallego, L., Redston, M. & Tuveson, D. A. (2006) Pathology of genetically engineered mouse models of pancreatic exocrine cancer: consensus report and recommendations, *Cancer research.* **66**, 95-106.

55. Mazur, P. K. & Siveke, J. T. (2012) Genetically engineered mouse models of pancreatic cancer: unravelling tumour biology and progressing translational oncology, *Gut.* **61**, 1488-500.
56. Payne, S. N., Maher, M. E., Tran, N. H., Van De Hey, D. R., Foley, T. M., Yueh, A. E., Leystra, A. A., Pasch, C. A., Jeffrey, J. J., Clipson, L., Matkowskyj, K. A. & Deming, D. A. (2015) PIK3CA mutations can initiate pancreatic tumorigenesis and are targetable with PI3K inhibitors, *Oncogenesis.* **4**, e169.
57. Collisson, E. A., Trejo, C. L., Silva, J. M., Gu, S., Korkola, J. E., Heiser, L. M., Charles, R. P., Rabinovich, B. A., Hann, B., Dankort, D., Spellman, P. T., Phillips, W. A., Gray, J. W. & McMahon, M. (2012) A central role for RAF-->MEK-->ERK signaling in the genesis of pancreatic ductal adenocarcinoma, *Cancer discovery.* **2**, 685-93.
58. Alagesan, B., Contino, G., Guimaraes, A. R., Corcoran, R. B., Deshpande, V., Wojtkiewicz, G. R., Hezel, A. F., Wong, K. K., Loda, M., Weissleder, R., Benes, C., Engelman, J. A. & Bardeesy, N. (2015) Combined MEK and PI3K inhibition in a mouse model of pancreatic cancer, *Clinical cancer research : an official journal of the American Association for Cancer Research.* **21**, 396-404.
59. Zhong, H., Sanchez, C., Spitzer, D., Plambeck-Suess, S., Gibbs, J., Hawkins, W. G., Denardo, D., Gao, F., Pufahl, R. A., Lockhart, A. C., Xu, M., Linehan, D., Weber, J. & Wang-Gillam, A. (2013) Synergistic effects of concurrent blockade of PI3K and MEK pathways in pancreatic cancer preclinical models, *PloS one.* **8**, e77243.
60. Son, J., Lyssiotis, C. A., Ying, H., Wang, X., Hua, S., Ligorio, M., Perera, R. M., Ferrone, C. R., Mullarky, E., Shyh-Chang, N., Kang, Y., Fleming, J. B., Bardeesy, N., Asara, J. M., Haigis, M. C., DePinho, R. A., Cantley, L. C. & Kimmelman, A. C. (2013) Glutamine supports pancreatic cancer growth through a KRAS-regulated metabolic pathway, *Nature.* **496**, 101-5.
61. Ying, H., Kimmelman, A. C., Lyssiotis, C. A., Hua, S., Chu, G. C., Fletcher-Sananikone, E., Locasale, J. W., Son, J., Zhang, H., Coloff, J. L., Yan, H., Wang, W., Chen, S., Viale, A., Zheng, H., Paik, J. H., Lim, C., Guimaraes, A. R., Martin, E. S., Chang, J., Hezel, A. F., Perry, S. R., Hu, J., Gan, B., Xiao, Y., Asara, J. M., Weissleder, R., Wang, Y. A., Chin, L., Cantley, L. C. & DePinho, R. A. (2012) Oncogenic Kras maintains pancreatic tumors through regulation of anabolic glucose metabolism, *Cell.* **149**, 656-70.
62. Bryant, K. L., Mancias, J. D., Kimmelman, A. C. & Der, C. J. (2014) KRAS: feeding pancreatic cancer proliferation, *Trends in biochemical sciences.* **39**, 91-100.
63. Baek, G., Tse, Y. F., Hu, Z., Cox, D., Buboltz, N., McCue, P., Yeo, C. J., White, M. A., DeBerardinis, R. J., Knudsen, E. S. & Witkiewicz, A. K. (2014) MCT4 defines a glycolytic subtype of pancreatic cancer with poor prognosis and unique metabolic dependencies, *Cell reports.* **9**, 2233-49.
64. Weinberg, F., Hamanaka, R., Wheaton, W. W., Weinberg, S., Joseph, J., Lopez, M., Kalyanaraman, B., Mutlu, G. M., Budinger, G. R. & Chandel, N. S. (2010) Mitochondrial metabolism and ROS generation are essential for Kras-mediated tumorigenicity, *Proceedings of the National Academy of Sciences of the United States of America.* **107**, 8788-93.
65. Landry, W. D. & Cotter, T. G. (2014) ROS signalling, NADPH oxidases and cancer, *Biochemical Society transactions.* **42**, 934-8.
66. Lee, J. K., Edderkaoui, M., Truong, P., Ohno, I., Jang, K. T., Berti, A., Pandol, S. J. & Gukovskaya, A. S. (2007) NADPH oxidase promotes pancreatic cancer cell survival

via inhibiting JAK2 dephosphorylation by tyrosine phosphatases, *Gastroenterology.* **133**, 1637-48.
67. DeNicola, G. M., Karreth, F. A., Humpton, T. J., Gopinathan, A., Wei, C., Frese, K., Mangal, D., Yu, K. H., Yeo, C. J., Calhoun, E. S., Scrimieri, F., Winter, J. M., Hruban, R. H., Iacobuzio-Donahue, C., Kern, S. E., Blair, I. A. & Tuveson, D. A. (2011) Oncogene-induced Nrf2 transcription promotes ROS detoxification and tumorigenesis, *Nature.* **475**, 106-9.
68. Paulson, A. S., Tran Cao, H. S., Tempero, M. A. & Lowy, A. M. (2013) Therapeutic advances in pancreatic cancer, *Gastroenterology.* **144**, 1316-26.
69. Kleger, A., Perkhofer, L. & Seufferlein, T. (2014) Smarter drugs emerging in pancreatic cancer therapy, *Annals of oncology : official journal of the European Society for Medical Oncology / ESMO*.
70. Almhanna, K. & Philip, P. A. Defining new paradigms for the treatment of pancreatic cancer, *Curr Treat Options Oncol.* **12**, 111-25.
71. Philip, P. A., Mooney, M., Jaffe, D., Eckhardt, G., Moore, M., Meropol, N., Emens, L., O'Reilly, E., Korc, M., Ellis, L., Benedetti, J., Rothenberg, M., Willett, C., Tempero, M., Lowy, A., Abbruzzese, J., Simeone, D., Hingorani, S., Berlin, J. & Tepper, J. (2009) Consensus report of the national cancer institute clinical trials planning meeting on pancreas cancer treatment, *J Clin Oncol.* **27**, 5660-9.
72. Cowan, R. W. & Maitra, A. (2014) Genetic progression of pancreatic cancer, *Cancer journal.* **20**, 80-4.
73. Yachida, S. & Iacobuzio-Donahue, C. A. (2013) Evolution and dynamics of pancreatic cancer progression, *Oncogene.* **32**, 5253-60.
74. Chu, T. M. (1997) Molecular diagnosis of pancreas carcinoma, *J Clin Lab Anal.* **11**, 225-31.
75. Witkiewicz, A. K., Knudsen, K. E., Dicker, A. P. & Knudsen, E. S. (2011) The meaning of p16(ink4a) expression in tumors: functional significance, clinical associations and future developments, *Cell Cycle.* **10**, 2497-503.
76. Bardeesy, N., Aguirre, A. J., Chu, G. C., Cheng, K. H., Lopez, L. V., Hezel, A. F., Feng, B., Brennan, C., Weissleder, R., Mahmood, U., Hanahan, D., Redston, M. S., Chin, L. & Depinho, R. A. (2006) Both p16(Ink4a) and the p19(Arf)-p53 pathway constrain progression of pancreatic adenocarcinoma in the mouse, *Proc Natl Acad Sci U S A.* **103**, 5947-52.
77. Serrano, M., Lin, A. W., McCurrach, M. E., Beach, D. & Lowe, S. W. (1997) Oncogenic ras provokes premature cell senescence associated with accumulation of p53 and p16INK4a, *Cell.* **88**, 593-602.
78. Narita, M., Nunez, S., Heard, E., Lin, A. W., Hearn, S. A., Spector, D. L., Hannon, G. J. & Lowe, S. W. (2003) Rb-mediated heterochromatin formation and silencing of E2F target genes during cellular senescence, *Cell.* **113**, 703-16.
79. Herreros-Villanueva, M., Hijona, E., Cosme, A. & Bujanda, L. (2012) Mouse models of pancreatic cancer, *World journal of gastroenterology.* **18**, 1286-94.
80. Serrano, M., Gomez-Lahoz, E., DePinho, R. A., Beach, D. & Bar-Sagi, D. (1995) Inhibition of ras-induced proliferation and cellular transformation by p16INK4, *Science.* **267**, 249-52.

81. Calbo, J., Marotta, M., Cascallo, M., Roig, J. M., Gelpi, J. L., Fueyo, J. & Mazo, A. (2001) Adenovirus-mediated wt-p16 reintroduction induces cell cycle arrest or apoptosis in pancreatic cancer, *Cancer gene therapy.* **8**, 740-50.
82. Chen, F., Li, Y., Lu, Z., Gao, J. & Chen, J. (2005) Adenovirus-mediated Ink4a/ARF gene transfer significantly suppressed the growth of pancreatic carcinoma cells, *Cancer Biol Ther.* **4**, 1348-54.
83. Lukas, J., Sorensen, C. S., Lukas, C., Santoni-Rugiu, E. & Bartek, J. (1999) p16INK4a, but not constitutively active pRb, can impose a sustained G1 arrest: molecular mechanisms and implications for oncogenesis, *Oncogene.* **18**, 3930-5.
84. Xiong, Y., Zhang, H. & Beach, D. (1993) Subunit rearrangement of the cyclin-dependent kinases is associated with cellular transformation, *Genes Dev.* **7**, 1572-83.
85. Pavletich, N. P. (1999) Mechanisms of cyclin-dependent kinase regulation: structures of Cdks, their cyclin activators, and Cip and INK4 inhibitors, *Journal of molecular biology.* **287**, 821-8.
86. Russo, A. A., Tong, L., Lee, J. O., Jeffrey, P. D. & Pavletich, N. P. (1998) Structural basis for inhibition of the cyclin-dependent kinase Cdk6 by the tumour suppressor p16INK4a, *Nature.* **395**, 237-43.
87. Malumbres, M. & Barbacid, M. (2006) Is Cyclin D1-CDK4 kinase a bona fide cancer target?, *Cancer Cell.* **9**, 2-4.
88. Serrano, M., Hannon, G. J. & Beach, D. (1993) A new regulatory motif in cell-cycle control causing specific inhibition of cyclin D/CDK4, *Nature.* **366**, 704-7.
89. Koh, J., Enders, G. H., Dynlacht, B. D. & Harlow, E. (1995) Tumour-derived p16 alleles encoding proteins defective in cell-cycle inhibition, *Nature.* **375**, 506-10.
90. Zuo, L., Weger, J., Yang, Q., Goldstein, A. M., Tucker, M. A., Walker, G. J., Hayward, N. & Dracopoli, N. C. (1996) Germline mutations in the p16INK4a binding domain of CDK4 in familial melanoma, *Nat Genet.* **12**, 97-9.
91. Bartkova, J., Lukas, J., Guldberg, P., Alsner, J., Kirkin, A. F., Zeuthen, J. & Bartek, J. (1996) The p16-cyclin D/Cdk4-pRb pathway as a functional unit frequently altered in melanoma pathogenesis, *Cancer Res.* **56**, 5475-83.
92. Lukas, J., Parry, D., Aagaard, L., Mann, D. J., Bartkova, J., Strauss, M., Peters, G. & Bartek, J. (1995) Retinoblastoma-protein-dependent cell-cycle inhibition by the tumour suppressor p16, *Nature.* **375**, 503-6.
93. Shapiro, G. I., Edwards, C. D., Kobzik, L., Godleski, J., Richards, W., Sugarbaker, D. J. & Rollins, B. J. (1995) Reciprocal Rb inactivation and p16INK4 expression in primary lung cancers and cell lines, *Cancer Res.* **55**, 505-9.
94. Kaye, F. J. (2002) RB and cyclin dependent kinase pathways: defining a distinction between RB and p16 loss in lung cancer, *Oncogene.* **21**, 6908-14.
95. Toogood, P. L., Harvey, P. J., Repine, J. T., Sheehan, D. J., VanderWel, S. N., Zhou, H., Keller, P. R., McNamara, D. J., Sherry, D., Zhu, T., Brodfuehrer, J., Choi, C., Barvian, M. R. & Fry, D. W. (2005) Discovery of a potent and selective inhibitor of cyclin-dependent kinase 4/6, *Journal of medicinal chemistry.* **48**, 2388-406.
96. Michaud, K., Solomon, D. A., Oermann, E., Kim, J. S., Zhong, W. Z., Prados, M. D., Ozawa, T., James, C. D. & Waldman, T. (2010) Pharmacologic inhibition of cyclin-dependent kinases 4 and 6 arrests the growth of glioblastoma multiforme intracranial xenografts, *Cancer Res.* **70**, 3228-38.

97. Rivadeneira, D. B., Mayhew, C. N., Thangavel, C., Sotillo, E., Reed, C. A., Grana, X. & Knudsen, E. S. (2010) Proliferative suppression by CDK4/6 inhibition: complex function of the retinoblastoma pathway in liver tissue and hepatoma cells, *Gastroenterology.* **138**, 1920-30.
98. Dean, J. L., Thangavel, C., McClendon, A. K., Reed, C. A. & Knudsen, E. S. (2010) Therapeutic CDK4/6 inhibition in breast cancer: key mechanisms of response and failure, *Oncogene.* **29**, 4018-32.
99. Markey, M. P., Angus, S. P., Strobeck, M. W., Williams, S. L., Gunawardena, R. W., Aronow, B. J. & Knudsen, E. S. (2002) Unbiased analysis of RB-mediated transcriptional repression identifies novel targets and distinctions from E2F action, *Cancer Res.* **62**, 6587-97.
100. Dean, J. L., McClendon, A. K., Hickey, T. E., Butler, L. M., Tilley, W. D., Witkiewicz, A. K. & Knudsen, E. S. Therapeutic response to CDK4/6 inhibition in breast cancer defined by ex vivo analyses of human tumors, *Cell Cycle.* **11**, 2756-61.
101. Dean, J. L., McClendon, A. K. & Knudsen, E. S. Modification of the DNA damage response by therapeutic CDK4/6 inhibition, *J Biol Chem*.
102. McClendon, A. K., Dean, J. L., Rivadeneira, D. B., Yu, J. E., Reed, C. A., Gao, E., Farber, J. L., Force, T., Koch, W. J. & Knudsen, E. S. CDK4/6 inhibition antagonizes the cytotoxic response to anthracycline therapy, *Cell Cycle.* **11**, 2747-55.
103. Konecny, G. E., Winterhoff, B., Kolarova, T., Qi, J., Manivong, K., Dering, J., Yang, G., Chalukya, M., Wang, H. J., Anderson, L., Kalli, K. R., Finn, R. S., Ginther, C., Jones, S., Velculescu, V. E., Riehle, D., Cliby, W. A., Randolph, S., Koehler, M., Hartmann, L. C. & Slamon, D. J. Expression of p16 and retinoblastoma determines response to CDK4/6 inhibition in ovarian cancer, *Clin Cancer Res.* **17**, 1591-602.
104. Finn, R. S., Dering, J., Conklin, D., Kalous, O., Cohen, D. J., Desai, A. J., Ginther, C., Atefi, M., Chen, I., Fowst, C., Los, G. & Slamon, D. J. (2009) PD 0332991, a selective cyclin D kinase 4/6 inhibitor, preferentially inhibits proliferation of luminal estrogen receptor-positive human breast cancer cell lines in vitro, *Breast Cancer Res.* **11**, R77.
105. Anders, L., Ke, N., Hydbring, P., Choi, Y. J., Widlund, H. R., Chick, J. M., Zhai, H., Vidal, M., Gygi, S. P., Braun, P. & Sicinski, P. (2011) A systematic screen for CDK4/6 substrates links FOXM1 phosphorylation to senescence suppression in cancer cells, *Cancer Cell.* **20**, 620-34.
106. Sadasivam, S., Duan, S. & DeCaprio, J. A. (2012) The MuvB complex sequentially recruits B-Myb and FoxM1 to promote mitotic gene expression, *Genes Dev.* **26**, 474-89.
107. Leonard, J. P., LaCasce, A. S., Smith, M. R., Noy, A., Chirieac, L. R., Rodig, S. J., Yu, J. Q., Vallabhajosula, S., Schoder, H., English, P., Neuberg, D. S., Martin, P., Millenson, M. M., Ely, S. A., Courtney, R., Shaik, N., Wilner, K. D., Randolph, S., Van den Abbeele, A. D., Chen-Kiang, S. Y., Yap, J. T. & Shapiro, G. I. Selective CDK4/6 inhibition with tumor responses by PD0332991 in patients with mantle cell lymphoma, *Blood.* **119**, 4597-607.
108. Schwartz, G. K., LoRusso, P. M., Dickson, M. A., Randolph, S. S., Shaik, M. N., Wilner, K. D., Courtney, R. & O'Dwyer, P. J. (2011) Phase I study of PD 0332991, a cyclin-dependent kinase inhibitor, administered in 3-week cycles (Schedule 2/1), *Br J Cancer.* **104**, 1862-8.

109. Flaherty, K. T., Lorusso, P. M., Demichele, A., Abramson, V. G., Courtney, R., Randolph, S. S., Shaik, M. N., Wilner, K. D., O'Dwyer, P. J. & Schwartz, G. K. (2012) Phase I, dose-escalation trial of the oral cyclin-dependent kinase 4/6 inhibitor PD 0332991, administered using a 21-day schedule in patients with advanced cancer, *Clin Cancer Res.* **18**, 568-76.
110. Lange, C. A. & Yee, D. (2011) Killing the second messenger: targeting loss of cell cycle control in endocrine-resistant breast cancer, *Endocr Relat Cancer.* **18**, C19-24.
111. Thangavel, C., Dean, J. L., Ertel, A., Knudsen, K. E., Aldaz, C. M., Witkiewicz, A. K., Clarke, R. & Knudsen, E. S. (2011) Therapeutically activating RB: reestablishing cell cycle control in endocrine therapy-resistant breast cancer, *Endocr Relat Cancer.* **18**, 333-45.
112. Guha, M. (2013) Blockbuster dreams for Pfizer's CDK inhibitor, *Nature biotechnology.* **31**, 187.
113. Dickson, M. A. (2014) Molecular Pathways: CDK4 Inhibitors for Cancer Therapy, *Clin Cancer Res.* **20**, 3379-83.
114. Rocca, A., Farolfi, A., Bravaccini, S., Schirone, A. & Amadori, D. (2014) Palbociclib (PD 0332991) : targeting the cell cycle machinery in breast cancer, *Expert opinion on pharmacotherapy.* **15**, 407-20.
115. Kwong, L. N., Costello, J. C., Liu, H., Jiang, S., Helms, T. L., Langsdorf, A. E., Jakubosky, D., Genovese, G., Muller, F. L., Jeong, J. H., Bender, R. P., Chu, G. C., Flaherty, K. T., Wargo, J. A., Collins, J. J. & Chin, L. (2012) Oncogenic NRAS signaling differentially regulates survival and proliferation in melanoma, *Nature medicine.* **18**, 1503-10.
116. Liu, F. & Korc, M. (2012) Cdk4/6 inhibition induces epithelial-mesenchymal transition and enhances invasiveness in pancreatic cancer cells, *Mol Cancer Ther.* **11**, 2138-48.
117. Chicas, A., Wang, X., Zhang, C., McCurrach, M., Zhao, Z., Mert, O., Dickins, R. A., Narita, M., Zhang, M. & Lowe, S. W. (2010) Dissecting the unique role of the retinoblastoma tumor suppressor during cellular senescence, *Cancer Cell.* **17**, 376-87.
118. Caldon, C. E., Sergio, C. M., Kang, J., Muthukaruppan, A., Boersma, M. N., Stone, A., Barraclough, J., Lee, C. S., Black, M. A., Miller, L. D., Gee, J. M., Nicholson, R. I., Sutherland, R. L., Print, C. G. & Musgrove, E. A. (2012) Cyclin E2 overexpression is associated with endocrine resistance but not insensitivity to CDK2 inhibition in human breast cancer cells, *Mol Cancer Ther.* **11**, 1488-99.
119. Roberts, P. J., Bisi, J. E., Strum, J. C., Combest, A. J., Darr, D. B., Usary, J. E., Zamboni, W. C., Wong, K. K., Perou, C. M. & Sharpless, N. E. (2012) Multiple roles of cyclin-dependent kinase 4/6 inhibitors in cancer therapy, *J Natl Cancer Inst.* **104**, 476-87.
120. Angus, S. P., Wheeler, L. J., Ranmal, S. A., Zhang, X., Markey, M. P., Mathews, C. K. & Knudsen, E. S. (2002) Retinoblastoma tumor suppressor targets dNTP metabolism to regulate DNA replication, *J Biol Chem.* **277**, 44376-84.
121. Infante, J. R., Somer, B. G., Park, J. O., Li, C. P., Scheulen, M. E., Kasubhai, S. M., Oh, D. Y., Liu, Y., Redhu, S., Steplewski, K. & Le, N. (2014) A randomised, double-blind, placebo-controlled trial of trametinib, an oral MEK inhibitor, in combination with

gemcitabine for patients with untreated metastatic adenocarcinoma of the pancreas, *Eur J Cancer*.
122. Leontieva, O. V. & Blagosklonny, M. V. (2013) CDK4/6-inhibiting drug substitutes for p21 and p16 in senescence: duration of cell cycle arrest and MTOR activity determine geroconversion, *Cell Cycle.* **12**, 3063-9.
123. Leontieva, O. V., Demidenko, Z. N. & Blagosklonny, M. V. (2013) MEK drives cyclin D1 hyperelevation during geroconversion, *Cell death and differentiation.* **20**, 1241-9.
124. (2014) Palbociclib ups PFS in HER2-/ER+ breast cancer, *Cancer Discov.* **4**, 624-5.
125. Musgrove, E. A. & Sutherland, R. L. (2009) Biological determinants of endocrine resistance in breast cancer, *Nat Rev Cancer.* **9**, 631-43.
126. Saif, M. W. (2013) Advancements in the management of pancreatic cancer: 2013, *JOP : Journal of the pancreas.* **14**, 112-8.
127. Vincent, A., Herman, J., Schulick, R., Hruban, R. H. & Goggins, M. (2011) Pancreatic cancer, *Lancet.* **378**, 607-20.
128. Maitra, A. & Hruban, R. H. (2008) Pancreatic cancer, *Annual review of pathology.* **3**, 157-88.
129. LaPak, K. M. & Burd, C. E. (2014) The molecular balancing act of p16(INK4a) in cancer and aging, *Molecular cancer research : MCR.* **12**, 167-83.
130. Franco, J., Witkiewicz, A. K. & Knudsen, E. S. (2014) CDK4/6 inhibitors have potent activity in combination with pathway selective therapeutic agents in models of pancreatic cancer, *Oncotarget.* **5**, 6512-25.
131. Heilmann, A. M., Perera, R. M., Ecker, V., Nicolay, B. N., Bardeesy, N., Benes, C. H. & Dyson, N. J. (2014) CDK4/6 and IGF1 receptor inhibitors synergize to suppress the growth of p16INK4A-deficient pancreatic cancers, *Cancer research.* **74**, 3947-58.
132. Witkiewicz, A. K., Borja, N. A., Franco, J., Brody, J. R., Yeo, C. J., Mansour, J., Choti, M. A., McCue, P. & Knudsen, E. S. (2015) Selective impact of CDK4/6 suppression on patient-derived models of pancreatic cancer, *Oncotarget.* **6**, 15788-801.
133. Cai, L. & Tu, B. P. (2012) Driving the cell cycle through metabolism, *Annual review of cell and developmental biology.* **28**, 59-87.
134. Sousa, C. M. & Kimmelman, A. C. (2014) The Complex landscape of pancreatic cancer metabolism, *Carcinogenesis*.
135. Viale, A., Pettazzoni, P., Lyssiotis, C. A., Ying, H., Sanchez, N., Marchesini, M., Carugo, A., Green, T., Seth, S., Giuliani, V., Kost-Alimova, M., Muller, F., Colla, S., Nezi, L., Genovese, G., Deem, A. K., Kapoor, A., Yao, W., Brunetto, E., Kang, Y., Yuan, M., Asara, J. M., Wang, Y. A., Heffernan, T. P., Kimmelman, A. C., Wang, H., Fleming, J. B., Cantley, L. C., DePinho, R. A. & Draetta, G. F. (2014) Oncogene ablation-resistant pancreatic cancer cells depend on mitochondrial function, *Nature.* **514**, 628-32.
136. Laplante, M. & Sabatini, D. M. (2009) mTOR signaling at a glance, *Journal of cell science.* **122**, 3589-94.
137. Laplante, M. & Sabatini, D. M. (2012) mTOR Signaling, *Cold Spring Harbor perspectives in biology.* **4**.
138. Lopez-Mejia, I. C. & Fajas, L. (2015) Cell cycle regulation of mitochondrial function, *Current opinion in cell biology.* **33**, 19-25.

139. Wang, C., Li, Z., Lu, Y., Du, R., Katiyar, S., Yang, J., Fu, M., Leader, J. E., Quong, A., Novikoff, P. M. & Pestell, R. G. (2006) Cyclin D1 repression of nuclear respiratory factor 1 integrates nuclear DNA synthesis and mitochondrial function, *Proceedings of the National Academy of Sciences of the United States of America.* **103**, 11567-72.
140. Hilgendorf, K. I., Leshchiner, E. S., Nedelcu, S., Maynard, M. A., Calo, E., Ianari, A., Walensky, L. D. & Lees, J. A. (2013) The retinoblastoma protein induces apoptosis directly at the mitochondria, *Genes Dev.* **27**, 1003-15.
141. Benevolenskaya, E. V. & Frolov, M. V. (2015) Emerging links between E2F control and mitochondrial function, *Cancer Res.* **75**, 619-23.
142. Ambrus, A. M., Islam, A. B., Holmes, K. B., Moon, N. S., Lopez-Bigas, N., Benevolenskaya, E. V. & Frolov, M. V. (2013) Loss of dE2F compromises mitochondrial function, *Developmental cell.* **27**, 438-51.
143. Clem, B. F. & Chesney, J. (2012) Molecular pathways: regulation of metabolism by RB, *Clinical cancer research : an official journal of the American Association for Cancer Research.* **18**, 6096-100.
144. Reynolds, M. R., Lane, A. N., Robertson, B., Kemp, S., Liu, Y., Hill, B. G., Dean, D. C. & Clem, B. F. (2014) Control of glutamine metabolism by the tumor suppressor Rb, *Oncogene.* **33**, 556-66.
145. Nicolay, B. N., Gameiro, P. A., Tschop, K., Korenjak, M., Heilmann, A. M., Asara, J. M., Stephanopoulos, G., Iliopoulos, O. & Dyson, N. J. (2013) Loss of RBF1 changes glutamine catabolism, *Genes Dev.* **27**, 182-96.
146. Nicolay, B. N., Danielian, P. S., Kottakis, F., Lapek, J. D., Jr., Sanidas, I., Miles, W. O., Dehnad, M., Tschop, K., Gierut, J. J., Manning, A. L., Morris, R., Haigis, K., Bardeesy, N., Lees, J. A., Haas, W. & Dyson, N. J. (2015) Proteomic analysis of pRb loss highlights a signature of decreased mitochondrial oxidative phosphorylation, *Genes & development.* **29**, 1875-89.
147. Varaljai, R., Islam, A. B., Beshiri, M. L., Rehman, J., Lopez-Bigas, N. & Benevolenskaya, E. V. (2015) Increased mitochondrial function downstream from KDM5A histone demethylase rescues differentiation in pRB-deficient cells, *Genes Dev.* **29**, 1817-34.
148. Blanchet, E., Annicotte, J. S., Lagarrigue, S., Aguilar, V., Clape, C., Chavey, C., Fritz, V., Casas, F., Apparailly, F., Auwerx, J. & Fajas, L. (2011) E2F transcription factor-1 regulates oxidative metabolism, *Nature cell biology.* **13**, 1146-52.
149. Lamb, J., Ramaswamy, S., Ford, H. L., Contreras, B., Martinez, R. V., Kittrell, F. S., Zahnow, C. A., Patterson, N., Golub, T. R. & Ewen, M. E. (2003) A mechanism of cyclin D1 action encoded in the patterns of gene expression in human cancer, *Cell.* **114**, 323-34.
150. Witkiewicz, A. K., McMillan, E. A., Balaji, U., Baek, G., Lin, W. C., Mansour, J., Mollaee, M., Wagner, K. U., Koduru, P., Yopp, A., Choti, M. A., Yeo, C. J., McCue, P., White, M. A. & Knudsen, E. S. (2015) Whole-exome sequencing of pancreatic cancer defines genetic diversity and therapeutic targets, *Nature communications.* **6**, 6744.
151. Knudsen, E. S. & Wang, J. Y. (1997) Dual mechanisms for the inhibition of E2F binding to RB by cyclin-dependent kinase-mediated RB phosphorylation, *Molecular and cellular biology.* **17**, 5771-83.
152. Tibes, R., Qiu, Y., Lu, Y., Hennessy, B., Andreeff, M., Mills, G. B. & Kornblau, S. M. (2006) Reverse phase protein array: validation of a novel proteomic technology and

utility for analysis of primary leukemia specimens and hematopoietic stem cells, *Mol Cancer Ther.* **5**, 2512-21.
153. Brunelle, J. K., Shroff, E. H., Perlman, H., Strasser, A., Moraes, C. T., Flavell, R. A., Danial, N. N., Keith, B., Thompson, C. B. & Chandel, N. S. (2007) Loss of Mcl-1 protein and inhibition of electron transport chain together induce anoxic cell death, *Molecular and cellular biology.* **27**, 1222-35.
154. Thomas, L. W., Lam, C. & Edwards, S. W. (2010) Mcl-1; the molecular regulation of protein function, *FEBS letters.* **584**, 2981-9.
155. Oltersdorf, T., Elmore, S. W., Shoemaker, A. R., Armstrong, R. C., Augeri, D. J., Belli, B. A., Bruncko, M., Deckwerth, T. L., Dinges, J., Hajduk, P. J., Joseph, M. K., Kitada, S., Korsmeyer, S. J., Kunzer, A. R., Letai, A., Li, C., Mitten, M. J., Nettesheim, D. G., Ng, S., Nimmer, P. M., O'Connor, J. M., Oleksijew, A., Petros, A. M., Reed, J. C., Shen, W., Tahir, S. K., Thompson, C. B., Tomaselli, K. J., Wang, B., Wendt, M. D., Zhang, H., Fesik, S. W. & Rosenberg, S. H. (2005) An inhibitor of Bcl-2 family proteins induces regression of solid tumours, *Nature.* **435**, 677-81.
156. Vander Heiden, M. G. (2011) Targeting cancer metabolism: a therapeutic window opens, *Nature reviews Drug discovery.* **10**, 671-84.
157. Lyssiotis, C. A., Son, J., Cantley, L. C. & Kimmelman, A. C. (2013) Pancreatic cancers rely on a novel glutamine metabolism pathway to maintain redox balance, *Cell cycle.* **12**, 1987-8.
158. Datar, S. A., Jacobs, H. W., de la Cruz, A. F., Lehner, C. F. & Edgar, B. A. (2000) The Drosophila cyclin D-Cdk4 complex promotes cellular growth, *The EMBO journal.* **19**, 4543-54.
159. Sancak, Y., Peterson, T. R., Shaul, Y. D., Lindquist, R. A., Thoreen, C. C., Bar-Peled, L. & Sabatini, D. M. (2008) The Rag GTPases bind raptor and mediate amino acid signaling to mTORC1, *Science.* **320**, 1496-501.
160. Vora, S. R., Juric, D., Kim, N., Mino-Kenudson, M., Huynh, T., Costa, C., Lockerman, E. L., Pollack, S. F., Liu, M., Li, X., Lehar, J., Wiesmann, M., Wartmann, M., Chen, Y., Cao, Z. A., Pinzon-Ortiz, M., Kim, S., Schlegel, R., Huang, A. & Engelman, J. A. (2014) CDK 4/6 Inhibitors Sensitize PIK3CA Mutant Breast Cancer to PI3K Inhibitors, *Cancer Cell.* **26**, 136-49.
161. Galluzzi, L., Kepp, O., Vander Heiden, M. G. & Kroemer, G. (2013) Metabolic targets for cancer therapy, *Nature reviews Drug discovery.* **12**, 829-46.
162. Sabharwal, S. S. & Schumacker, P. T. (2014) Mitochondrial ROS in cancer: initiators, amplifiers or an Achilles' heel?, *Nat Rev Cancer.* **14**, 709-21.
163. Gorrini, C., Harris, I. S. & Mak, T. W. (2013) Modulation of oxidative stress as an anticancer strategy, *Nature reviews Drug discovery.* **12**, 931-47.
164. Taylor-Harding, B., Aspuria, P. J., Agadjanian, H., Cheon, D. J., Mizuno, T., Greenberg, D., Allen, J. R., Spurka, L., Funari, V., Spiteri, E., Wang, Q., Orsulic, S., Walsh, C., Karlan, B. Y. & Wiedemeyer, W. R. (2015) Cyclin E1 and RTK/RAS signaling drive CDK inhibitor resistance via activation of E2F and ETS, *Oncotarget.* **6**, 696-714.
165. Barton, C. M., McKie, A. B., Hogg, A., Bia, B., Elia, G., Phillips, S. M., Ding, S. F. & Lemoine, N. R. (1995) Abnormalities of the RB1 and DCC tumor suppressor genes: uncommon in human pancreatic adenocarcinoma, *Molecular carcinogenesis.* **13**, 61-9.

166. McClendon, A. K., Dean, J. L., Rivadeneira, D. B., Yu, J. E., Reed, C. A., Gao, E., Farber, J. L., Force, T., Koch, W. J. & Knudsen, E. S. (2012) CDK4/6 inhibition antagonizes the cytotoxic response to anthracycline therapy, *Cell Cycle.* **11**, 2747-55.
167. Alt, J. R., Cleveland, J. L., Hannink, M. & Diehl, J. A. (2000) Phosphorylation-dependent regulation of cyclin D1 nuclear export and cyclin D1-dependent cellular transformation, *Genes & development.* **14**, 3102-14.
168. Fajas, L. (2013) Re-thinking cell cycle regulators: the cross-talk with metabolism, *Frontiers in oncology.* **3**, 4.
169. Jewell, J. L., Russell, R. C. & Guan, K. L. (2013) Amino acid signalling upstream of mTOR, *Nature reviews Molecular cell biology.* **14**, 133-9.
170. Efeyan, A., Zoncu, R. & Sabatini, D. M. (2012) Amino acids and mTORC1: from lysosomes to disease, *Trends in molecular medicine.* **18**, 524-33.
171. Rebsamen, M. & Superti-Furga, G. (2015) SLC38A9: a lysosomal amino acid transporter at the core of the amino acid-sensing machinery that controls MTORC1, *Autophagy*, 0.
172. Xie, D. & Xie, K. (2015) Pancreatic cancer stromal biology and therapy, *Genes & Diseases.* **2**, 133-143.
173. Neesse, A., Algul, H., Tuveson, D. A. & Gress, T. M. (2015) Stromal biology and therapy in pancreatic cancer: a changing paradigm, *Gut.* **64**, 1476-84.
174. Bainbridge, P. (2013) Wound healing and the role of fibroblasts, *Journal of wound care.* **22**, 407-8, 410-12.
175. Erez, N., Truitt, M., Olson, P., Arron, S. T. & Hanahan, D. (2010) Cancer-Associated Fibroblasts Are Activated in Incipient Neoplasia to Orchestrate Tumor-Promoting Inflammation in an NF-kappaB-Dependent Manner, *Cancer cell.* **17**, 135-47.
176. Augsten, M. (2014) Cancer-associated fibroblasts as another polarized cell type of the tumor microenvironment, *Frontiers in oncology.* **4**, 62.
177. Karagiannis, G. S., Poutahidis, T., Erdman, S. E., Kirsch, R., Riddell, R. H. & Diamandis, E. P. (2012) Cancer-associated fibroblasts drive the progression of metastasis through both paracrine and mechanical pressure on cancer tissue, *Molecular cancer research : MCR.* **10**, 1403-18.
178. Castells, M., Thibault, B., Delord, J. P. & Couderc, B. (2012) Implication of tumor microenvironment in chemoresistance: tumor-associated stromal cells protect tumor cells from cell death, *International journal of molecular sciences.* **13**, 9545-71.
179. Pickard, A., Cichon, A. C., Barry, A., Kieran, D., Patel, D., Hamilton, P., Salto-Tellez, M., James, J. & McCance, D. J. (2012) Inactivation of Rb in stromal fibroblasts promotes epithelial cell invasion, *The EMBO journal.* **31**, 3092-103.
180. Al-Ansari, M. M., Hendrayani, S. F., Shehata, A. I. & Aboussekhra, A. (2013) p16(INK4A) represses the paracrine tumor-promoting effects of breast stromal fibroblasts, *Oncogene.* **32**, 2356-64.
181. Korc, M. (2003) Pathways for aberrant angiogenesis in pancreatic cancer, *Molecular cancer.* **2**, 8.
182. Luo, J., Guo, P., Matsuda, K., Truong, N., Lee, A., Chun, C., Cheng, S. Y. & Korc, M. (2001) Pancreatic cancer cell-derived vascular endothelial growth factor is biologically active in vitro and enhances tumorigenicity in vivo, *International journal of cancer.* **92**, 361-9.

183. Kollmann, K., Heller, G., Schneckenleithner, C., Warsch, W., Scheicher, R., Ott, R. G., Schafer, M., Fajmann, S., Schlederer, M., Schiefer, A. I., Reichart, U., Mayerhofer, M., Hoeller, C., Zochbauer-Muller, S., Kerjaschki, D., Bock, C., Kenner, L., Hoefler, G., Freissmuth, M., Green, A. R., Moriggl, R., Busslinger, M., Malumbres, M. & Sexl, V. (2013) A kinase-independent function of CDK6 links the cell cycle to tumor angiogenesis, *Cancer cell.* **24**, 167-81.
184. Lin, J., Yan, X. J. & Chen, H. M. (2007) Fascaplysin, a selective CDK4 inhibitor, exhibit anti-angiogenic activity in vitro and in vivo, *Cancer chemotherapy and pharmacology.* **59**, 439-45.
185. Hiraoka, N., Onozato, K., Kosuge, T. & Hirohashi, S. (2006) Prevalence of FOXP3+ regulatory T cells increases during the progression of pancreatic ductal adenocarcinoma and its premalignant lesions, *Clinical cancer research : an official journal of the American Association for Cancer Research.* **12**, 5423-34.
186. Yamamoto, T., Yanagimoto, H., Satoi, S., Toyokawa, H., Hirooka, S., Yamaki, S., Yui, R., Yamao, J., Kim, S. & Kwon, A. H. (2012) Circulating CD4+CD25+ regulatory T cells in patients with pancreatic cancer, *Pancreas.* **41**, 409-15.
187. Mielgo, A. & Schmid, M. C. (2013) Impact of tumour associated macrophages in pancreatic cancer, *BMB reports.* **46**, 131-8.
188. Veiga-Fernandes, H. & Rocha, B. (2004) High expression of active CDK6 in the cytoplasm of CD8 memory cells favors rapid division, *Nature immunology.* **5**, 31-7.
189. Yang, Y., Ma, B., Li, L., Jin, Y., Ben, W., Zhang, D., Jiang, K., Feng, S., Huang, L. & Zheng, J. (2014) CDK2 and CDK4 play important roles in promoting the proliferation of SKOV3 ovarian carcinoma cells induced by tumor-associated macrophages, *Oncology reports.* **31**, 2759-68.
190. Murakami, Y., Mizoguchi, F., Saito, T., Miyasaka, N. & Kohsaka, H. (2012) p16(INK4a) exerts an anti-inflammatory effect through accelerated IRAK1 degradation in macrophages, *J Immunol.* **189**, 5066-72.
191. (2012) Comprehensive molecular portraits of human breast tumours, *Nature.* **490**, 61-70.
192. Cancello, G., Maisonneuve, P., Rotmensz, N., Viale, G., Mastropasqua, M. G., Pruneri, G., Veronesi, P., Torrisi, R., Montagna, E., Luini, A., Intra, M., Gentilini, O., Ghisini, R., Goldhirsch, A. & Colleoni, M. (2010) Prognosis and adjuvant treatment effects in selected breast cancer subtypes of very young women (<35 years) with operable breast cancer, *Annals of oncology : official journal of the European Society for Medical Oncology / ESMO.* **21**, 1974-81.
193. Dent, R., Trudeau, M., Pritchard, K. I., Hanna, W. M., Kahn, H. K., Sawka, C. A., Lickley, L. A., Rawlinson, E., Sun, P. & Narod, S. A. (2007) Triple-negative breast cancer: clinical features and patterns of recurrence, *Clinical cancer research : an official journal of the American Association for Cancer Research.* **13**, 4429-34.
194. Reis-Filho, J. S. & Tutt, A. N. (2008) Triple negative tumours: a critical review, *Histopathology.* **52**, 108-18.
195. Lehmann, B. D., Bauer, J. A., Chen, X., Sanders, M. E., Chakravarthy, A. B., Shyr, Y. & Pietenpol, J. A. (2011) Identification of human triple-negative breast cancer subtypes and preclinical models for selection of targeted therapies, *The Journal of clinical investigation.* **121**, 2750-67.

196. Zardavas, D., Irrthum, A., Swanton, C. & Piccart, M. (2015) Clinical management of breast cancer heterogeneity, *Nature reviews Clinical oncology.* **12**, 381-94.
197. Andre, F. & Zielinski, C. C. (2012) Optimal strategies for the treatment of metastatic triple-negative breast cancer with currently approved agents, *Annals of oncology : official journal of the European Society for Medical Oncology / ESMO.* **23 Suppl 6**, vi46-51.
198. Wahba, H. A. & El-Hadaad, H. A. (2015) Current approaches in treatment of triple-negative breast cancer, *Cancer biology & medicine.* **12**, 106-16.
199. Herschkowitz, J. I., He, X., Fan, C. & Perou, C. M. (2008) The functional loss of the retinoblastoma tumour suppressor is a common event in basal-like and luminal B breast carcinomas, *Breast cancer research : BCR.* **10**, R75.
200. Burkhart, D. L. & Sage, J. (2008) Cellular mechanisms of tumour suppression by the retinoblastoma gene, *Nature reviews Cancer.* **8**, 671-82.
201. Willis, S., De, P., Dey, N., Long, B., Young, B., Sparano, J. A., Wang, V., Davidson, N. E. & Leyland-Jones, B. R. (2015) Enriched transcription factor signatures in triple negative breast cancer indicates possible targeted therapies with existing drugs, *Meta gene.* **4**, 129-41.
202. Knudsen, E. S., McClendon, A. K., Franco, J., Ertel, A., Fortina, P. & Witkiewicz, A. K. (2015) RB loss contributes to aggressive tumor phenotypes in MYC-driven triple negative breast cancer, *Cell Cycle.* **14**, 109-22.
203. Robinson, T. J., Liu, J. C., Vizeacoumar, F., Sun, T., Maclean, N., Egan, S. E., Schimmer, A. D., Datti, A. & Zacksenhaus, E. (2013) RB1 status in triple negative breast cancer cells dictates response to radiation treatment and selective therapeutic drugs, *PloS one.* **8**, e78641.